



N3B – Los Alamos
 600 6th Street
 Los Alamos, New Mexico 87544
 (303) 489-2471



Environmental Management
 Los Alamos Field Office
 P.O. Box 1663, MS M984
 Los Alamos, New Mexico 87545
 (505) 665-5658/FAX (505) 606-2132

Date: **AUG 06 2018**
 Refer To: N3B-18-0145

John Kieling, Bureau Chief
 Hazardous Waste Bureau
 New Mexico Environment Department
 2905 Rodeo Park Drive East, Building 1
 Santa Fe, NM 87505-6303

Subject: Submittal of the Interim Measures Final Report for Soil-Vapor Extraction of Volatile Organic Compounds from Material Disposal Area L, Technical Area 54

Dear Mr. Kieling:

Enclosed please find two hard copies with electronic files of the Interim Measures Final Report for Soil-Vapor Extraction of Volatile Organic Compounds from Material Disposal Area L, Technical Area 54. Pursuant to Section XXIII.C of the Compliance Order on Consent, a pre-submission review meeting was held with the U.S. Department of Energy Environmental Management Los Alamos Field Office, Newport News Nuclear BWXT – Los Alamos, LLC (N3B), and the New Mexico Environment Department (NMED) on July 17, 2018, to discuss N3B's responses to draft comments provided by NMED. The enclosed draft incorporates information from that meeting.

If you have any questions, please contact Danny Katzman at (505) 309-1371 (danny.katzman@em-la.doe.gov) or Cheryl Rodriguez at (505) 665-5330 (cheryl.rodriguez@em.doe.gov).

Sincerely,

Joseph A. Legare
 Program Manager
 Environmental Remediation Program

Sincerely,

David S. Rhodes, Director
 Office of Quality and Regulatory Compliance
 Environmental Management
 Los Alamos Field Office

JL/DR/DK/CR

Enclosure(s): Two hard copies with electronic files – Interim Measures Final Report for Soil-Vapor Extraction of Volatile Organic Compounds from Material Disposal Area L, Technical Area 54 (EM2018-0008)

Cy: (letter with enclosure[s])
Danny Katzman, N3B, ER Program
Kent Rich, N3B, ER Program
Cheryl Rodriguez, DOE-EM-LA

Cy: (letter with electronic enclosure[s])
Laurie King, EPA Region 6, Dallas, TX
Steve Yanicak, NMED-DOE-OB, LANL MS M894
emla.docs@em.doe.gov
N3B Records
Public Reading Room (EPRR and HPRR)
PRS Database

Cy: (letter emailed without enclosure[s])
David Rhodes, DOE-EM-LA
David Nickless, DOE-EM-LA
Nick Lombardo, N3B
Frazer Lockhart, N3B
Joe Legare, N3B, ER Program
Erich Evered, N3B, ER Program

August 2018
EM2018-0008


Interim Measures Final Report for Soil-Vapor Extraction of Volatile Organic Compounds from Material Disposal Area L, Technical Area 54

Newport News Nuclear BWXT – Los Alamos, LLC (N3B), under the U.S. Department of Energy Office of Environmental Management Contract No. 89303318CEM000007 (the Los Alamos Legacy Cleanup Contract), has prepared this document pursuant to the Compliance Order on Consent, signed June 24, 2016. The Compliance Order on Consent contains requirements for the investigation and cleanup, including corrective action, of contamination at Los Alamos National Laboratory. The U.S. government has rights to use, reproduce, and distribute this document. The public may copy and use this document without charge, provided that this notice and any statement of authorship are reproduced on all copies.

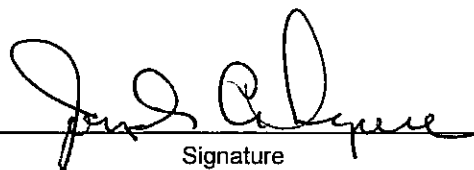
Interim Measures Final Report for Soil-Vapor Extraction of Volatile Organic Compounds from Material Disposal Area L, Technical Area 54

August 2018


Responsible program director:

Erich Evered		Program Director	RCRA Remediation Program	7/26/18
--------------	---	---------------------	--------------------------------	---------

Responsible N3B representative:

Joseph A. Legare		Program Manager	N3B Environmental Remediation Program	7/26/18
Printed Name	Signature	Title	Organization	Date

Responsible DOE-EM-LA representative:

David S. Rhodes		Office Director	Quality and Regulatory Compliance	8/6/18
Printed Name	Signature	Title	Organization	Date

EXECUTIVE SUMMARY

This interim measures (IM) final report summarizes the results from 10 mo of continuous soil-vapor extraction (SVE) operation at two vapor-extraction wells at Material Disposal Area (MDA) L, Technical Area 54. The SVE-West system began operation on January 9, 2015, and the SVE-East system began operation on January 26, 2015. Both the East and West systems were turned off for the winter on November 18, 2015. During the period of operation, the two SVE units removed 553 kg (1217 lb) of total organic vapor mass. The mass was primarily removed from within an approximately 150-ft radius surrounding the extraction wells. Following the initial 10-mo SVE operation, short duration (2-d) rebound testing was performed in 2016. A final 25-d rebound test on SVE-East was performed in June 2017. These rebound tests were performed to provide additional insight into plume behavior and to create a data set for model validation.

Baseline and annual pore-gas monitoring samples were collected from 185 pore-gas sampling ports in 28 boreholes within and surrounding MDA L. Quarterly pore-gas monitoring samples were collected from a subset of ports in 14 boreholes located within a 150-ft radius of the SVE units. Pore-gas sampling results confirm SVE operation has reduced the concentrations at the majority of sampling ports to below their baseline values. The radius of influence of both SVE wells is at least 150 ft, increasing the previous estimates from shorter duration SVE testing.

Data collected during the IM has been analyzed and used to calibrate and validate a three-dimensional numerical model of the site. The numerical model was used to explore scenarios of hypothetical future releases at the site and present suggestions to support the selection and design of a final remedy for MDA L. Recommendations include the following:

1. Conduct semiannual monitoring of boreholes located in the source region (“sentry boreholes”) to allow early detection of potential container failure. Sentry boreholes on the western side of MDA L include boreholes 54-27641 and 54-24240. On the eastern side of MDA L, sentry boreholes include boreholes 54-24241, 54-24238, and 54-27642.
2. Monitor peripheral boreholes once every 2 yr for evidence of plume expansion.
3. Conduct semiannual monitoring of deep borehole 54-24399 to further characterize long-term trends of volatile organic compound (VOC) concentrations in the basalt and to provide data needed to support the Corrective Measures Evaluation process (e.g., updating the conceptual model for transport and developing Tier II screening levels and cleanup goals).
4. Activate the eastern SVE unit if total VOC concentrations in any ports in the eastern sentry boreholes rise above 2000 ppmv, with a trend of consistent increase with each consecutive measurement for ports to depths of 100 ft. Once observed, the eastern SVE system should be activated within a period of 2 yr.
5. Activate the western SVE unit if total VOC concentrations in any ports in the western sentry boreholes rise above 2000 ppmv, with a trend of consistent increase with each consecutive measurement for ports to depths of 100 ft. Once observed, the western SVE system should be activated within a period of 2 yr.

CONTENTS

1.0	INTRODUCTION	1
1.1	Background.....	2
2.0	OPERATION OF SVE UNITS	2
2.1	Description of SVE Units	2
2.2	Data Collection Methods and Results	3
2.2.1	Effluent Gas from SVE Units.....	4
2.2.2	Calculation of Mass Removal from SVE Effluent and Gas Flow Rate.....	4
2.2.3	Subsurface Pore-Gas Sampling.....	5
2.2.4	Subsurface Pore-Gas Sampling at Borehole 54-24399.....	5
2.3	Gas Sampling Schedule	6
2.3.1	Effluent Sampling from SVE Units	6
2.3.2	Subsurface Pore-Gas Data	6
2.4	Summary of SVE System Operations	7
3.0	SUMMARY OF SUBSURFACE PORE-GAS BASELINE RESULTS	7
4.0	SUMMARY OF SVE RESULTS	7
4.1	Effluent Mass Removal.....	7
4.2	Concentrations in the SVE Effluent.....	8
4.3	Subsurface Plume Changes Relative to Baseline 2014.....	8
4.3.1	Weston Data Interpolations.....	9
4.3.2	Effectiveness of SVE at Selected Monitoring Wells.....	10
4.4	Monitoring Well 54-24399.....	11
4.5	Differential Pressure Measurements	13
4.6	Rebound Data.....	14
5.0	NUMERICAL ANALYSIS	15
5.1	MDA L Vapor Plume Modeling Review	15
5.2	November 2014 Base Simulation	16
5.3	Predicted Plume Behavior Compared with Measured SVE Response	16
5.4	Predicted Plume Behavior Compared with Measured Monitoring Borehole Data	16
5.5	Simulated Rebound	17
5.6	Simulated Sudden Failure of Buried Drums	17
5.6.1	Drum Failure in Absence of SVE	18
5.6.2	Simulated SVE Remediation Following Sudden Drum Failure	18
6.0	DEVIATIONS	19
6.1	Sampling Ports	19
6.2	Active Extraction Duration	19
6.3	Deep Borehole 54-24399 Dual-Packer Failure	19
7.0	CONCLUSIONS	20
8.0	RECOMMENDATIONS	20
9.0	REFERENCES AND MAP DATA SOURCES	21
9.1	References	21
9.2	Map Data Sources	23

Figures

Figure 1.1-1 View of MDA L with disposal units, surface structures, pore-gas monitoring boreholes, SVE boreholes, and 150-ft ROI of extraction wells..... 25

Figure 2.1-1 Diagram of SVE-East and SVE-West system piping and instrumentation 26

Figure 2.1-2 SVE-East unit..... 27

Figure 2.2-1 Subsurface sampling train 27

Figure 2.2-2 Permanent packer installed in borehole 54-24399 in August 2016 28

Figure 2.2-3 Surface completion of the permanent packer at borehole 54-24399..... 28

Figure 2.2-4 Top of the permanent packer showing the OMEGA pressure transducer, one sample line, and the nitrogen inflation line..... 29

Figure 2.2-5 Schematic of the completed single packer installation in borehole 54-24399 30

Figure 4.1-1 Cumulative mass removal and cumulative volume of pore gas pumped from the subsurface from both SVE units as a function of time 31

Figure 4.1-2 Weekly mass removal rate from both SVE units as a function of time 32

Figure 4.2-1 Effluent concentration versus time for SVE-West and SVE-East 33

Figure 4.2-2 Effluent concentration ratios versus time for (A) SVE-West and (B) SVE-East 34

Figure 4.3-1 Comparison of subsurface VOC concentrations before SVE (baseline 2014) and after 10-plus mo of SVE pumping (November 2015) 35

Figure 4.3-2 Comparison of post-SVE and pre-SVE subsurface VOC concentrations for seven analytes passing Tier II screening. Labeled points are all from borehole 54-24238 36

Figure 4.3-3 Baseline 2014 1,1,1-TCA plume data interpolated from borehole data..... 37

Figure 4.3-4 April 2015 1,1,1-TCA plume data interpolated from borehole data 38

Figure 4.3-5 Baseline 2014 TCE plume data interpolated from borehole data..... 39

Figure 4.3-6 April 2015 TCE plume data interpolated from borehole data 40

Figure 4.3-7 DCA[1,2], TCE, PCE, and 1,1,1-TCA concentration data for borehole 54-27641 41

Figure 4.3-8 DCA[1,2], TCE, PCE, and 1,1,1-TCA concentration data for borehole 54-24240 42

Figure 4.3-9 DCA[1,2], TCE, PCE, and 1,1,1-TCA concentration data for borehole 54-02022..... 43

Figure 4.3-10 DCA[1,2], TCE, PCE, and 1,1,1-TCA concentration data for borehole 54-24243 44

Figure 4.3-11 DCA[1,2], TCE, PCE, and 1,1,1-TCA concentration data for borehole 54-24241 45

Figure 4.3-12 DCA[1,2], TCE, PCE, and 1,1,1-TCA concentration data for borehole 54-27642..... 46

Figure 4.3-13 DCA[1,2], TCE, PCE, and 1,1,1-TCA concentration data for borehole 54-02089..... 47

Figure 4.3-14 DCA[1,2], TCE, PCE, and 1,1,1-TCA concentration data for borehole 54-24238..... 48

Figure 4.4-1 TCA[1,1,1] in borehole 54-24399 sampled using SUMMA canisters, relative to the Tier 1 screening level..... 49

Figure 4.4-2 TCE in borehole 54-24399 sampled using SUMMA canisters, relative to the Tier 1 screening level..... 49

Figure 4.4-3 PCE in borehole 54-24399 sampled using SUMMA canisters, relative to the Tier 1 screening level 50

Figure 4.4-4 DCA[1,2] in borehole 54-24399 sampled using SUMMA canisters, relative to the Tier 1 screening level..... 50

Figure 4.4-5	Methylene chloride in borehole 54-24399 sampled using SUMMA canisters, relative to the Tier 1 screening level.....	51
Figure 4.4-6	Concentration of 1,1,1-TCA in borehole 54-01015.....	51
Figure 4.4-7	LumaSense Photoacoustic Gas Monitor measurements of 1,1,1-TCA from borehole 54-24399 during 12 d in April 2017. Pressure measured beneath the packer is also shown.....	52
Figure 4.4-8	Ratio of 1,1,1-TCA to toluene plotted versus 1,1,1-TCA concentration comparing borehole 54-24399 with borehole 54-24241	52
Figure 4.6-1	TCA[1,1,1] concentrations in effluent from SVE-West versus time including three short duration (2-d) rebound tests in 2016.....	53
Figure 4.6-2	Concentration in effluent from SVE-East versus time including three short duration (2-d) rebound tests in 2016 and a 25-d rebound test in June 2017.....	54
Figure 4.6-3	Subsurface plume concentrations in 2017 versus baseline (2014) concentrations for seven analytes	55
Figure 5.1-1	Locations of the MDA L outline, example monitoring boreholes, SVE units, and simulated leaking subsurface sources	56
Figure 5.2-1	Simulated 1,1,1-TCA concentration compared with data for the 2014 baseline pre-SVE initial state.....	57
Figure 5.2-2	Simulated 1,1,1-TCA concentration on a plane 60 ft below the ground surface of MDA L	58
Figure 5.3-1	Predicted versus measured concentrations of 1,1,1-TCA at SVE-West	59
Figure 5.3-2	Predicted versus measured 1,1,1-TCA concentrations at SVE-East	59
Figure 5.3-3	Predicted versus measured 1,1,1-TCA concentrations at SVE-East for the recalibrated simulation	60
Figure 5.4-1	Simulated versus measured 1,1,1-TCA concentration in borehole 54-27641	61
Figure 5.4-2	Simulated versus measured 1,1,1-TCA concentration in borehole 54-24241	62
Figure 5.4-3	Simulated versus measured 1,1,1-TCA concentration in borehole 54-24243	63
Figure 5.5-1	Simulated rebound for SVE-East compared with measured SUMMA data from SVE-East effluent.....	63
Figure 5.5-2	Simulated active extraction concentrations and rebound for SVE-West compared with measured SUMMA data	64
Figure 5.6-1	Location of sudden drum failure and three existing monitoring wells	65
Figure 5.6-2	Borehole 54-24238 response to sudden release of 1 drum (200 L) of 1,1,1-TCA	65
Figure 5.6-3	Borehole 54-27642 response to sudden release of 1 drum (200 L) of 1,1,1-TCA	66
Figure 5.6-4	Borehole 54-24241 response to sudden release of 1 drum (200 L) of 1,1,1-TCA	66
Figure 5.6-5	Concentrations in monitoring borehole 54-27642 for a simulated five-drum sudden failure of TCA followed by 7 y of SVE	67
Figure 5.6-6	Mass removal by active SVE of 1,1,1-TCA versus time for the five-drum case	68

Tables

Table 2.2-1	List of 62 Organic Compounds Analyzed by EPA Method TO-15 during SVE Operations	69
Table 2.2-2	Subsurface Vapor-Monitoring Locations, Port Depths, and Corresponding Sampling Intervals Used for Baseline and Annual Monitoring.....	70
Table 2.2-3	Subsurface Vapor-Monitoring Locations, Port Depths, and Corresponding Sampling Intervals Used for Quarterly Sampling within 150-ft Radius of the SVE Units.....	75
Table 4.1-1	Mass Removed for Detected Organic Compounds during SVE Operation	79
Table 4.1-2	Flow Rate Data for SVE-West	81
Table 4.1-3	Flow Rate Data for SVE-East	85
Table 4.3-1	MDA L CME Tier I+II Screening Calculations.....	89
Table 4.3-2	Differential Pressure Data at Sampling Ports Monitored during SVE Operations	90
Table 5.6-1	Distances from Example Observation Points to SVE-East and Sudden Drum Failure Location.....	95

Appendixes

Appendix A	Spreadsheet Containing Dwyer Orifice Plate Calculations (on CD included with this document)
Appendix B	Analytical Suites and Results (on CD included with this document)
Appendix C	Example Calculations for Effluent Mass Removal
Appendix D	Video Log of Borehole 54-24399 (on DVD included with this document)
Appendix E	Flow Rate Data for SVE-West and SVE-East (on CD included with this document)

Plate

Plate 1	Graphical Summary of Pore-Gas Monitoring Results for MDA L
---------	--

1.0 INTRODUCTION

This interim measures (IM) final report summarizes results from a soil-vapor extraction (SVE) operation at two extraction wells at Material Disposal Area (MDA) L, Technical Area 54 (TA-54), within the boundaries of Los Alamos National Laboratory (LANL or the Laboratory). These activities were conducted in accordance with the “Interim Measures Work Plan for Soil-Vapor Extraction of Volatile Organic Compounds from Material Disposal Area L, Technical Area 54, Revision 1” (hereafter, the IMWP) (LANL 2014, 261843). The IMWP was submitted to the New Mexico Environment Department (NMED) on September 15, 2014, in response to requirements in NMED’s “Approval with Modifications, Interim Measures Work Plan for Soil-Vapor Extraction of Volatile Organic Compounds from Material Disposal, Area L,” dated July 17, 2014 (NMED 2014, 525053). Following 6 mo of operation, a progress report was submitted to NMED on September 28, 2015 (LANL 2015, 600930). In May, 2016, LANL submitted to NMED an annual progress report (LANL 2016, 601484).

The data in this IM report were collected from August 2014 to August 2017. Though initial plans were to run the SVE IM for a full year, concerns over damage to the system caused by freezing of condensation in the winter months led to modification of the plan, and the SVE units were shut down in November 2015. Following the initial 10 mo SVE operation, short duration (2-d) rebound testing was performed in 2016 with the goal of gathering more data on plume behavior. A final 25-d rebound test was undertaken in June 2017 using the eastern SVE unit.

Remediation of the vapor plume by SVE is included as part of the recommended final remedy in the “Corrective Measures Evaluation Report for Material Disposal Area L, Solid Waste Management Unit 54-006, at Technical Area 54, Revision 2” (hereafter, the CME report) to meet the remedial action objective of preventing groundwater from being impacted above a regulatory standard by the transport of volatile organic compounds (VOCs) to groundwater through soil vapor (LANL 2011, 205756). The depth to regional groundwater beneath MDA L is on the order of 285 m (935 ft), whereas the vapor plume is predominantly within the Bandelier Tuff in the upper 90 m (300 ft) of the subsurface. The tuff units beneath the surface at MDA L are underlain by a thick (nearly 150-m [500-ft]) sequence of Cerros del Rio basalts. There is uncertainty regarding the long-term transport of vapors downward through the basalt toward the water table. Therefore, it is desirable to contain the plume above the basalt. The SVE IM is a proactive step to remove VOC mass, to decrease maximum VOC concentrations within the plume, to reduce the current extent of the vapor plume so it remains well-contained within the upper tuff units, and to gather design information for a potential final corrective measures remedy. The CME report was withdrawn by the U.S. Department of Energy (DOE) in October 2016 (DOE 2016, 601899) based on an updated schedule of environmental cleanup activities at TA-54. The CME report will be updated and resubmitted in the future in accordance with the revised schedule.

To better characterize the transport properties of the Cerros del Rio basalts, a gas-phase tracer test was implemented in conjunction with the SVE IM. Results from the tracer test in the Cerros del Rio basalts yield estimates of effective diffusivity that are orders of magnitude above simple porous diffusion. The enhanced diffusivity is a result of tight coupling between the atmosphere and the subsurface pressure in the basalt. The impact of enhanced vapor diffusivity in the basalt is to move contaminants more rapidly in all directions. This may shorten the arrival time of contaminants at the regional aquifer; however, because of later spreading in three dimensions, the mass flux to a given location at the top of the regional aquifer could be reduced relative to that predicted with a simpler one-dimensional diffusion calculation. However, variability in VOC data from boreholes in the basalts suggests that a more complex conceptual model may be needed to explain transport through this horizon.

1.1 Background

MDA L operated from the early 1960s to 1986 as the designated disposal area for nonradiological liquid chemical wastes, including containerized and uncontainerized liquid wastes; bulk quantities of treated aqueous waste; batch-treated salt solutions and electroplating wastes, including precipitated heavy metals; and small-batch quantities of treated lithium hydride. Waste was disposed of in 1 pit, 3 impoundments, and 34 shafts (Plate 1).

Disposal Shafts 1 through 34 were dry-drilled directly into the Tshirege Member of the Bandelier Tuff. The shafts range from 3 to 8 ft in diameter and from 15 to 65 ft in depth. The 34 disposal shafts were used to dispose of containerized and uncontainerized liquid chemical wastes and precipitated solids from the treatment of aqueous waste. Before 1982, containerized liquids were disposed of without the addition of absorbents. Small containers were typically dropped into a shaft. Larger drums were lowered by crane and arranged in layers of one drum in a 3- or 4-ft-diameter shaft, four to five drums in a 6-ft-diameter shaft, or six drums in an 8-ft-diameter shaft. The space around the drums was filled with crushed tuff, and a 6-in. layer of crushed tuff was placed between each layer of drums. Uncontainerized liquid wastes were also disposed of in the shafts. Between 1982 and 1985, only containerized wastes (including organic and inorganic liquids, precipitated heavy metals, and stabilized heavy metals) were disposed of in the shafts. These shafts are the primary source for the subsurface VOC vapor plume that is present beneath MDA L (LANL 2011, 205756).

Soil-vapor monitoring boreholes located within and around MDA L have been used to characterize the nature and extent of the subsurface vapor plume at the site since 1986. Figure 1.1-1 shows the pore-gas monitoring boreholes at MDA L. Concentrations in the subsurface VOC plume are generally highest within 150 ft below ground surface (bgs) and decrease significantly with depth to the top of the Cerros del Rio basalts. Concentrations measured in the basalt are quite low, with values less than 1 ppmv.

The CME report used a two-tiered screening approach to identify the VOCs present at high enough concentrations within the vapor plume to potentially impact groundwater above a regulatory standard if they migrated to groundwater (LANL 2011, 205756). The analysis found vapor concentrations for 1,1,1-trichloroethane (1,1,1-TCA); trichloroethene (TCE); tetrachloroethene (PCE or PERC); methylene chloride; 1,2-dichloropropane (1,2-DCP); 1,1-dichloroethene (1,1-DCE); 1,2-dichloroethane (1,2-DCA); and 1,4-dioxane present within the tuff units at concentrations that exceed their Tier II screening levels (LANL 2011, 205756). However, the assumptions used in the Tier II screening analysis are not consistent with field measurements of VOC concentration variability and barometric pumping in the basalt.

The hydrogeologic framework for the contaminated subsurface at MDA L is based on years of data collection, including results from a 2006 pilot SVE test at the site (LANL 2006, 094152). The current IM uses the same two wells used during the pilot test: SVE-East and SVE-West (Figure 1.1-1). Data gathered in 2006 and subsequent analysis (Stauffer et al. 2007, 097871; Stauffer et al. 2011, 255584) were used to create three-dimensional (3-D) numerical simulations that provided expected total mass removal from the two SVE units during the IM.

2.0 OPERATION OF SVE UNITS

2.1 Description of SVE Units

The two SVE systems have a main blower unit rated to 129 standard cubic feet per minute (scfm) at vacuum equal to 42.5 kPa (120 in. of water), a knock-out trap for liquid, various in-line flow and pressure-measurement instruments, and an off-gas stack to the atmosphere (Figure 2.1-1). The SVE blower systems are 11-ft long × 3-ft wide skid-mounted Model 4L SVE Blower Package systems provided by Catalytic Combustion Corp. of Bloomer, WI (Figure 2.1-2).

The SVE units pull subsurface gas from the open uncased part of the boreholes, 65 to 215 ft bgs on the east SVE well and 65 to 115 ft bgs on the west SVE well. Condensed liquid (water) is removed in the SVE unit knock-out tank, and the effluent gas is filtered with a rough particulate filter to protect the blower from large particulate material that may be present. Untreated effluent gas from each SVE unit is then discharged through a stack located 21 ft above ground surface. Samples representative of the extracted gas are collected from a sample port (SP1) located between the blower and the exhaust stack. Each unit is equipped with a manual air dilution valve (V1) that is closed at all times (Figure 2.1-1).

The gas-flow rate is measured at each wellhead using a Dwyer Series PE Orifice Plate Flow Meter (Model PE-H-2) equipped with a Dwyer 0–25 in. of water Magnehelic Differential Pressure Gage. Flow rate is calculated using the measured differential pressure across the orifice plate, line pressure, and temperature using a formula provided by the manufacturer of the flow meter (Appendix A, on CD included with this document). This calculation is also corrected for a local atmospheric pressure of 80 kPa. Output from the calculation are in scfm. Readings from the differential pressure gage, pipeline temperature, and pressure are recorded by the operator and used to calculate the instantaneous flow rate per Detailed Operating Procedure ER-DOP-20242, “Soil Vapor Extraction System Setup, Operation, and Monitoring Procedure.” During the first 3 wk of operation, each system was monitored 7 d/wk. Following the first 3 wk of operation, each system was inspected and monitored by the operator a minimum of 4 d (Mondays through Thursdays) each week.

2.2 Data Collection Methods and Results

SUMMA canisters were used for both SVE gas effluent and subsurface pore-gas sampling. Evacuated canisters were attached to valved T-ports and allowed to equilibrate to atmospheric pressure before sealing. All SUMMA samples were analyzed by an independent analytical laboratory, Eurofins Air Toxics, Inc., using U.S. Environmental Protection Agency (EPA) Method TO-15. Eurofins Air Toxic is a National Environmental Laboratory Accreditation Program–certified laboratory. The data are entered into the Environmental Information Management (EIM) database and undergo a secondary validation. EIM is the official database for environmental data collected by both the Laboratory and NMED. Table 2.2-1 lists the organic compounds analyzed by EPA Method TO-15 from samples collected from the effluent streams of the active SVE units and subsurface pore-gas sampling ports. Analytical results from samples collected during SVE operation are presented in Appendix B (on CD included with this document).

All data analyzed by Eurofins Air Toxics using the EPA Method TO-15 are reported to the Laboratory in units of ppbv. To convert from ppbv to ppmv, one divides by 1000. Both ppmv and ppbv are used in this report. Concentrations expressed as ppmv or ppbv are independent of temperature or pressure. NMED has also requested that the Laboratory provide concentrations in $\mu\text{g}/\text{m}^3$, and these units are included in Appendix B. To convert between the two units, one must know the molecular weight of the contaminant and that of air as well as the density of air, which is a function of temperature and pressure. Air is a mixture of many gases but can be approximated as having a molecular weight of 29 g/mol. The primary VOC at MDA L, TCA, has a molecular weight of 133 g/mol. Assuming the density of air on the mesa (top elevation, average atmospheric pressure, and temperature of 2072 m, 80 kPa, and 10°C: 6800 ft, 11.6 psi, and 50°F) is approximately 1 kg/m³, a concentration of 1000 ppmv TCA can be converted to $\mu\text{g}/\text{m}^3$ as follows:

$$\begin{aligned}
 1000 \text{ ppmv} &= 1000 \text{ moles TCA}/1\text{e}6 \text{ moles air} \\
 1000 \text{ moles TCA} * 133 \text{ g/mol} * 1\text{e}6 \text{ } \mu\text{g/g} &= 133.\text{e}9 \text{ } \mu\text{g TCA} \\
 1\text{e}6 \text{ moles Air} * 29 \text{ g/mol} * 1 \text{ m}^3/\text{kg} * 1\text{e-}3 \text{ kg/g} &= 29,000 \text{ m}^3 \\
 &\text{yielding} \\
 133.\text{e}9 \text{ } \mu\text{g}/29,000 \text{ m}^3 &= 4.6\text{e}6 \text{ } \mu\text{g}/\text{m}^3
 \end{aligned}$$

Within Laboratory databases, units of ppbv provided by the analytical laboratory are converted to $\mu\text{g}/\text{m}^3$ using the assumption of constant gas density at standard pressure and temperature (101.325 kPa, 25°C) with conversion factors for each compound based on individual molecular weights. Because the actual pressures and temperatures are not constant for each measured sample, this required assumption of the conversion from ppbv to $\mu\text{g}/\text{m}^3$ introduces an error into the $\mu\text{g}/\text{m}^3$ values that could be up to 20% (Stauffer et al. 2007, 097871).

2.2.1 Effluent Gas from SVE Units

Effluent gas from each SVE system was sampled in accordance with the sampling plan outlined in the IMWP (LANL 2014, 261843). Section 12[2] of ER-DOP-20242 outlines the steps taken to collect the gas sample from sampling port SP1 on each unit (Figure 2.1-1). Data were collected by connecting tubing from port SP1 to the SUMMA canister. Port SP1 was then opened, followed by opening of the SUMMA canister valve. Samples were collected in SUMMA canisters more frequently early in the operation of the system. As operation of the system continued and the vapor concentrations of VOCs were observed to level out, the sampling frequency decreased. Section 2.3.1 of this report presents the SVE effluent sampling schedule.

2.2.2 Calculation of Mass Removal from SVE Effluent and Gas Flow Rate

Calculation of mass removal is based on two principles: numerical integration of the flow rate and concentration data and interpolation of the results to the desired date. Numerical integration is based on the trapezoid method, and the interpolation is always linear. No results are extrapolated beyond the last measurement.

The first step in the numerical integration is the calculation of the volume of the gas pumped. The flow rate versus time curves are integrated, producing two curves of volume pumped versus time: one each for the SVE-East and SVE-West units. Total pumped volume versus time is produced by adding the SVE-East and SVE-West curves. The addition process includes interpolation of the results from the SVE-West volume versus time curve to time concurrent with data collection used to generate the SVE-East curve. This is necessary because the SVE-West and SVE-East flow rate and concentration data are not measured at exactly the same time.

In the second step, concentration versus time columns are (virtually) constructed, transferred to the concentration versus volume scale (using volume pumped values from the first step) and numerically integrated, producing total mass removed. The “concentration” in this process may be a concentration of the individual compound or a total concentration (sum of all VOC concentrations). Finally, the SVE-West and SVE-East mass removal curves are added together using interpolation. Example calculations for effluent mass removal are included in Appendix C.

VOC concentrations from SUMMA samples are reported by the analytical laboratory in ppbv units. Laboratory values are stored in the EIM database as “Laboratory Result.” The EIM database recalculates the ppbv concentrations to $\mu\text{g}/\text{m}^3$ values using molar mass, and standard temperature and pressure (101.325 kPa, 25°C). Recalculated values (in $\mu\text{g}/\text{m}^3$) are stored by the database as “Reported Result,” and these data were used to calculate total mass removed.

2.2.3 Subsurface Pore-Gas Sampling

Subsurface pore-gas sampling was performed in accordance with the current version of Standard Operating Procedure EP-ERSS-SOP-5074, "Sampling Subsurface Vapor." Baseline and annual monitoring samples were collected from pore-gas sampling ports in 28 boreholes (Table 2.2-2). Quarterly samples were collected from a subset of ports in 14 boreholes located within a 150-ft radius of the SVE units (Table 2.2-3).

Sampling involves a set of steps for each well and port. This process begins when a well is opened and a radiological control technician (RCT) monitors the well for radioactivity. If the activity levels are less than $20 \mu\text{Ci}/\text{m}^3$, each port is opened and the RCT monitors the area above each port within 2 in. of the opening. If any ports are found to be higher than $20 \mu\text{Ci}/\text{m}^3$, the port is allowed to breath and then is monitored again. Next, the sampling team records static subsurface pressure with a handheld digital manometer. Once static pressure has been measured, the sample port is connected to the sample train shown in Figure 2.2-1.

The sample train consists of tubing that connects the sample port to a pair of isolation valves. The isolation valves allow the SUMMA canister to be bypassed during purging. The sample train continues past the isolation valves into a Sierra Instruments Top-Trak Mass Flow Meter that displays the purge rate and total purge volume in standard liters per minute. The flow meter is connected to a Brailsford & Company single-head portable pump that produces a flow rate of 4 to 5 L/min. Exhaust from the pump is routed through a Geotech MultiRAE portable screening instrument that measures CH_4 , O_2 , VOC, and CO_2 . The MultiRAE is the final piece of the sample train, and exhaust from this instrument is allowed to vent to the atmosphere.

After the sampling train is assembled, the isolation valves are opened (SUMMA is closed at this point), and the sample port is purged for 10 min at a flow rate of 4 to 5 L/min. At the beginning of purge, the ambient surface air concentrations of CH_4 , O_2 , VOC, and CO_2 are recorded on a purge form. After 10 min, CH_4 , O_2 , VOC, and CO_2 readings are taken and recorded every minute for 3 min. If readings are stable and within 10% of one another, the pump is turned off and the isolation valves are closed. Next, the valve on the SUMMA canister is opened and the vacuum pressure is checked to ensure the SUMMA canister is at the required initial vacuum. The isolation valve on the sample port side of the sampling train is then opened to allow subsurface gas to flow into the SUMMA canister. Once the pressure gauge equilibrates back from the lower SUMMA suction pressure to ambient pressure, the SUMMA valve is closed. The time of the sample collection is recorded in the log book, on the purge form, on the chain of custody, and on the identification tag of the sample. At the completion of each sampling day, the SUMMA samples were taken to the Laboratory's Sample Management Office for shipment to the analytical laboratory.

In some cases, sample ports were determined to be either fully blocked or partially blocked. In an effort to ensure data quality, ports that were either fully or partially blocked on two consecutive sampling events were assumed to be adversely impacted and were subsequently removed from the sampling plan.

2.2.4 Subsurface Pore-Gas Sampling at Borehole 54-24399

Borehole 54-24399 is the deepest borehole at MDA L with an open interval in the Cerros del Rio basalts. A dedicated packer system and sampling line are used to collect samples at borehole 54-24399. In the past, a drill rig was used for lowering and raising a single and double packer system into the borehole. Because of issues with packer destruction on sharp basalt, the Laboratory installed a permanent packer in August 2016 (Figure 2.2-2).

The permanent packer was placed with its bottom at 566.7 ft bgs within the casing of the wellbore. To sample borehole 54-24399, the packer is inflated with pure nitrogen (99.99%) from a surface port to the desired inflation pressure according to the manufacturer's specification. The sample train is then connected to one of the two ports on the surface completion (Figure 2.2-3). The packer has two sample ports, one pulling air from 566.7 ft bgs and one pulling air from 587.8 ft bgs. The port labeled "Sample" is open to 587.8 ft bgs while the port labeled "Tracer" is open to 566.7 ft bgs (Figure 2.2-3). There is also an OMEGA PX429-015AI-EH extra-high-accuracy 0–15 psi ($\pm 0.05\%$) pressure transducer mounted on the top of the packer that is open to a feed-through port to monitor pressure immediately below the packer at 566.7 ft bgs (Figure 2.2-4). This transducer is connected to the surface through a grey wire shown in Figure 2.2-3 and is connected to a data logger and records 6-min averages of pressure. The pressure transducer was used to demonstrate the close coupling between the atmosphere and the subsurface pressure within the basalt. A schematic of the packer completion is shown in Figure 2.2-5 and includes rock types as seen in the video log (August 2015) of borehole 54-24399 (Appendix D, on DVD included with this document). The depth to the bottom of the casing was revised from 568 ft to 566.7 ft bgs after review of the video log and original drilling log (LANL 2005, 092591).

2.3 Gas Sampling Schedule

2.3.1 Effluent Sampling from SVE Units

Gas samples were collected in SUMMA canisters from the two SVE systems effluent sample ports (SP1) according to the following schedule:

1. Day 1 and Day 2 of operation: Four samples were collected each day.
2. Next 3 wk: One sample was collected each day (closure of the Laboratory prevented collection of one daily sample during this period).
3. Next 9 to 11 wk: One sample was collected weekly (generally on Wednesday of each week).
4. Beginning April 15, 2015, for SVE-West and May 6, 2015, for SVE-East: One sample was collected monthly on the first Wednesday of each month.
5. Monthly sampling of the SVE system effluent continued until the SVE units were shut down in November 2015.
6. Short duration, 2-d rebound sampling (SVE-West April, June, August 2016; SVE-East April, June, November 2016) included a minimum of five SUMMA samples collected for each test.
7. The 25-d rebound test on SVE-East, June 5–29 2017, collected 14 SUMMA samples with higher frequency in the first 4 d.

2.3.2 Subsurface Pore-Gas Data

Baseline subsurface samples were collected from pore-gas sampling ports in 28 boreholes from late August to early October 2014. Annual sample collection at these 28 boreholes was repeated in February 2016 and February 2017. In addition, 8 quarters of subsurface samples from 14 boreholes located within a 150-ft radius of the SVE wells were collected in April 2015, July 2015, November 2015, May 2016, August 2016, November 2016, May 2017, and August 2017. Analytical results are included in Appendix B. Blockages and radiological screening results prevented sampling at some ports during annual and quarterly sampling. Tables 2.2-2 and 2.2-3 show the ports from wells sampled during each round, and notes are included to indicate why certain samples could not be collected. If a port failed because of blockage or partial blockage for two quarters in a row, the port was removed from the sampling plan.

2.4 Summary of SVE System Operations

The SVE-West system operated from January 9, 2015, to November 18, 2015, at an average flow rate of 99.3 scfm. During this period, the system was operational 99.0% of the available time. The system shut down five times: on January 24, 2015, because of a sitewide power failure; on February 23, 2015, because of ice buildup in the water knock-out tank; and on August 8, October 21, and October 22, 2015, when lightning caused power outages in the area. The SVE-West system was also shut down for very short periods for maintenance.

The SVE-East system operated from January 26, 2015, to November 18, 2015, at an average flow rate of 97.5 scfm. During this period, the system was operational 99.0% of the available time. The system shut down four times: on February 23, 2015, because of ice buildup in the water knock-out tank; and on August 8, October 21, and October 22, 2015, when lightning caused power outages in the area. The SVE-East system was also shut down for very short periods for maintenance.

Water has condensed in the knock-out tank of both systems during periods of cold weather. Generally, water vapor in extracted pore gas condenses and is captured in the knock-out tank when the ambient air temperature drops below freezing for an extended period of time. More water was generated in the SVE-West unit probably because it is shaded in winter and does not warm from exposure to the sun. Approximately 200 gal. of condensed water was generated through November 2015 from the operation of both SVE units. The condensed water was characterized as nonradioactive and nonhazardous and was disposed of at the Laboratory's Sanitary Wastewater System Consolidation treatment facility.

3.0 SUMMARY OF SUBSURFACE PORE-GAS BASELINE RESULTS

Baseline pore-gas samples were collected in August and September 2014 from 185 individual gas sampling ports in 28 boreholes within and surrounding MDA L. These data were used to estimate the total plume mass of two primary constituents: 1,1,1-TCA and TCE. These constituents were selected because they have historically constituted more than 60% of the estimated plume mass (Stauffer et al. 2005, 090537; Stauffer et al. 2007, 097871; LANL 2011, 205756; Stauffer et al. 2011, 255584). The mass of 1,1,1-TCA and TCE was calculated using 3-D data-interpolation techniques described more fully by Weston Solutions, Inc. (Weston 2015, 600886). Assumptions in this technique include fixed subsurface water saturation within each geological unit, fixed Henry's Law partitioning into subsurface pore water, fixed sorption parameters, and a small component (0.05%) of organic carbon within the subsurface. Given these assumptions, the baseline 1,1,1-TCA plume mass in September 2014 was estimated to be 740 kg (1628 lb), while the TCE plume mass was estimated to be 343 kg (755 lb).

4.0 SUMMARY OF SVE RESULTS

4.1 Effluent Mass Removal

From January 9, 2015, to November 18, 2015, the combined VOC mass removal from the two SVE units is calculated to be 553 kg (1217 lb). Figure 4.1-1 shows the cumulative VOC mass removal versus time for both SVE units as well as the cumulative volume of pore gas pumped from the subsurface by both SVE units. The slopes of both the mass removal and volume pumped curves changed when the SVE-East unit became active on January 26, 2015.

Figure 4.1-2 shows the rate of mass removal for the combined extraction from both SVE units in pounds per week. The activation of SVE-East on January 26, 2015, resulted in an increase in mass removal from 35 lb/wk to nearly 60 lb/wk. The mass-removal rate then decreased over time to 23 lb/wk in July 2015. By

November 2015, the rate decreased to about 17 lb/wk. The long tail in the mass removal curve shows the SVE systems continue to be effective after 10 mo of operation.

Table 4.1-1 lists the mass removed for each detected organic compound during SVE operations. Out of 62 analytes measured using the TO-15 panel, only 24 have reported detections in the SVE effluent. Of the total 1217 lb removed, 1,1,1-TCA was the highest constituent at over 44% (541 lb); TCE composed 21% of the mass extracted (259 lb); Freon-113 (1,1,2-trichloro-1,2,2-trifluoroethane) was third at 10% (117 lb); and PCE was the fourth most prevalent component in the effluent at 9% (110 lb). Other compounds with significant mass removal include 1,2-DCA (46 lb); 1,1-DCE (34 lb); 1,2-DCP (29 lb); and chloroform (24 lb). Together these constituents composed 95% of the total extracted mass.

Tables 4.1-2 and 4.1-3 list the flow rates for SVE-West and SVE-East, respectively. These flow rates were calculated using observed wellhead pressures and orifice plate pressure differentials as described in section 2.1. Flow rate data for SVE-West and SVE-East are included in Appendix E (on CD included with this document).

4.2 Concentrations in the SVE Effluent

Concentration reductions in the effluent from the two SVE units are presented in Figure 4.2-1. The five analytes with the greatest mass removal (TCA, TCE, PCE, 1,2-DCA, and Freon-113) were selected to illustrate the decreases in concentrations in the effluent with time. Effluent concentrations from both systems decrease with time for all analytes, with larger decreases in concentrations seen for SVE-West. On both east and west sides of the site, PCE concentrations are reduced by smaller fractions of their initial values than are other constituents, possibly related to stronger liquid partitioning for PCE. The larger reduction in all concentrations on the west side of MDA L is likely because the SVE-West system is located closer to the western source region than is the SVE-East system to the eastern source region (Figure 1.1-1).

Figure 4.2-2 shows how the molar ratios of these compounds evolved during the 10 mo of continuous SVE operation and during rebound tests through June 2017. Molar ratio is defined as the number of moles of a given compound divided by the total number of moles of organics measured in the TO-15 suite. Because ppbv is a measure of molar volumetric concentration (volume fraction per total volume) and volume is directly proportional to the number of moles, molar ratio is derived by dividing the ppbv of a given analyte by the sum of all measured analytes in ppbv at a given port (see Appendix B for the lists of analytes found at each port). Initially, for SVE-West, TCE decreased rapidly as a mole fraction of the plume while PCE increased. Beginning around August 2015, TCE reached a steady percentage while TCA began to drop with a further increase of PCE molar fraction. For SVE-East, small changes occurred in the percentages of the major constituents, with TCA decreasing and TCE; 1,2-DCA; and PCE increasing while Freon-113 appeared to maintain a relatively constant mole fraction.

4.3 Subsurface Plume Changes Relative to Baseline 2014

Plate 1 presents color bars for the main constituents at each of the 2015 quarterly sampling locations compared with baseline 2014 data at a range of depths. The sum of each color segment is the total ppmv of a given sample. Most of the concentration plots have the same maximum scale (600 ppmv), allowing for comparison of relative plume concentrations. The maximum scale for boreholes 54-02089 and 54-24238 is 1200 ppmv because of the increases in concentrations observed in July and November 2015. On the east side of the site, boreholes 54-02002, 54-24243, and 54-24241 show large decreases in measured total organics as a result of SVE operations. On the west side, boreholes 54-24240, 54-27641, and 54-02001 show the strongest decreases in concentration from SVE operations. Boreholes 54-02089 and 54-24238, located in the eastern source region, both show increases in concentrations. Two logical hypotheses for

the increases at these boreholes are (1) increased leakage from containers in the source region near these two boreholes and (2) migration of existing higher vapor concentrations from north of these two boreholes toward the SVE-East well. Further analysis will be required to differentiate between these two hypotheses, and continued monitoring in borehole 54-24238 is recommended.

Figure 4.3-1 plots individual concentrations for seven analytes from each port in the boreholes around SVE-East and SVE-West that were sampled for both the baseline 2014 and the November 2015 events (553 points in total). Data in this plot are for 1,1,1-TCA; TCE; PCE; 1,2-DCA; 1,1-DCE; 1,2-DCP; and methylene chloride. Dashed black lines above and below the red 1:1 line show typical $\pm 30\%$ uncertainty in reproducibility of subsurface gas concentration measurements. Baseline 2014 concentrations are plotted on the horizontal axis and November 2015 concentrations are plotted on the vertical axis. Figure 4.3-1 shows the decreasing trend in concentrations that occurred during the first 10 mo of SVE operation. If the SVE system had no impact on subsurface concentrations, the data would plot on or close to the 1:1 line shown in red in the figure. However, most of the points fall below the 1:1 line, indicating the SVE system has reduced the concentrations at the majority of sample ports below their baseline values. Points are colored by borehole, indicating the boreholes that are the most impacted. In this figure, several points from boreholes 54-02089 (purple triangles) and 54-24238 (green circles) are labeled to highlight increasing concentration during the SVE IM.

Figure 4.3-2 shows how concentrations of the same seven analytes described in the previous paragraph responded over three quarters of sampling. The green points from April 2015 have slightly more scatter around the 1:1 line, while July 2015 and November 2015 both show the majority of the measurements to be well below the 2014 baseline sampling concentrations. Shown in the figure are the increases in concentration of several VOCs in borehole 54-24238 during 2015.

4.3.1 Weston Data Interpolations

Figures 4.3-3 and 4.3-4 show images of the 1,1,1-TCA plume generated by data interpolation for the baseline 2014 and April 2015 data, respectively (Weston 2015, 600887). Data are shown with dots, while the interpolation is shown on a contoured color scale with both color contour lines and contour shading. The contour intervals are based on multiples of Tier I screening values used in the CME report (LANL 2011, 205756). Tier I screening uses only Henry's Law partitioning to determine if a given vapor concentration exceeds groundwater standards, assuming the vapor is in contact with groundwater (Table 4.3-1). The post-SVE image (Figure 4.3-4) shows a decrease in both the spatial extent of most individual concentration contours and the magnitude of concentrations of the 1,1,1-TCA plume.

Figures 4.3-5 and 4.3-6 show similar information for TCE (Weston 2015, 600887). Again, the extent of a given contour is reduced, and for TCE, maximum concentration contours are absent in the interpolated data set for April 2015. For example, the highest concentration of TCE in Figure 4.3-5 on the west side of the site is well into the 250 times (red) color shading, while in April 2015 (Figure 4.3-6) the maximum concentration contour shading is reduced to 100 times (orange) the Tier I screening value.

Using the interpolated data set, a comparison of April 2015 mass estimates with those of the baseline 2014 estimates suggests substantial ($\sim 30\%$) SVE-induced mass reductions in both the 1,1,1-TCA and TCE plumes over the first 3 to 4 mo of SVE operations.

4.3.2 Effectiveness of SVE at Selected Monitoring Wells

In Figures 4.3-7 through 4.3-14, data from a subset of 8 monitoring wells are presented showing concentration versus depth for 1,2-DCA; TCE; PCE; and 1,1,1-TCA for each of the 10 quarters after the start of SVE operation compared with baseline 2014 data. In all of the depth-dependent plots, baseline 2014 data are shown in light blue. The three 2015 data sets show concentration changes during the active SVE phase; the six data sets from 2016 and 2017 show concentration changes during the rebound phase.

4.3.2.1 SVE-West

Figures 4.3-7 and 4.3-8 show concentration data from boreholes 54-27641 and 54-24240, respectively, both within a 30-ft radius of SVE-West. These boreholes show large concentration reductions within 110 ft bgs, and mass removal appears to be especially effective in the top 80 ft bgs in borehole 54-24240, where concentration had dropped several orders of magnitude by November 2015, just before the SVE units were turned off. This region may be impacted by flow of fresh air from the atmospheric boundary being pulled toward the low-pressure region created by the SVE system. The effectiveness of the SVE is observed to decrease with depth in borehole 54-27641, especially at depths below 150 ft. The data from April 2015 show an anomalous increase in concentration at the 340-ft depth; however, this anomaly is not observed in the subsequent quarters of data, where concentrations return to values measured in the pre-SVE baseline sampling. Observed rebound in these two wells is strongest in monitoring borehole 54-24240, implying that continued vapor-phase releases from buried drums are localized closer to this well than to borehole 54-27641, where observed rebound was lower. In both cases, rebound in the upper 60 ft is noticeably higher, coincident with the depth of the waste shafts. Note that both concentration reduction and rebound of PCE is nearly constant with depth. This trend may be related to the lower vapor pressure of PCE and increased pore-water storage of this chemical.

Figure 4.3-9 shows concentration data from borehole 54-02022, located more than 150 ft from SVE-West. This monitoring well shows concentration decreases to a depth of 200 ft. Data from April 2015 are again anomalous, showing concentration increases above the pre-SVE baseline at depths below 150 ft; however, both the July 2015 and November 2015 sampling rounds show decreases in all four analytes at all depths. The strong decreases of both TCA and TCE at 200 ft bgs suggest the radius of influence (ROI) for the SVE-West extraction well may be greater than 150 ft. Rebound in this well was fairly minimal, which is expected given its distance from the source region. In this well, PCE does not recover as dramatically as in borehole 54-24240; however, suction at the larger radius to borehole 54-02022 was much lower during SVE, and pre-SVE concentrations were also lower in borehole 54-02022.

4.3.2.2 SVE-East

Figures 4.3-10 and 4.3-11 show data for boreholes 54-24243 and 54-24241, located 54 ft and 83 ft radially from SVE-East, respectively. Both show strong impacts from SVE, with concentration decreases by factors of between 1/3 to 1/100 in many ports. Both of these boreholes show strong SVE impacts to total depth. Rebound from the minimum measured concentrations for the four VOCs presented is significant at all depths, with some shallower values rising toward pre-SVE conditions, with PCE concentrations in borehole 54-24241 rebounding the most of the constituents. One anomaly in the data is for 1,2-DCA in borehole 54-24241, where concentrations have risen nearly 4 times the pre-SVE values at ports above 100 ft bgs. A possible explanation for this increase would be leakage from a container with a relatively higher ratio of 1,2-DCA, as the other constituents in these shallow ports do not show similar increases in concentration above pre-SVE values. Note that 1,2-DCA concentrations below 100 ft bgs show little change over the course of the IM.

Borehole 54-27642 is located about 130 radial ft from SVE-East and shows reductions in concentration with greater efficiency at shallow depths (Figure 4.3-12). Borehole 54-27642 is located near the edge of the paved portion of the site and shows appreciable reductions in concentration to 175 ft bgs, with less impact observed at greater depths. The large reductions in concentration in this borehole also suggest that the 150-ft ROI may be conservative with respect to design of a corrective measures SVE system as discussed in the CME report (LANL 2011, 205756). Rebound in this well is significant, with TCE and PCE both rebounding to near pre-SVE values by August 2017. DCA[1,2] at 120 and 340 ft bgs increases above the pre-SVE concentrations, although not dramatically. TCA[1,1,1] rebounds to pre-SVE concentrations at the deepest port (340 ft), while near-surface rebound is less pronounced.

Boreholes 54-02089 and 54-24238 are approximately 70 ft and 100 ft from the SVE-East extraction well and are fairly close to the eastern disposal shafts (Figure 1.1-1). Many of the ports in these wells show increased concentrations for all analytes, particularly at the deepest 89-ft ports (Figures 4.3-13 and 4.3-14). Only in the shallowest ports are concentrations reduced by SVE and only for certain analytes (TCA in both holes, and all four analytes shown in 54-02089). The data from borehole 54-24238 are very similar to what is predicted in simulations of increased leakage from the source region and could imply a recent increase in leakage from a buried container (drum) near this well. Another hypothesis for the increasing concentrations is that suction from the SVE unit could be pulling higher existing vapor concentrations located to the north in a region with no monitoring boreholes toward the eastern SVE well. Continued monitoring at this location should be undertaken to ensure that the observed concentration increase is not a significant release that is just arriving at this location.

4.3.2.3 Gradient Reversals

In section 3.3.1 of the IMWP (LANL 2014, 261843), it was hypothesized that

[with] maximum concentrations lower in the source regions, vapor transport will reverse direction, and VOCs will diffuse from deeper in the plume back toward the surface. This reversal of the diffusion gradient would limit deeper migration into the underlying basalt and potentially toward groundwater.

Borehole 54-27641 clearly demonstrates such a reversal in concentration gradient. Figure 4.3-7 shows that before SVE operations, concentrations were highest near the surface with lower concentrations at depth, a situation that would move mass to depth from high to low concentrations via diffusion. Thus, in Figure 4.3-7 for the 2014 baseline curve, 1,1,1-TCA mass at 150 ft bgs would diffuse downward along the concentration gradient. However, this trend has been reversed by the impacts of the SVE system. At the end of the active SVE operation in November 2015, when the primary mass transport mechanism switches from advection back to diffusion, the concentration gradient (from high to low concentration) at 150 ft bgs has reversed to an upward direction, meaning that diffusion will transport mass at 150 ft bgs following the concentration gradient toward the surface and will aid in remediation. Similar gradient reversals have been observed in borehole 54-24240 at 100 ft bgs and in borehole 54-24243 at 80 ft bgs. However, reversal of the concentration gradient is not ubiquitous, and boreholes 54-27642, 54-02022, and 54-24241 show concentration reductions at all depths without reversals of their concentration gradients over the 10-mo SVE IM.

4.4 Monitoring Well 54-24399

The deepest monitoring well at MDA L, 54-24399, installed in 2005, lies near the center of MDA L and is cased from the surface to a depth of approximately 567 ft bgs. The original plan to collect data from a 1-ft interval at the top of the uncased section (568–569 ft bgs) using a dual-packer system was abandoned after the July 2015 sampling event when the lower packer was damaged during sampling after it came in

contact with vesicular basalt. Logbooks from this sampling event conclude that the sample taken was valid. Video logs of the open hole show a short section of massive basalt near the top of the uncased section followed by vesicular basalt, some having large voids and very sharp rock formations (Appendix D). Note that the depths indicated in the video are inaccurate because of cable stretch.

Because of the risk of damage to packers from sampling the borehole below the casing, sampling with the dual-packer system was removed from the sampling plan and a permanent single packer was installed in August 2016 (Figure 2.2-2). The new permanent packer has several benefits including (1) a simpler sampling process needing no drill rig, (2) a substantial reduction in borehole breathing due to new construction of the well head (Figure 2.2-3), and (3) the ability to maintain longer periods of packer inflation to ensure isolation of the deep basalt.

TCA[1,1,1] data collected from May 2005 through August 2017 at borehole 54-24399 are shown in Figure 4.4-1. Concentrations were measured using a variety of sampling techniques, including a dual packer that isolated a 1-ft interval near the bottom of the casing; a single packer lowered from a drill rig and set at the base of the casing; and the latest permanent packer, which has been used since August 2016. The horizontal line in the figure is the Tier I screening level for this compound calculated as simple equilibrium partitioning from the gas phase into hypothetical drinking water; the vertical line is the date of the installation of the permanent packer. Data show a high degree of variability through time, with TCA values spanning a range from a low of 13 ppbv to a high of 4800 ppbv on November 14, 2016. Typically, values from the open section of borehole before installation of the permanent packer were often much lower than those collected using a double packer to isolate a 1-ft section near the base of the casing. After installation of the permanent packer, values from two ports in the open hole show a similar pattern, with higher concentrations at the port near the base of the casing than those measured 21 ft deeper.

Data for other VOCs are shown in Figures 4.4-2 through 4.4-5 and closely follow the same trends as 1,1,1-TCA. The concentrations of TCE; PCE; 1,2-DCA; and methylene chloride all exceed Tier I screening levels, especially in samples taken following the installation of the permanent packer. It is likely that the previous open borehole arrangement allowed significant breathing in borehole 54-24399, reducing concentrations through passive venting. The new completion on this well has reduced breathing to nearly zero with an O-ring pulled tightly onto the top of the wellhead by the weight of 587 ft of 1-in. galvanized pipe. The new configuration allows more representative samples to be collected from this well. However, the variability in the data are not expected given the measured barometric pumping within the basalt, which should rapidly homogenize concentrations. This observation may point to annular flow outside the casing from the base of the Bandelier Tuff to the bottom of the casing. Such flow could occur if the borehole 54-24399 completion did not seal the formation from the open hole in which the casing was installed. Because of the large voids in the basalt, it is unlikely that the hole was sealed between the formation and the casing, potentially creating a short circuit from the base of the Bandelier Tuff to the 566.7-ft monitoring point. This scenario would also help explain the higher readings seen in the vicinity of the bottom of the casing compared with measurements from 21 ft below the casing in the open hole from the same sampling date (Figure 4.4-2 through 4.4-5).

Two other boreholes at this site are completed in the basalt and provide a limited but important data set to compare with the behavior of 54-24399. Boreholes 54-01015 and 54-01016 angle under the site from the north and approach 54-24399 to within 243 and 95 lateral feet, although ports in each do not reach the total depth of the bottom of the casing in 54-24399. Data from borehole 54-01015 show an increase in 1,1,1-TCA concentration since the installation of the permanent packer (Figure 4.4-6). Data from borehole 54-01016 do not show an increase and concentrations are below 200 ppbv in all samples.

Figure 4.4-7 shows 1,1,1-TCA data collected during a sulfur hexafluoride tracer test performed in borehole 54-24399 in April 2017 (LANL 2017, 602792). These data were collected over 12 d, during which the permanent packer was continuously inflated. Data from this experiment were collected using a LumaSense Photoacoustic Gas Monitor model number 1412i and provide 1-m time resolution measurements.

Deep samples show concentrations of CO₂ (>1000 ppmv) well above atmospheric (400 ppmv) and are diagnostic of sample quality, e.g., microbial respiration at depth producing CO₂ should be relatively constant implying that CO₂ concentrations <1000 ppm are symptomatic of unintentionally diluted samples. Included in Figure 4.4-7 is the subsurface pressure signal beneath the packer during the experiment. These data show 1,1,1-TCA concentrations varying by nearly 2 orders of magnitude, closely tied to changes in subsurface pressure. Conclusions of the tracer study support Neeper (2002, 098639), who hypothesized that observed large variations in pressure in the deep basalt beneath MDA L will drive significant advective flow. The conceptual model for transport in the deep basalt continues to evolve in light of the recent tracer test data from borehole 54-24399.

Borehole 54-24399 was an open conduit for 11 years (2005–2016) before installation of the permanent packer in August 2016, having a well cap that allowed significant airflow. During this time, strong flows of air out of the borehole were regularly observed, and the borehole was visited as part of tours to the site to show passive vapor extraction in action. However, airflow regularly reversed direction, pulling surface air into the deep borehole. MDA L is a staging area for transport of waste and thus often has trucks idling for hours at a time. Additionally, for installation of temporary packer systems before August 2016, a running drill rig would be parked at the open hole for each sampling event. Exhaust from these vehicles may have been pulled into the deep borehole and could have added a component of vehicle exhaust (benzene, ethylbenzene, toluene, and xylenes [BTEX]) to deep samples. In an attempt to determine if 11 years of barometrically induced breathing in borehole 54-24399 caused measurable changes in the chemical composition, the ratio of 1,1,1-TCA to toluene from boreholes 54-24399 and 54-24241 were compared (Figure 4.4-8). The deep samples do show a shift to lower 1,1,1-TCA/toluene values and may support the hypothesis that exhaust has impacted the deep basalt. However, installation of the new packer has greatly reduced barometric breathing to the surface through borehole 54-24399, and the exhaust signature is expected to dissipate over time.

4.5 Differential Pressure Measurements

Subsurface differential pressure measurements were made at pore-gas sampling ports in boreholes sampled during SVE operations. Measurements were made during the baseline sampling in August and September 2014, in April 2015, in July 2015, and in November 2015. For these measurements, one input on a digital manometer is connected to a subsurface gas sampling port, while the other input is left open to the atmosphere. The manometer then records the difference in pressure between the subsurface port and the atmosphere. Table 4.3-2 shows the results of the pressure measurements for 189 ports in the 28 boreholes for the baseline and a subset of these for the three quarterly sampling events (April 2015, July 2015, and November 2015) that occurred during SVE operations.

To evaluate these data, it is helpful to first review measurements made at MDA L in the 1990s. Neeper (2002, 098639) presents atmospheric and differential subsurface pressure data from boreholes near MDA L. These data show that the atmosphere can change pressure by more than 1.5 kPa over the span of a few days (Neeper 2002, 098639, Figure 3). Subsurface pressure changes in response to atmospheric pressure; however, pressure changes in the subsurface are shifted in time and reduced in amplitude, based on the formation's connection to the atmosphere at a particular depth. The amplitude of subsurface pressures within the Bandelier Tuff decreases, and maximum deviations from average pressure are shifted to later times with increasing depth. Neeper (2002, 098639) presents data collected

from a borehole located 100 m (328 ft) to the east of the site that show almost no pressure difference between the atmosphere and a port at the depth of 11 m (36 ft). However, at depths of 77 m and 103 m (250 ft and 338 ft), the amplitude of the pressure wave is depressed, and the phase is shifted such that maximum differential pressure between atmospheric pressure and downhole pressure varies between +0.6 kPa and -0.6 kPa, with the maximum downhole deviation from average pressure occurring up to 0.33 d after the maximum atmospheric deviation.

Given the variability expected in subsurface differential pressure, it is difficult to attribute many of the measured values presented in Table 4.3-2 to the SVE systems. However, some ports at boreholes 54-24240, 54-24241, and 54-27641 show strong signals that are likely impacted by the SVE suction. Additionally, some of the shallower pressure measurements should be less impacted by shifts in magnitude and phase, allowing smaller pressure differences to be attributed to the suction from the SVE units. Further analysis using daily pressure variations at the time of the sampling could allow more refined estimates of the extent of pressure propagation from the SVE units and may reduce unexpected variability observed in data collected between April 2015 and February 2016. Such analysis requires the use of layered permeability models to separate out the effects of natural-phase shift and amplitude reduction from those caused by the SVE systems at individual ports.

4.6 Rebound Data

To more fully evaluate SVE strategies for MDA L, the Laboratory collected and analyzed data related to plume rebound following shutdown of the SVE units in November 2015. Rebound sampling is important to the development of a long-term strategy for using SVE as a vapor-plume control at MDA L. Rebound sampling also helps determine whether, and to what degree, ongoing VOC releases from the shafts are occurring. This is because very little VOC mass is adsorbed to the tuff or dissolved into pore water and therefore must be coming from the source in the shafts. Thus, repartitioning of previously released mass is unlikely to result in significant rebound. Large rebound would more likely be indicative of ongoing release from source.

For the rebound analysis, there are two types of plume rebound data collected. First, quarterly and annual monitoring data from the surrounding boreholes can be used to see if subsurface concentrations are rebounding because of continued leakage in the source area. Second, rebound concentrations from the exhaust from the SVE units can guide development of restart intervals for long-term planning.

Quarterly and annual monitoring data for boreholes surrounding the SVE boreholes are a vital part of the rebound analysis and have been collected through August 2017. However, because the SVE systems pull vapor from a large volume of the subsurface, the rebound characteristics of the SVE restarts provide data to complement point measurements of rebound gathered in the quarterly and annual subsurface vapor sampling.

For the rebound testing, the Laboratory restarted the SVE units for 2-d periods to allow integrated rebound assessment. These brief restarts were done in April, June, and September 2016. Because of an electrical issue with the SVE-East unit, rebound sampling in September 2016 was delayed until late November 2016. Based on continued higher concentrations in the SVE-East rebound samples, a single 25-d rebound test in June 2017 was performed. Concentration data (1,1,1-TCA) from the rebound tests are shown relative to the concentrations measured during active SVE in Figures 4.6-1 and 4.6-2. TCA rebound on the west side of MDA L is not as significant as on the east side. During the rebound sampling it was estimated that 5–8 lb were extracted for each 2-d test, while the 25-d test resulted in nearly 80 additional pounds of VOC removed from SVE-East. Thus, the total rebound mass removal is on the order of 110–130 lb. Rebound molar concentration ratios appear to return partway toward those seen at the beginning of the SVE IM (Figure 4.2-2).

The impact of the 10 mo of SVE operation in 2015 on the subsurface plume can be seen by plotting baseline concentrations in 2014 versus concentrations in 2017 (Figure 4.6-3). The bulk of the data show that the plume in 2017 remains below measured baseline conditions. Concentrations have increased for monitoring wells 54-24238 and 54-02089. The increase is especially pronounced for 1,1,1-TCA and methylene chloride. Increases in these two compounds may suggest a leak from buried source containers (drums) near boreholes 54-24238 and 54-02089 or alternatively, migration of higher concentrations from the north towards the SVE-West borehole.

5.0 NUMERICAL ANALYSIS

This sections contains a brief review of previous modeling work in support of decision analysis undertaken at MDA L, followed by a description of the generation of an initial pre-SVE simulated plume corresponding to the period just before the IM was initiated in January 2015. Simulation results generated in December 2014 are presented for predicted plume behavior and are then compared with those results obtained during the SVE IM. Differences between predicted and observed behavior are discussed with emphasis on how these differences impact previous recommendations for long-term corrective measures.

5.1 MDA L Vapor Plume Modeling Review

A 3-D numerical model of the VOC vapor plume in the subsurface at MDA L was developed using a site-scale numerical model. The porous flow simulator Finite Element Heat and Mass Transfer (FEHM) is used for all calculations (Zyvoloski et al. 1997, 070147). The numerical simulations account for diffusion, advection, partitioning between liquid and vapor, variable saturation and porosity, an atmospheric boundary, four discrete source release locations, an asphalt cover, and topography. Figure 5.1-1 shows the numerical 3-D model domain and the site boundary of MDA L. The numerical domain contains more than 140,000 finite-volume elements with a lateral spacing of 25 ft. The domain extends from the topographic surface to the water table and contains two high-resolution regions around the SVE boreholes.

The site-scale numerical model has evolved over many years (1999–2017) and has been used to evaluate the nature and extent of the subsurface plume at MDA L associated with waste disposal. As a surrogate for the entire plume, the contaminant with the highest subsurface concentrations (1,1,1-TCA) was selected to reduce the complexity of the simulations. The numerical model includes a 2006 SVE pilot test of less than 1-mo duration that was used to calibrate permeability at MDA L by matching flow rate versus pressure drop simultaneously with concentrations in the exhaust gas (Vrugt et al. 2008, 104951). The calibrated model parameters were then used to initiate model validation that started from the pre-SVE test in 2006 and was used to predict plume concentrations in the year 2010. Results from this effort yielded a data/model correlation coefficient (r^2) for over 150 data model pairs of greater than 90%. The ability of the model to align with data after 4 yr that include two active SVE demonstration tests provided confidence that the model captures the dominant physical transport processes at this site. The validated numerical model was next used to explore scenarios related to the possible role of SVE as a corrective measure at MDA L (LANL 2011, 205756; Stauffer et al. 2011, 255584). Previous analysis showed that SVE has the potential to effectively remove significant quantities of VOCs from the subsurface (Stauffer et al. 2007, 104950; Stauffer et al. 2007, 097871). Suggestions regarding sampling frequency and location were made based on these results to allow for rapid detection of any sudden changes in the plume (Stauffer et al. 2007, 097871). Estimates of the ROIs of the SVE pilot test wells (~37 m [120 ft]) were given and a suggested SVE system for long-term plume control was presented (LANL 2011, 205756). To judge the quality of the model throughout the modeling process, spatially dependent 1,1,1-TCA concentration data from the site and the predicted (modeled) concentrations are compared through linear regression.

5.2 November 2014 Base Simulation

The last model update, before the current SVE interim measure, was performed in 2011 for the MDA L corrective measures evaluation (CME) (LANL 2011, 205756). To generate an updated model that represents the subsurface TCA plume, the output of the 2011 CME model, which correlated well with the 2011 plume data, was used as the starting point. The two source regions were then assumed to leak with fixed concentrations until 2014 (Figure 5.1-1). During the fixed leakage simulations, diffusion is assumed to be the only process moving mass in the subsurface. Figure 5.2-1 shows predicted concentrations for three simulations with fixed leakage from 2011–2014; the simulations assume three different fixed source concentrations (500 ppmv, 300 ppmv, or 200 ppmv) with both the eastern and western source regions leaking with the same concentrations for a particular simulation. When the two source regions are fixed at 500 ppmv, the model generates concentrations that are higher than the data. The simulations with 200 ppmv and 300 ppmv are quite similar; however, using a least squares regression between model and data, a fixed concentration of 300 ppmv in the source regions leads to the best match between the model and data from the set of 100–1000 ppmv, run in discrete leakage steps of 100 ppmv. Also included in Figure 5.2-1 are the +30% data reproducibility bounds on either side of the model = data line. Simulated results on a plane 60 ft below the ground surface are shown in Figure 5.2-2 where the two source regions are visible with higher concentrations.

5.3 Predicted Plume Behavior Compared with Measured SVE Response

Predictions for the first 10 mo of SVE operations were used to inform the project and NMED on expected VOC mass removal rates. Estimates were on the order of less than 2000 lb of VOC production during the SVE IM. After 10 mo of SVE IM data were collected, predicted effluent concentrations from both SVE-West and SVE-East were compared with the effluent data. The effluent predictions were calculated in December 2014 before the SVE system was started in January 2015, with pumping assumed to run continuously on both east and west units for a full year. The SVE-West predictions of effluent concentration based on the previously calibrated permeabilities and assumption of 300 ppmv constant source concentration are similar to the effluent data (Figure 5.3-1). However, SVE-East effluent predictions, shown in Figure 5.3-2, are consistently higher than the measured data. The less accurate model for the SVE-East side of MDA L may be related to two unexplained differences that have been observed. First, unexplained increases in concentrations at ports in boreholes 54-02089 and 54-24243 push the data higher than the baseline. Second, the suction required at SVE-East to pull 100 scfm (25 kPa) during the 2015 IM is significantly higher than suction required in 2006 to pull the same gas flow rate (19 kPa). In addition to these unexplained issues, the initial state of the SVE pumping calculations may play a role in the data/model mismatch on the eastern side of MDA L.

To address the mismatch in the SVE-East prediction, a second calibration was performed. For this calibration, permeabilities were modified on the east side with the constraint that the suction of 25 kPa be maintained while pulling 100 scfm. Figure 5.3-3 shows the improved fit using the new calibration data. In the new calibration, the constant source was also lowered from 300 to 200 ppmv. The new calibration permeability field, suction, and flow rate were used for all remaining simulations in this report.

5.4 Predicted Plume Behavior Compared with Measured Monitoring Borehole Data

Simulated concentrations at subsurface monitoring locations are next compared with measured data. The locations of the monitoring boreholes used in the comparison are shown in Figure 5.1-1. On the west side of MDA L, borehole 54-27641 is located near the source region, and the simulation at this well is in good agreement with measured data. Figure 5.4-1 shows the evolution of 1,1,1-TCA concentrations in the subsurface, with values dropping over time to a minimum in February 2016, just after the active SVE period ended. At depths shallower than 100 ft bgs, concentrations in this borehole have rebounded to less

than 30% of their original values. Model predictions track fairly closely, especially in February 2016. One exception is the simulated rebound at 180 ft bgs in February and August 2017 that is not seen in the data.

Simulated concentrations in the subsurface on the east side of MDA L are less correlated with the data, especially at depths greater than 100 ft (Figure 5.4-2). Some disconnection between the model and data is expected, given that the starting concentrations in the simulations for borehole 54-24241 are approximately 50% higher than the measured 2014 data. Also, at borehole 54-24243, which is located approximately 50 ft east of the SVE-East unit, initial model concentrations are 50% lower than measured concentrations in the 2014 baseline sampling (Figure 5.4-3). One cause of the model/data differences is the location of the simulated source leakage, which is included in the simulations to provide enough continuous leakage to maintain measured concentrations through time. The distribution of these source locations has not been varied and is meant to capture the general plume behavior. Therefore, a 100% agreement between the model and data is not expected at all points around the plume.

5.5 Simulated Rebound

Simulations of plume rebound after the 10-mo period of active SVE are next presented. These simulations are run with a leak rate equal to the simulated leak rate on January 9, 2015, just before the SVE systems were turned on. Using the new calibration that achieved a better fit to effluent versus time, the fixed leak rate was based on a constant concentration in the source regions of 200 ppmv over the period of 2010 through January 9, 2015. These simulations use the newly calibrated geological unit permeabilities for the west side of the site. As seen in Figure 5.5-1, the simulations overestimate the rebound on the east side until June 2017 when simulated rebound falls quite close to measured rebound. On the west side, simulated rebound is quite close to measured values, until September 2016 when the simulated rebound is lower than the measured values (Figure 5.5-2). This could suggest an increase in leakage from the underground source over the period of June to September 2016. Borehole 54-24240 does show an increase in 1,1,1-TCA concentrations from May 2016 through August 2017, with concentrations at the shallowest port rising from less than 50 ppmv to over 150 ppmv during this period (Figure 4.3-8).

As a whole, the rebound data show that the site is not rebounding quickly to pre-SVE conditions. Over 18 mo after the active system was shut down in November of 2015, concentrations from the SVE-East unit have recovered to approximately half of the pre-SVE condition. This is not surprising considering the continued reduction in concentration seen in data from the surrounding boreholes (Figures 4.3-7 through 4.3-14). Given the 2006 SVE Pilot Test had a long-lasting impact on the VOC plume (LANL 2011, 205756), it is reasonable to expect that concentrations at many ports will remain lower than they were at the start of the 2015 SVE IM.

However, uncertainty remains on the mass of VOC still contained in the underground source, and data from MDA L clearly show that some ports are measuring continued slow leakage from buried source containers. This is especially evident in boreholes 54-24238 and 54-02089 where concentrations have risen above the September 2014 baseline, and in the case of TCA in borehole 54-24238, where concentrations have risen from 230 ppmv to 560 ppmv (Figure 4.3-14).

5.6 Simulated Sudden Failure of Buried Drums

To address the possibility that buried drums of waste pose the potential for sudden failure, an analysis was conducted using the latest calibrated numerical model to explore scenarios of drum failure, monitoring behavior, and post-failure SVE performance. For this analysis, between one and five drums (200 L per drum) of pure liquid 1,1,1-TCA are assumed to be released suddenly. The analysis further assumes that this mass of solvent (264 kg per drum) is spread at the maximum 1,1,1-TCA vapor pressure (160,000 ppmv at 20°C)

into a region of the model domain 40–80 ft bgs within the source region. A single source region on the east side was chosen to allow behavior at a range of distances to be characterized through the location of the release relative to existing monitoring boreholes (Figure 5.6-1). The release location and the boreholes chosen characterize the potential for observations and span the distances from any known location of solvent-containing drums (or containers) to an existing observation well (Table 5.6-1). This analysis should therefore provide predictions sufficient to develop a robust monitoring strategy for detecting sudden drum/container failure at MDA L. All simulations of sudden drum/container failure were initiated on June 30, 2017, following the final SVE-East rebound study.

5.6.1 Drum Failure in Absence of SVE

Next, simulation results are presented for cases where drum failure occurs with no subsequent SVE operation, and simulations are run for 10 yr to June 2027. First, the evolution of concentration in the closest monitoring borehole, 54-24238, for the case of a single 200-L drum of TCA failing is shown in Figure 5.6-2. Because this borehole is quite close to the drum failure, concentrations in the monitoring ports spike quickly to greater than 1000 ppmv (1E6 ppbv). Concentrations for the next closest monitoring borehole, 54-27642, are shown in Figure 5.6-3. In this borehole, maximum concentrations of nearly 5000 ppmv are seen in the upper 100 ft bgs within approximately 1 yr. At the furthest analyzed monitoring borehole from the release, 54-24241, concentrations increase an order of magnitude within 2 yr for ports above 100 ft bgs (Figure 5.6-4). Results for simulations with five drum failures are even more extreme and easily detected at the three example distances from the release.

Results showing the arrival at three distances resulting from one drum failing suggest that by using existing monitoring boreholes, a reasonable metric for detecting drum failure of VOC from the source area can be constructed. The distance from the release to borehole 54-24241 is the maximum distance explored and is greater than the distance from any potential release location to an existing borehole. The distance from borehole 54-27642 to the simulated sudden release is more representative of the maximum distance any leak would be from an existing borehole, and simulation results from this location suggest that a conservative metric for detection of such a release would be an increase in total VOC concentration to over 2000 ppmv within a period of 2 yr, with a trend of consistent increase with each consecutive measurement for ports to depths of 100 ft within an impacted borehole. Further, given that there are multiple monitoring boreholes immediately surrounding both the east and west shaft clusters, a logical path forward would be to assign this group of monitoring boreholes to be “sentry boreholes” and focus monitoring on these moving forward. Given the 1–2-yr time scale for a sudden release signal to arrive at the sentry boreholes, a logical interval for sampling these boreholes would be every 6 mo. Since no known source exists outside of the source locations, monitoring of peripheral boreholes could be reduced in frequency to create a sitewide plume measurement once every 2 yr.

5.6.2 Simulated SVE Remediation Following Sudden Drum Failure

In this section, results are presented that demonstrate the ability of the existing SVE-East borehole to remediate a sudden drum failure. For this simulation, a five-drum release is evaluated, with the failure happening on June 29, 2017. The saturated vapor pressure of 1,1,1-TCA is fixed in the failure region from 40 to 80 ft bgs for 166 d to generate vapor-phase mass equal to five 200-L drums. It is assumed that 3 yr are needed to notice the sudden release, stand up the remediation, and initiate SVE on June 29, 2020. SVE is allowed to run continuously for 7 yr to June 29, 2027, with a goal of remediating the sudden drum failure. This is likely a longer continuous operation than would be conducted in practice; however, the results from this simulation can guide decisions on what length of time would be appropriate for remediating a failure of this magnitude.

Figure 5.6-5 shows the results from the five-drum sudden failure simulation including 7 yr of SVE operation starting in June 2020 for borehole 54-27642. Borehole 54-27642 is 138 ft from the SVE-East unit, at the outside of the radius of influence shown in Figure 1.1-1. A dramatic increase in concentration is seen in the first year for ports to 116 ft bgs. Concentrations rise from 40 to 50 ppmv in these shallowest three ports to over 20,000 ppmv. The port at 175 ft bgs shows a more gradual rise to almost 1000 ppmv. Diffusion in the rocks leads to a slow drop in the shallow ports until the SVE system is turned on June 29, 2020. At this time, the concentrations in all ports drop quickly. By June 2022, after just 2 yr of SVE, concentrations at all ports have returned to pre-failure values.

The impact of SVE on the total plume can be seen in Figure 5.6-6, where the total 1,1,1-TCA plume mass in the vapor phase (1500 kg), largely from the five-drum failure (1351 kg), has been reduced to less than 300 kg in only 2 yr of active extraction. This simulation provides a defensible estimate for creating a plan for remediating hypothetical drum failures and shows that the site operators would have ample time to turn on the SVE system after detection.

6.0 DEVIATIONS

This section describes deviations from the IMWP (LANL 2014, 261843). The deviations discussed below include ports that could not be sampled, a reduction from 1 full year of operation, and issues with the usage of a dual-packer system in borehole 54-24399.

6.1 Sampling Ports

Several ports listed in Table 2.2-3 were found to be either fully or partially blocked. If ports were partially or fully blocked for two consecutive sampling rounds, these ports were assumed to be suspect and were removed from the sampling plan. Additionally, radiological concerns caused some ports to be temporarily removed from the sampling plan in November 2015. RCT monitoring detected gas concentrations of greater than 20 $\mu\text{g}/\text{m}^3$ in 18 ports (Table 2.2-3). However, this issue was resolved, and an RCT-approved method for sampling allowed these 18 ports to be sampled in future quarterly sampling events.

6.2 Active Extraction Duration

The SVE system was run from January 2015 to November 2015. This is a deviation from the initial plan to run the system for a full year. The decision to stop the SVE units in November 2015 was based on production of condensate from the SVE units during times when temperatures dropped below freezing. Subsurface vapor, containing both water vapor and VOC gases, condenses in the SVE system and accumulates in the 20-gal. liquid storage container (Figure 2.1-1). This liquid must be characterized because of the dissolved VOC component. Furthermore, the liquid must be removed from the storage container on a regular basis because several gallons per day can accumulate during cold weather. To avoid issues with condensate, the decision was made to shut down the SVE units in November 2015.

6.3 Deep Borehole 54-24399 Dual-Packer Failure

During the April 2015 sampling event, the dual-packer sampling system used to isolate a 1-ft interval (568–569 ft bgs) directly beneath the casing of borehole 54-24399 was badly damaged. The lower packer was shredded when it came in contact with very sharp basalt. The sharp nature of the vesicular basalt can be observed in the video log of borehole 54-24399 (Appendix D). The video log shows a limited region of massive basalt directly below the casing (less than 2 ft), followed by a large void area. To avoid further problems with packer destruction, the decision was made to install a permanent single packer.

In August 2016, a permanent single packer was installed at the bottom of the casing (566.7 ft bgs) to collect pore-gas samples in the open portion of the borehole. The permanent single packer hangs from the surface on a 1-in. steel pipe, pulling a new well cap firmly down onto an O-ring in an effort to minimize barometrically pumped flow into and out of the well. Two gas sampling ports penetrate the packer and are connected to ports on the surface well cap. The first port samples directly beneath the packer (566.7 ft bgs) while the second port ends 21 ft below the bottom of the packer at 587.8 ft bgs. A pressure transducer is mounted on the top of the packer with its pressure sampling port located directly beneath the packer at 566.7 ft bgs. The final connection on the packer top is used to connect a 50-psi nitrogen line for packer inflation.

7.0 CONCLUSIONS

During the first year of SVE operation, the two SVE units removed 553 kg (1217 lb) of total organic vapor mass. The mass was primarily removed from within an approximately 150-ft radius surrounding each of the extraction wells. Mass removal was higher initially and continued at a removal rate of nearly 17 lb/mo after 10 mo of operation.

Rebound of the plume during 18 mo after the end of the active SVE IM was slow, with most observation ports rebounding to no more than 50% of their original concentrations. Two wells in the eastern shaft cluster (54-02089 and 54-24238) showed increases in concentration above baseline sampling, which may be the result of an active leak.

The long-term ability of the SVE system to remove significant quantities of vapor-phase organics has been demonstrated, and data collected during the IM has been analyzed further as part of ongoing efforts to support the selection and design of a final remedy for MDA L. Simulations show that the current SVE boreholes are capable of remediating a sudden release of solvents and that such remediation could happen over a relatively short period (2 yr of SVE).

8.0 RECOMMENDATIONS

The following recommendations are based on 10 mo of SVE operation at MDA L followed by 18 mo of plume rebound and include results from a tracer test performed in the deep Cerros del Rio basalt.

1. Conduct semiannual monitoring of boreholes located in the source region (sentry boreholes) to allow early detection of potential container failure. Sentry boreholes on the western side of MDA L are boreholes 54-27641 and 54-24240. On the eastern side of MDA L, sentry boreholes include boreholes 54-24241, 54-24238, and 54-27642.
2. Monitor peripheral boreholes once every 2 yr for evidence of plume expansion.
3. Conduct semiannual monitoring of borehole 54-24399 to further characterize long-term trends of VOC concentrations in the deep basalt and to provide data needed to support the CME process (e.g., updating the conceptual model for transport and developing Tier II screening levels and cleanup goals).
4. Activate the eastern SVE unit if total VOC concentrations in any ports in the east sentry boreholes rise above 2000 ppmv, with a trend of consistent increase with each consecutive measurement for ports to depths of 100 ft. Once observed, the eastern SVE system should be activated within a period of 2 yr.
5. Activate the western SVE unit if total VOC concentrations in any ports in the western sentry boreholes rise above 2000 ppmv, with a trend of consistent increase with each consecutive measurement for ports to depths of 100 ft. Once observed, the western SVE system should be activated within a period of 2 yr.

9.0 REFERENCES AND MAP DATA SOURCES

9.1 References

The following reference list includes documents cited in this report. Parenthetical information following each reference provides the author(s), publication date, and ERID, ESHID, or EMID. This information is also included in text citations. ERIDs were assigned by the Laboratory's Associate Directorate for Environmental Management (IDs through 599999); ESHIDs were assigned by the Laboratory's Associate Directorate for Environment, Safety, and Health (IDs 600000 through 699999); and EMIDs are assigned by N3B (IDs 700000 and above). IDs are used to locate documents in N3B's Records Management System and in the Master Reference Set. The NMED Hazardous Waste Bureau and N3B maintain copies of the Master Reference Set. The set ensures that NMED has the references to review documents. The set is updated when new references are cited in documents.

DOE (U.S. Department of Energy), October 12, 2016. "Withdrawal of Three Corrective Measures Evaluations and Suggested Priorities for New Mexico Environment Department Review of Documents," U.S. Department of Energy letter to J. Kieling (NMED-HWB) from D. Rhodes DOE-EM), Los Alamos, New Mexico. (DOE 2016, 601899)

LANL (Los Alamos National Laboratory), September 2005. "Investigation Report for Material Disposal Area L, Solid Waste Management Unit 54-006, at Technical Area 54," Los Alamos National Laboratory document LA-UR-05-5777, Los Alamos, New Mexico. (LANL 2005, 092591)

LANL (Los Alamos National Laboratory), November 2006. "Summary Report: 2006 In Situ Soil Vapor Extraction Pilot Study at Material Disposal Area L, Technical Area 54, Los Alamos National Laboratory," Los Alamos National Laboratory document LA-UR-06-7900, Los Alamos, New Mexico. (LANL 2006, 094152)

LANL (Los Alamos National Laboratory), September 2011. "Corrective Measures Evaluation Report for Material Disposal Area L, Solid Waste Management Unit 54-006, at Technical Area 54, Revision 2," Los Alamos National Laboratory document LA-UR-11-4798, Los Alamos, New Mexico. (LANL 2011, 205756)

LANL (Los Alamos National Laboratory), September 2014. "Interim Measures Work Plan for Soil-Vapor Extraction of Volatile Organic Compounds from Material Disposal Area L, Technical Area 54, Revision 1," Los Alamos National Laboratory document LA-UR-14-26472, Los Alamos, New Mexico. (LANL 2014, 261843)

LANL (Los Alamos National Laboratory), September 2015. "Interim Measures Progress Report for Soil-Vapor Extraction of Volatile Organic Compounds from Material Disposal Area L, Technical Area 54," Los Alamos National Laboratory document LA-UR-15-26893, Los Alamos, New Mexico. (LANL 2015, 600930)

LANL (Los Alamos National Laboratory), May 2016. "Interim Measures Progress Report for Soil-Vapor Extraction of Volatile Organic Compounds from Material Disposal Area L, Technical Area 54," Los Alamos National Laboratory document LA-UR-16-23065, Los Alamos, New Mexico. (LANL 2016, 601484)

LANL (Los Alamos National Laboratory), December 2017. "Summary of a Gas Transport Tracer Test in the Deep Cerros Del Rio Basalts, Mesita del Buey, Los Alamos NM," Los Alamos National Laboratory document LA-UR-17-31351, Los Alamos, New Mexico. (LANL 2017, 602792)

- Neeper, D.A., 2002. "Investigation of the Vadose Zone Using Barometric Pressure Cycles," *Journal of Contaminant Hydrology*, Vol. 54, pp. 59-80. (Neeper 2002, 098639)
- NMED (New Mexico Environment Department), July 17, 2014. "Approval with Modifications, Interim Measures Work Plan for Soil-Vapor Extraction of Volatile Organic Compounds from Material Disposal Area L, Technical Area 54," New Mexico Environment Department letter to P. Maggione (DOE-NA-LA) and J.D. Mousseau (LANL) from J.E. Kieling (NMED-HWB), Santa Fe, New Mexico. (NMED 2014, 525053)
- Stauffer, P., K. Birdsell, and W. Rice, March 7–11, 2011. "3-D Model Validation in Support of Site Closure, Material Disposal Area L, Los Alamos, NM," Paper 11545, Waste Management 2011 Conference, March 7–11, 2011, Phoenix, AZ. (Stauffer et al. 2011, 255584)
- Stauffer, P.H., K.H. Birdsell, M.S. Witkowski, and J.K. Hopkins, 2005. "Vadose Zone Transport of 1,1,1-Trichloroethane: Conceptual Model Validation through Numerical Simulation," *Vadose Zone Journal*, Vol. 4, pp. 760–773. (Stauffer et al. 2005, 090537)
- Stauffer, P.H., J.K. Hopkins, and T. Anderson, February 25–March 1, 2007. "A Soil Vapor Extraction Pilot Study in a Deep Arid Vadose Zone, Part 2: Simulations in Support of Decision Making Processes," Waste Management Conference 2007, February 25–March 1, 2007, Tucson, Arizona. (Stauffer et al. 2007, 104950)
- Stauffer, P.H., J.K. Hopkins, T. Anderson, and J. Vrugt, July 11, 2007. "Soil Vapor Extraction Pilot Test at Technical Area 54, Material Disposal Area L: Numerical Modeling in Support of Decision Analysis," Los Alamos National Laboratory document LA-UR-07-4890, Los Alamos, New Mexico. (Stauffer et al. 2007, 097871)
- Vrugt, J.A., P.H. Stauffer, T. Wöhling, B.A. Robinson, and V.V. Vesselinov, May 2008. "Inverse Modeling of Subsurface Flow and Transport Properties: A Review with New Developments," *Vadose Zone Journal*, Vol. 7, No. 2, pp. 843–864. (Vrugt et al. 2008, 104951)
- Weston (Weston Solutions, Inc.), May 2015. "Final Baseline Data Evaluation for Soil Vapor Extraction at Material Disposal Area L, Solid Waste Management Unit 54-006, at Technical Area 54," report prepared for Los Alamos National Laboratory, Los Alamos, New Mexico. (Weston 2015, 600886)
- Weston (Weston Solutions, Inc.), September 2015. "Draft Final Evaluation of Data from the First Quarter of Soil Vapor Extraction at Material Disposal Area L, Solid Waste Management Unit 54-006, at Technical Area 54," report prepared for Los Alamos National Laboratory, Los Alamos, New Mexico. (Weston 2015, 600887)
- Zyvoloski, G.A., B.A. Robinson, Z.V. Dash, and L.L. Trease, July 1997. "Summary of the Models and Methods for the FEHM Application — A Finite-Element Heat- and Mass-Transfer Code," Los Alamos National Laboratory report LA-13307-MS, Los Alamos, New Mexico. (Zyvoloski et al. 1997, 070147)

9.2 Map Data Sources

Hypsography, 20 and 100 Foot Contour Intervals; Los Alamos National Laboratory, ENV-Environmental Remediation and Surveillance Program; 1991

Materials Disposal Areas; Los Alamos National Laboratory, ENV-Environmental Remediation and Surveillance Program; ER2004-0221; 1:2,500 Scale Data; 23 April 2004

Waste Storage Features; Los Alamos National Laboratory, ENV-Environmental Remediation and Surveillance Program, ER2005-0748; 1:2,500 Scale Data; 06 October 2005

Security fence: Security and Industrial Fences and Gates; Los Alamos National Laboratory, KSL Site Support Services, Planning, Locating and Mapping Section; 06 January 2004; as published 29 November 2010.

Paved roads: Paved Road Arcs; Los Alamos National Laboratory, KSL Site Support Services, Planning, Locating and Mapping Section; 06 January 2004; as published 29 November 2010.

Unpaved roads: Dirt Road Arcs; Los Alamos National Laboratory, KSL Site Support Services, Planning, Locating and Mapping Section; 06 January 2004; as published 29 November 2010.

Structures: Structures; Los Alamos National Laboratory, KSL Site Support Services, Planning, Locating and Mapping Section; 06 January 2004; as published 29 November 2010.

Locations: ER Project Locations; Los Alamos National Laboratory, ESH&Q Waste and Environmental Services Division, 2010-2E; 1:2,500 Scale Data; 04 October 2010.

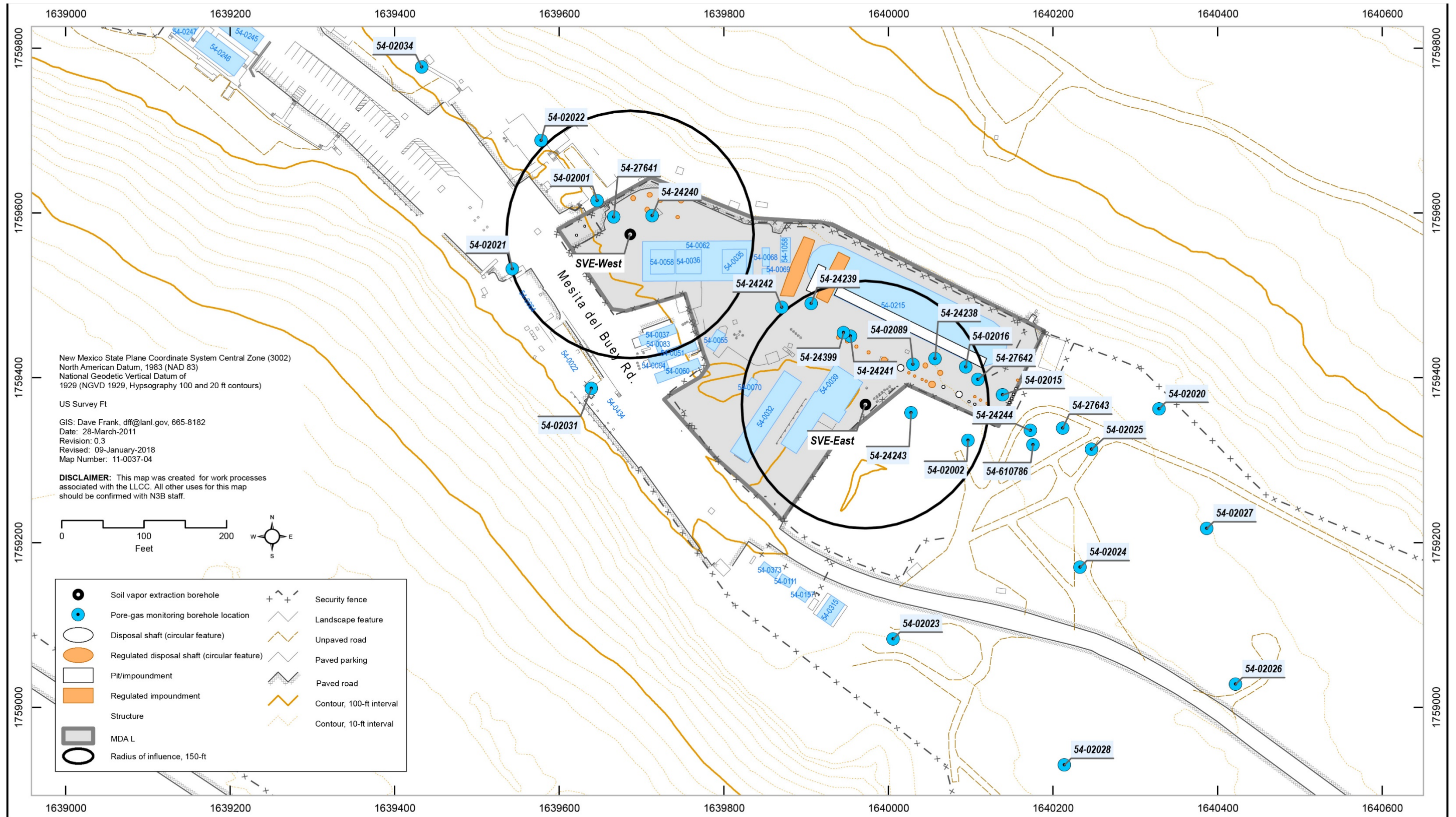


Figure 1.1-1 View of MDA L with disposal units, surface structures, pore-gas monitoring boreholes, SVE boreholes, and 150-ft ROI of extraction wells

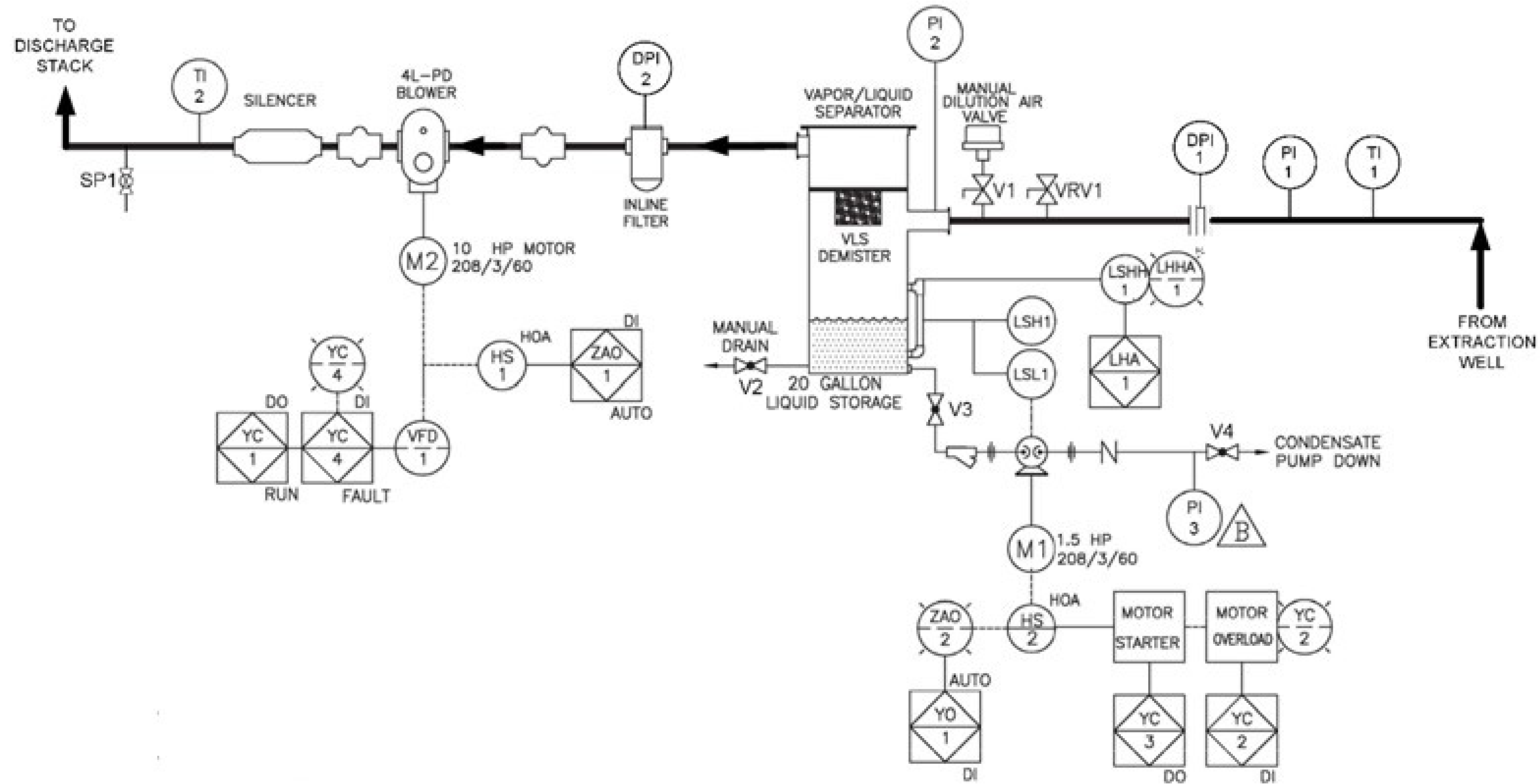


Figure 2.1-1 Diagram of SVE-East and SVE-West system piping and instrumentation



Figure 2.1-2 SVE-East unit

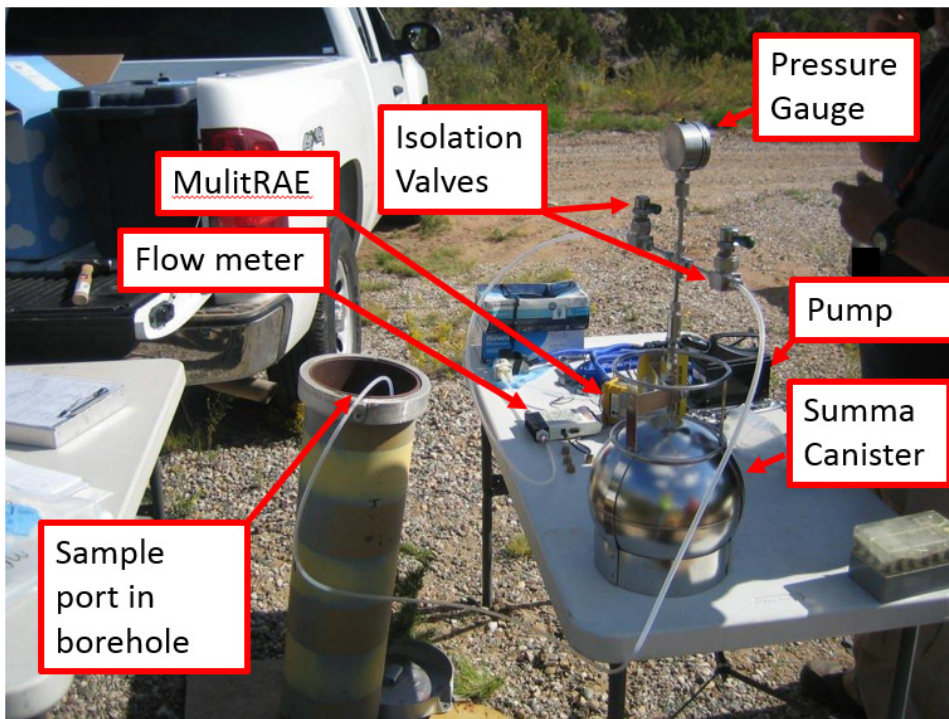


Figure 2.2-1 Subsurface sampling train



Figure 2.2-2 Permanent packer installed in borehole 54-24399 in August 2016



Figure 2.2-3 Surface completion of the permanent packer at borehole 54-24399



Figure 2.2-4 Top of the permanent packer showing the OMEGA pressure transducer, one sample line, and the nitrogen inflation line

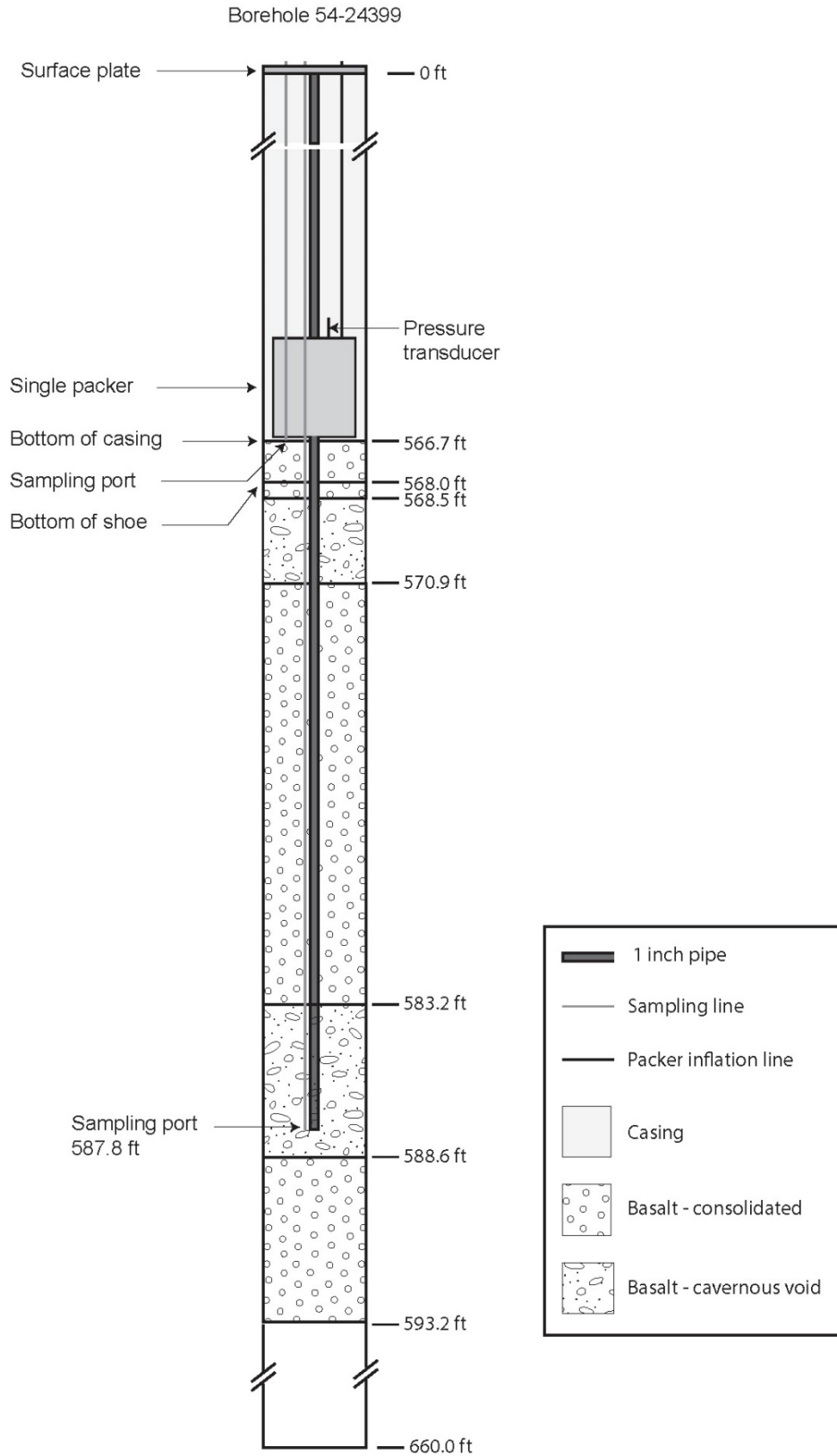


Figure 2.2-5 Schematic of the completed single packer installation in borehole 54-24399

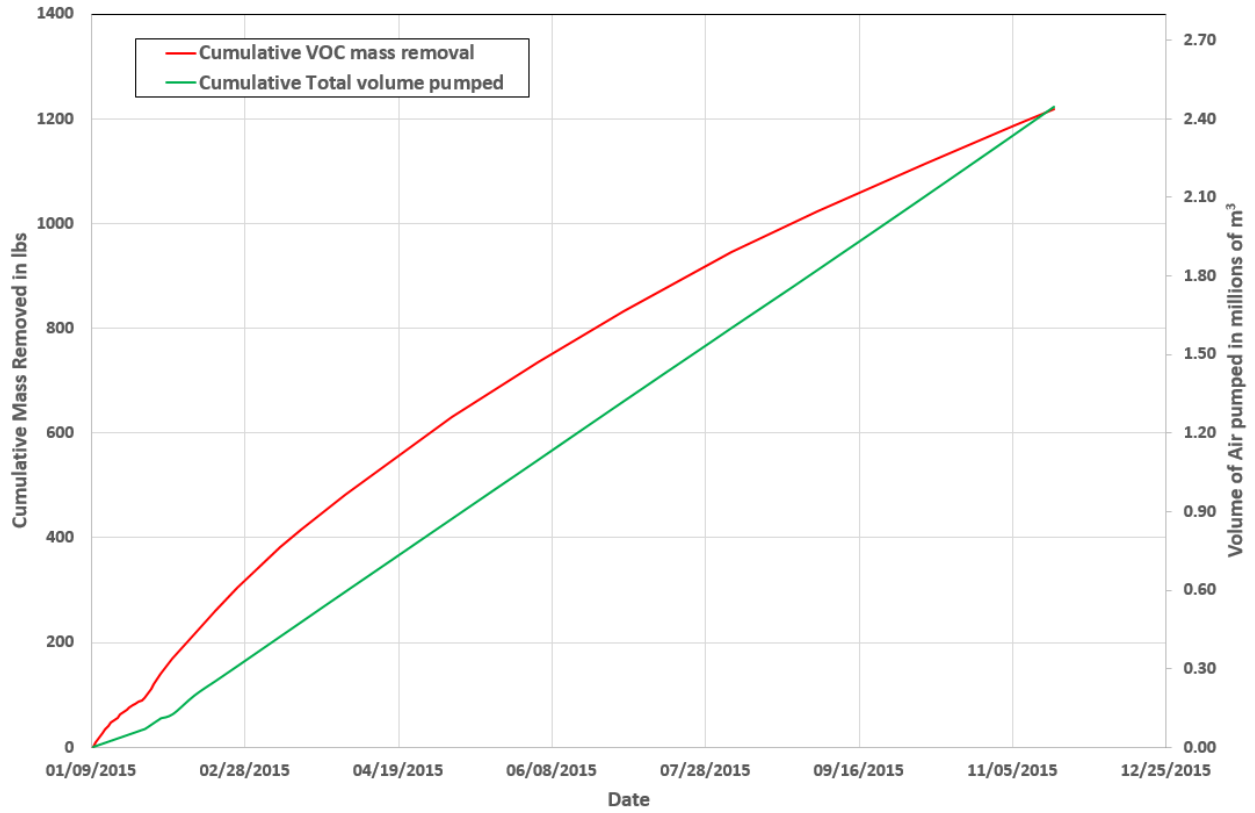


Figure 4.1-1 Cumulative mass removal and cumulative volume of pore gas pumped from the subsurface from both SVE units as a function of time

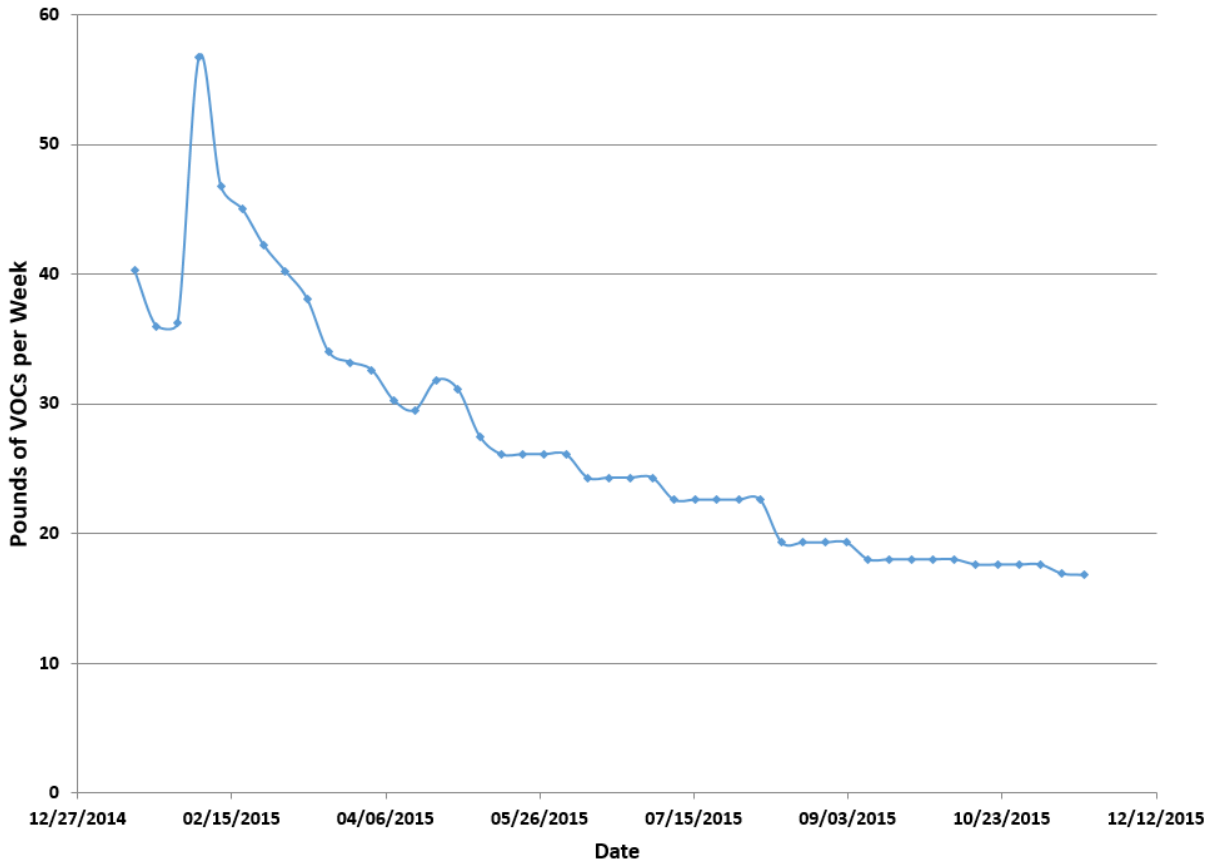


Figure 4.1-2 Weekly mass removal rate from both SVE units as a function of time

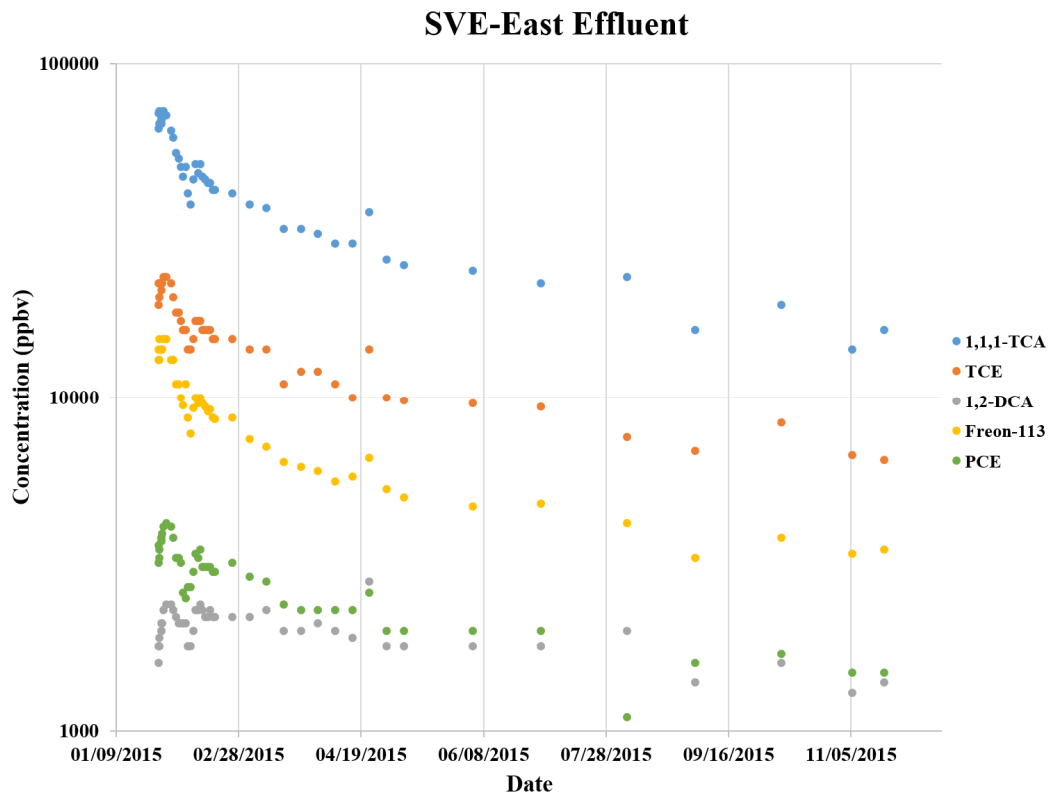
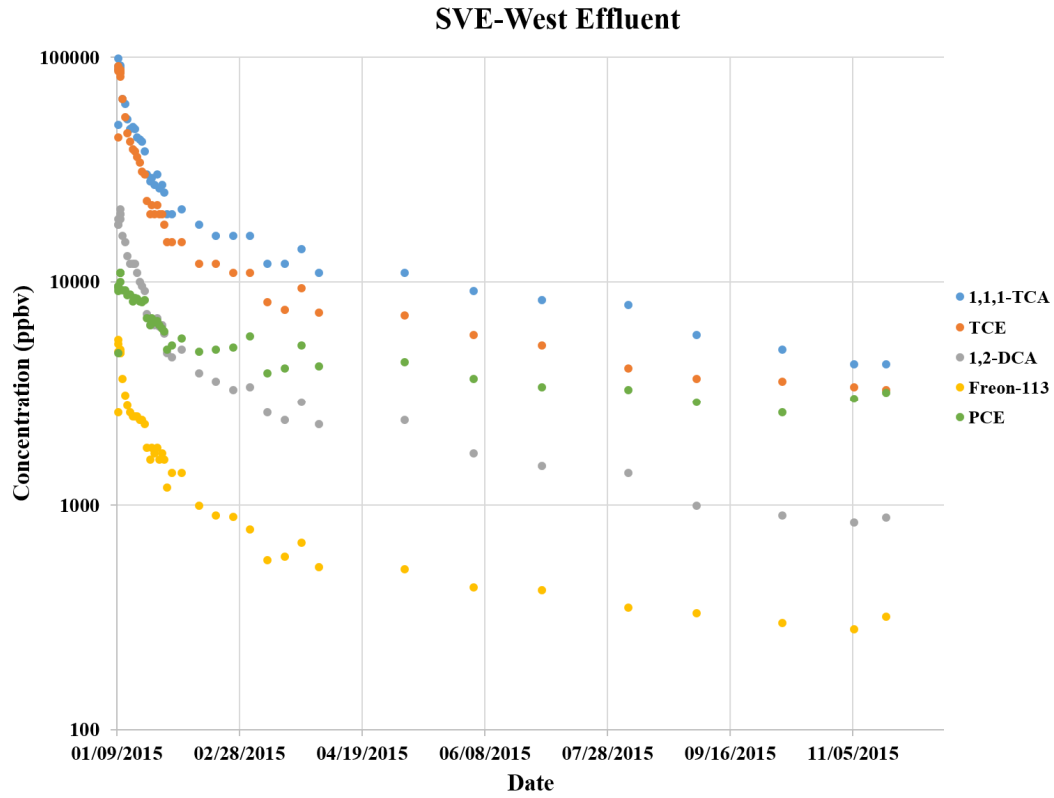


Figure 4.2-1 Effluent concentration versus time for SVE-West and SVE-East

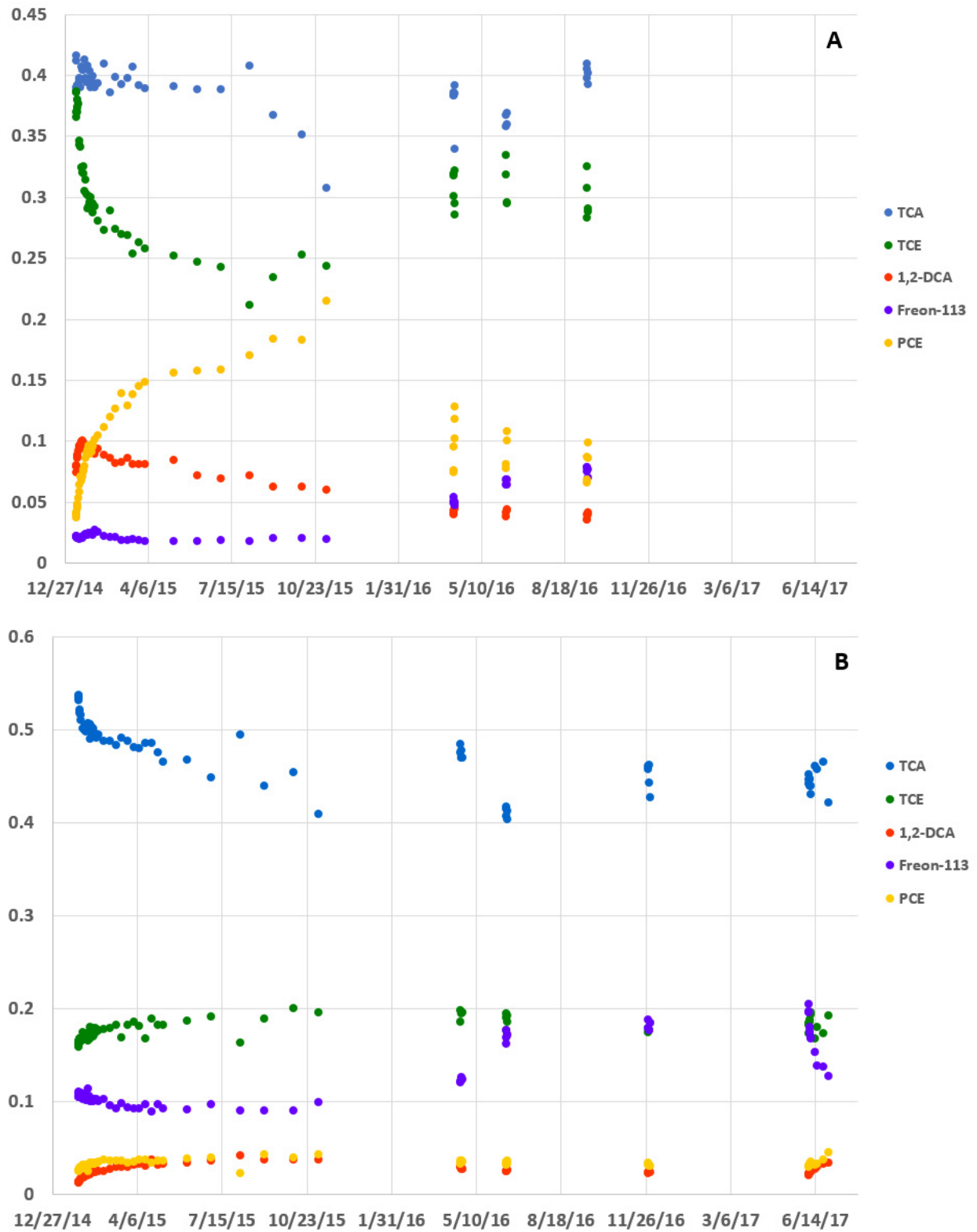


Figure 4.2-2 Effluent concentration ratios versus time for (A) SVE-West and (B) SVE-East

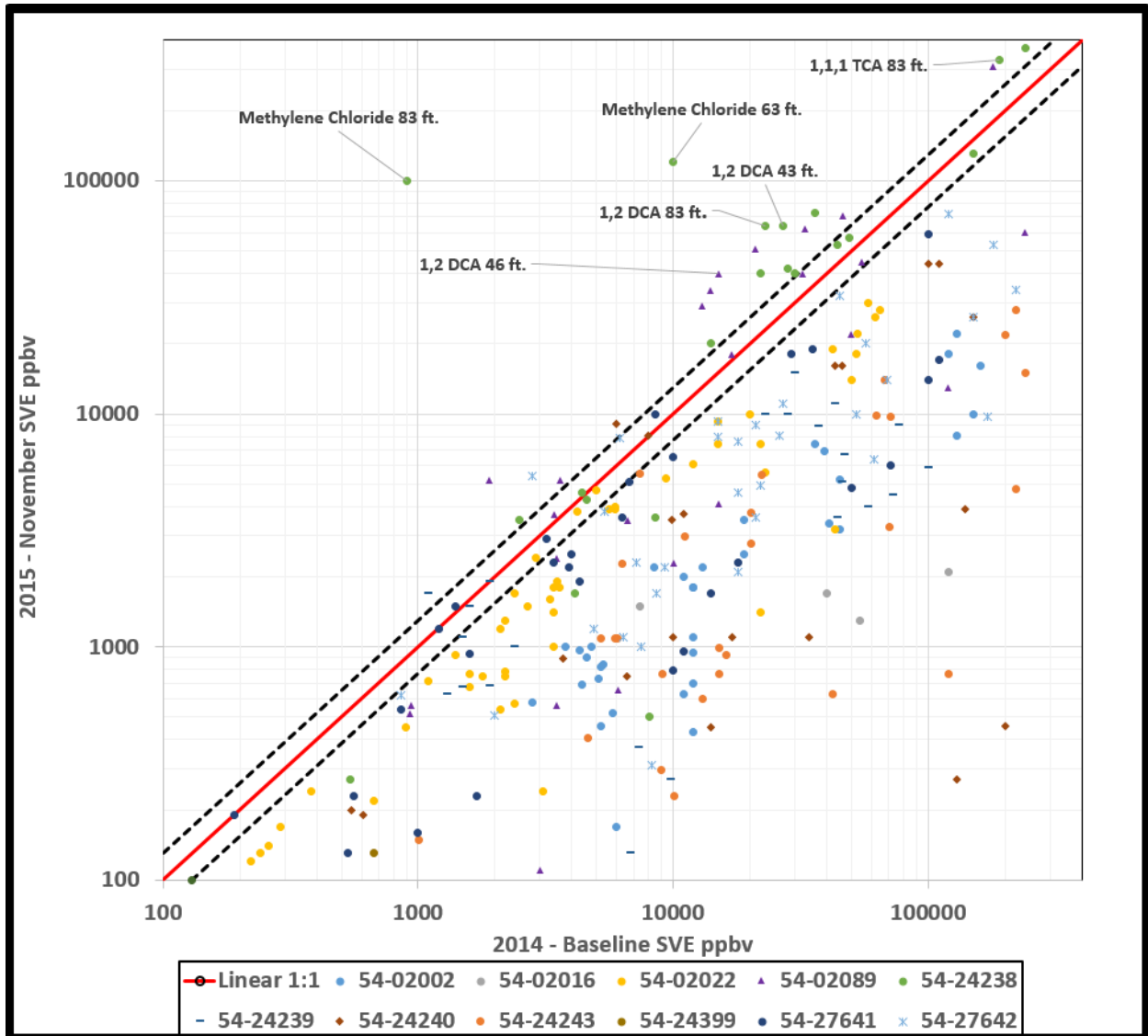


Figure 4.3-1 Comparison of subsurface VOC concentrations before SVE (baseline 2014) and after 10-plus mo of SVE pumping (November 2015)

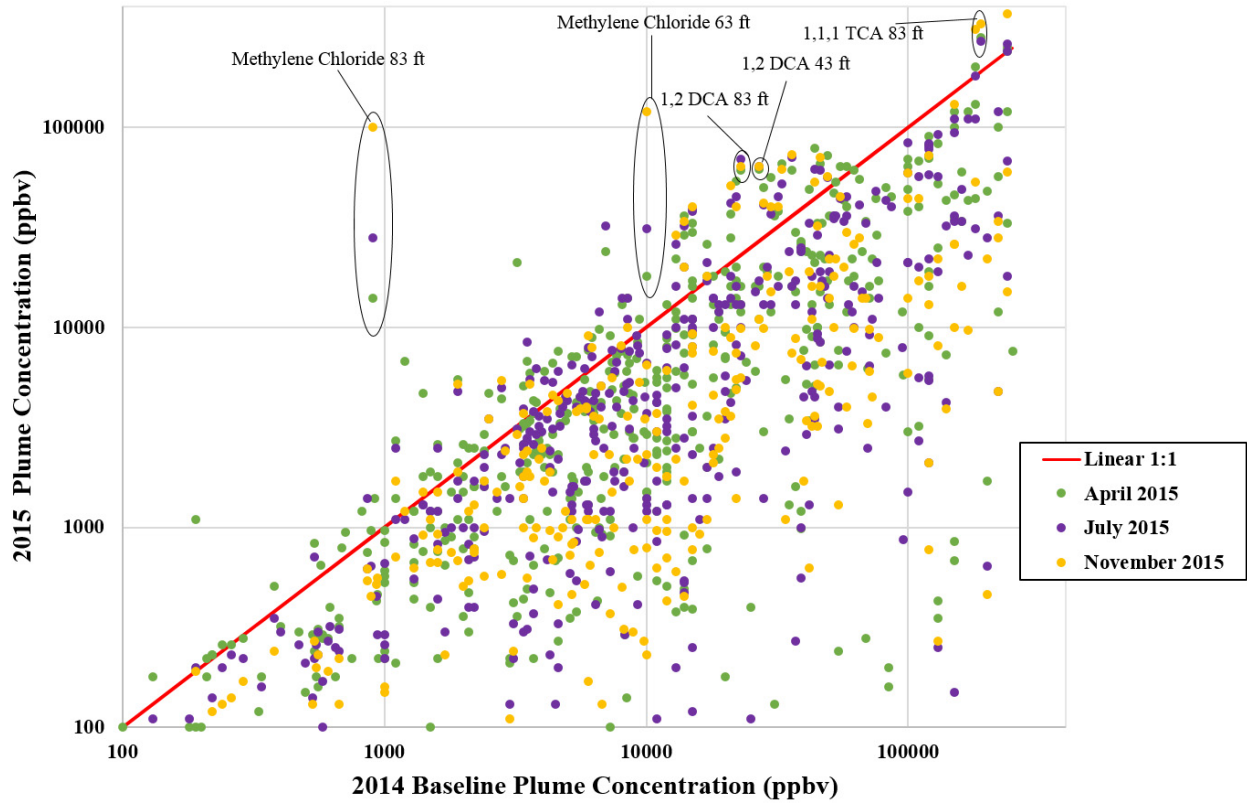


Figure 4.3-2 Comparison of post-SVE and pre-SVE subsurface VOC concentrations for seven analytes passing Tier II screening. Labeled points are all from borehole 54-24238.

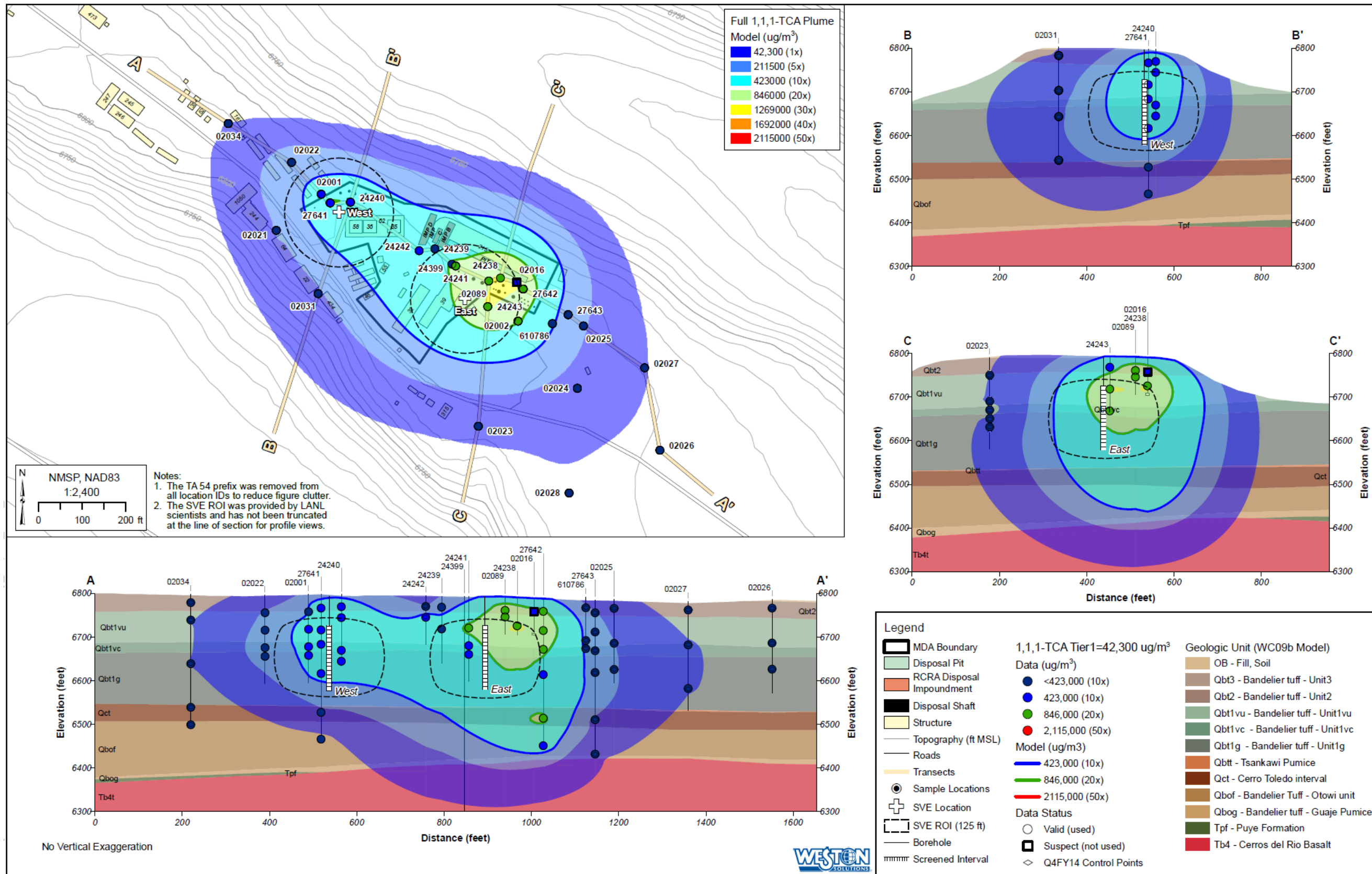


Figure 4.3-3 Baseline 2014 1,1,1-TCA plume data interpolated from borehole data

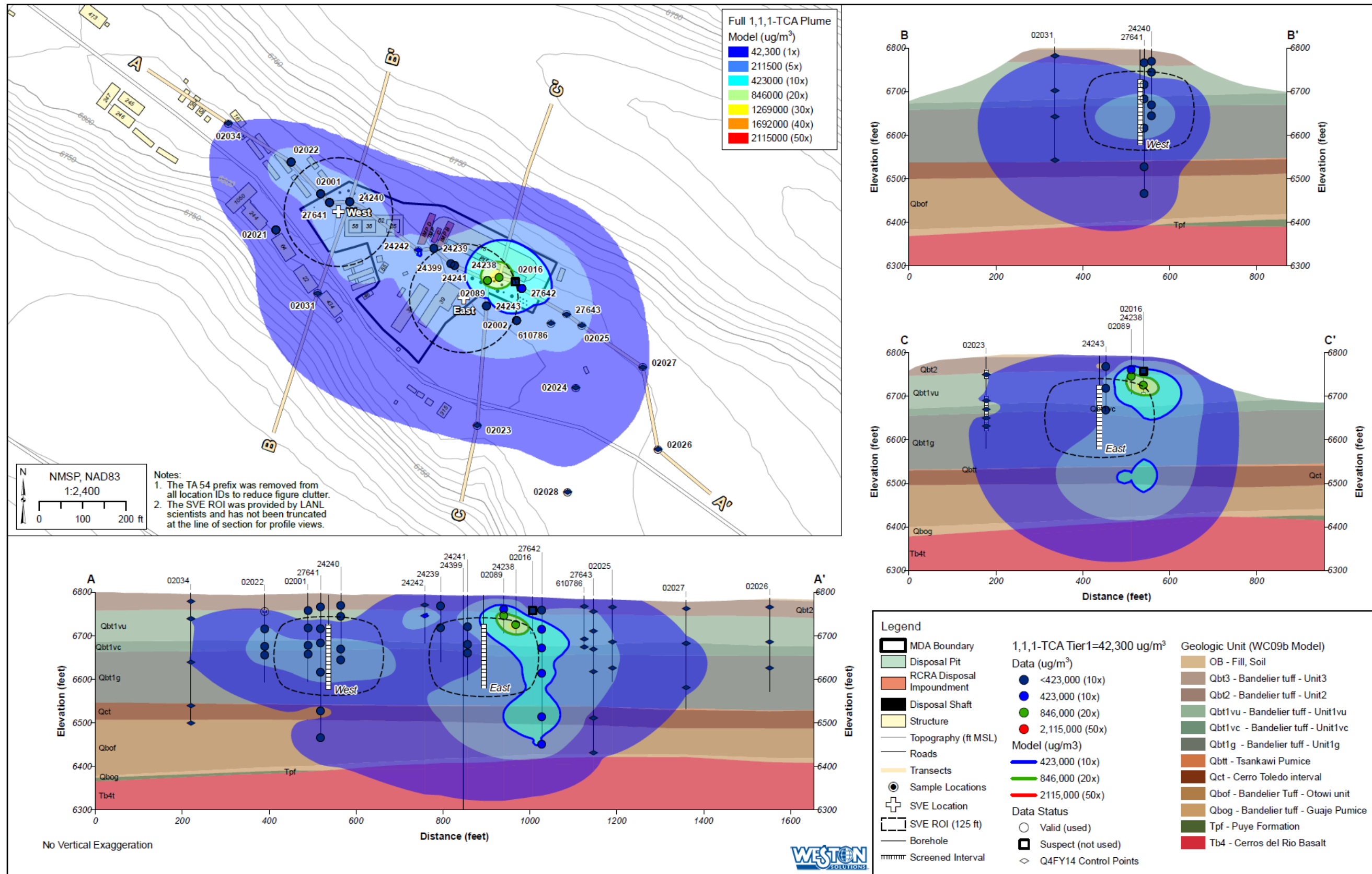


Figure 4.3-4 April 2015 1,1,1-TCA plume data interpolated from borehole data

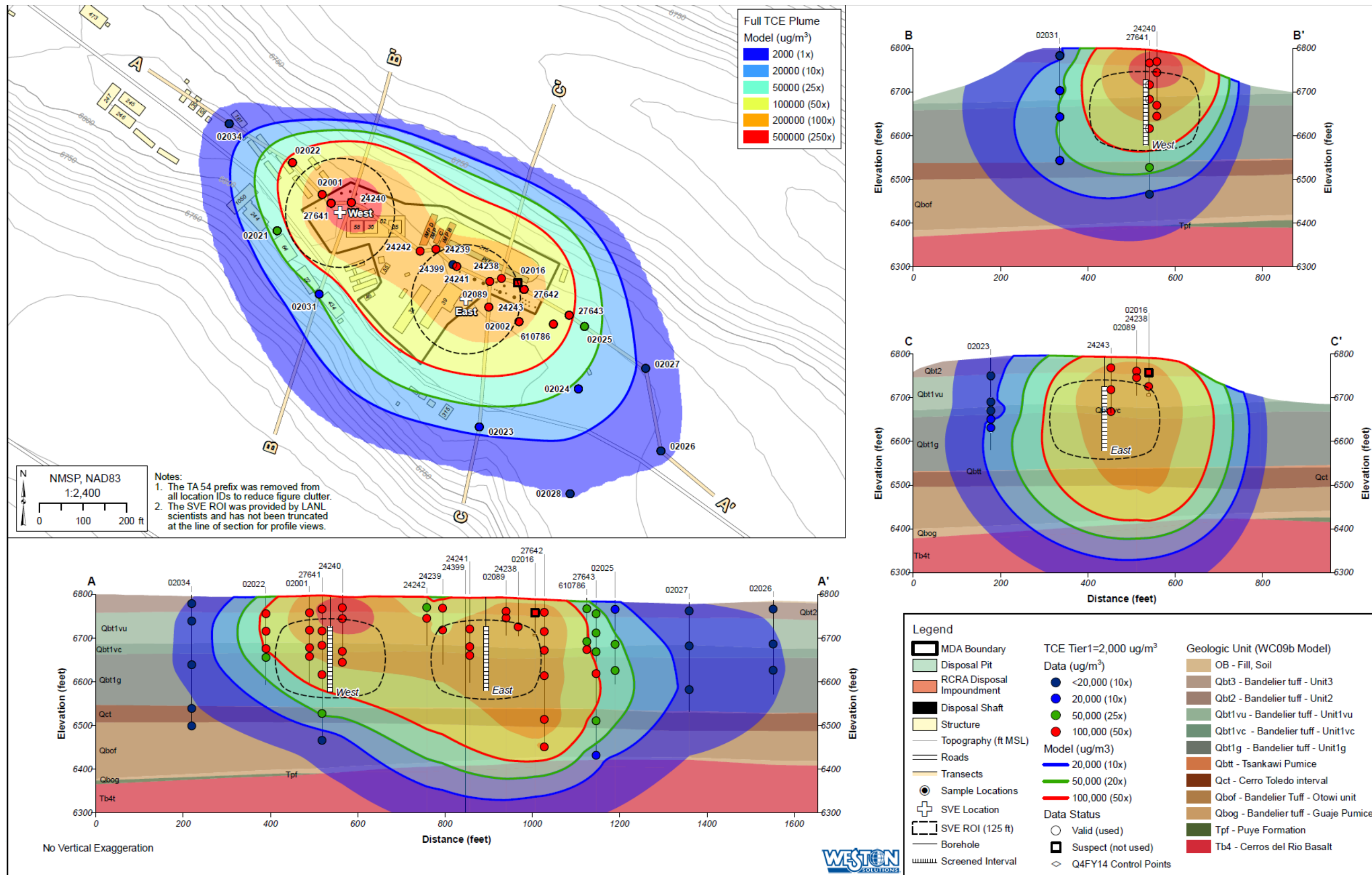


Figure 4.3-5 Baseline 2014 TCE plume data interpolated from borehole data

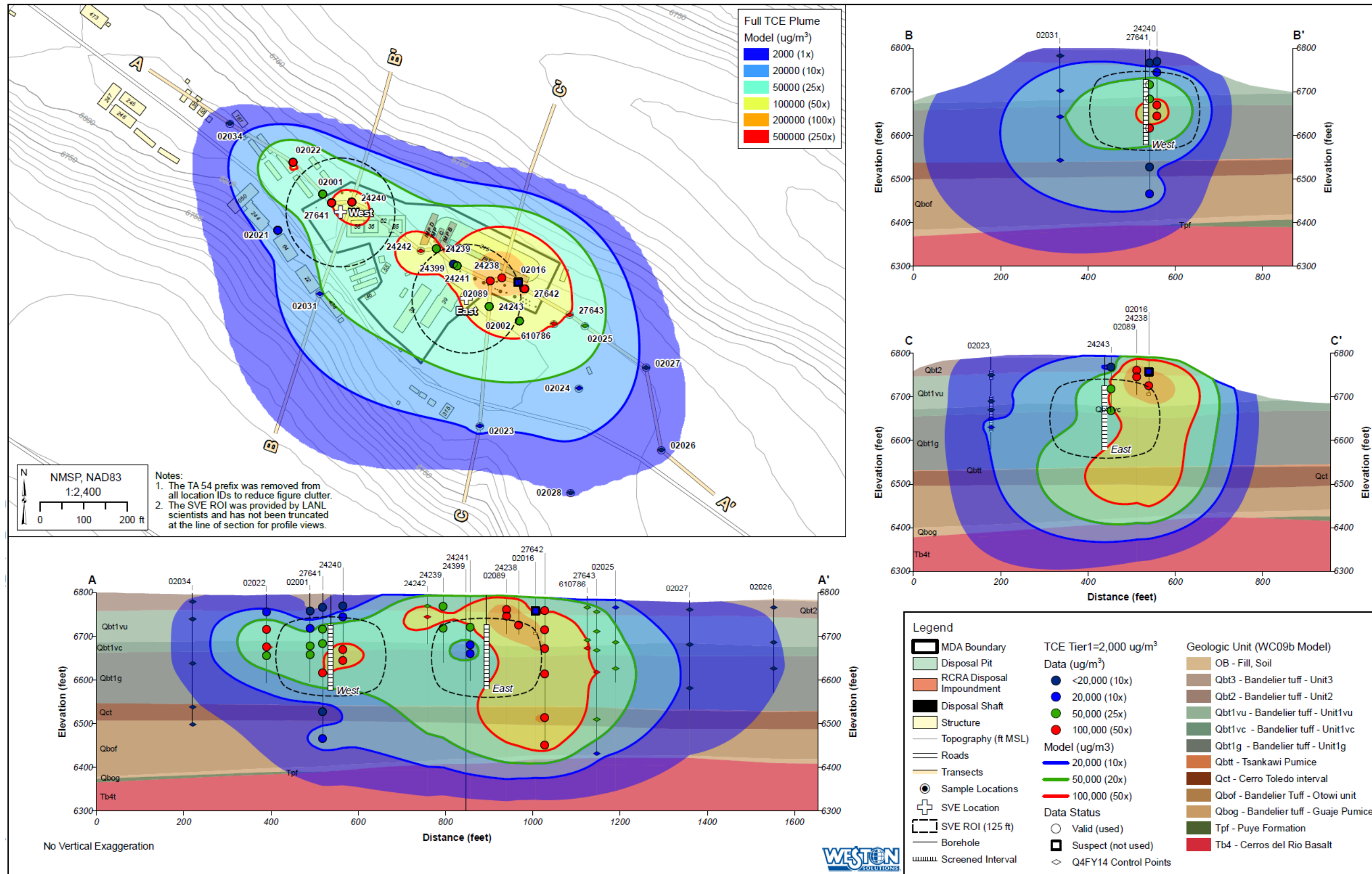


Figure 4.3-6 April 2015 TCE plume data interpolated from borehole data

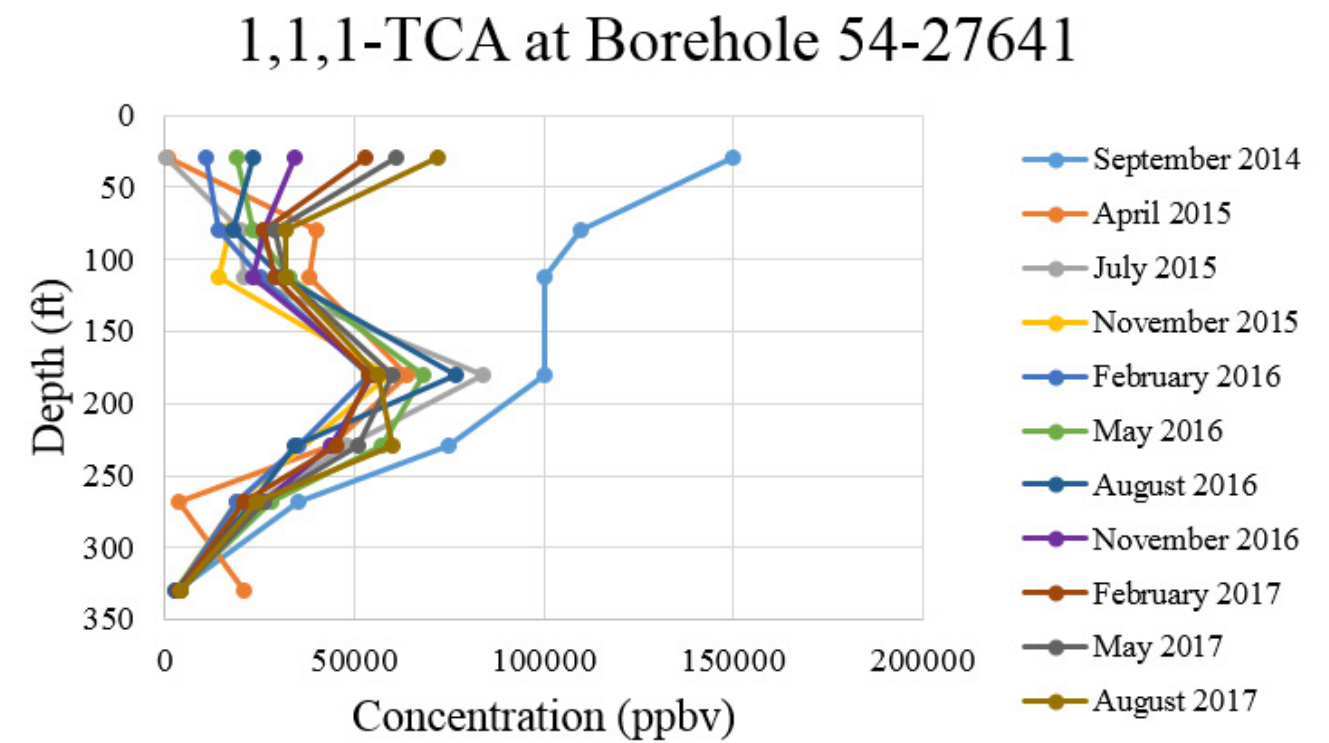
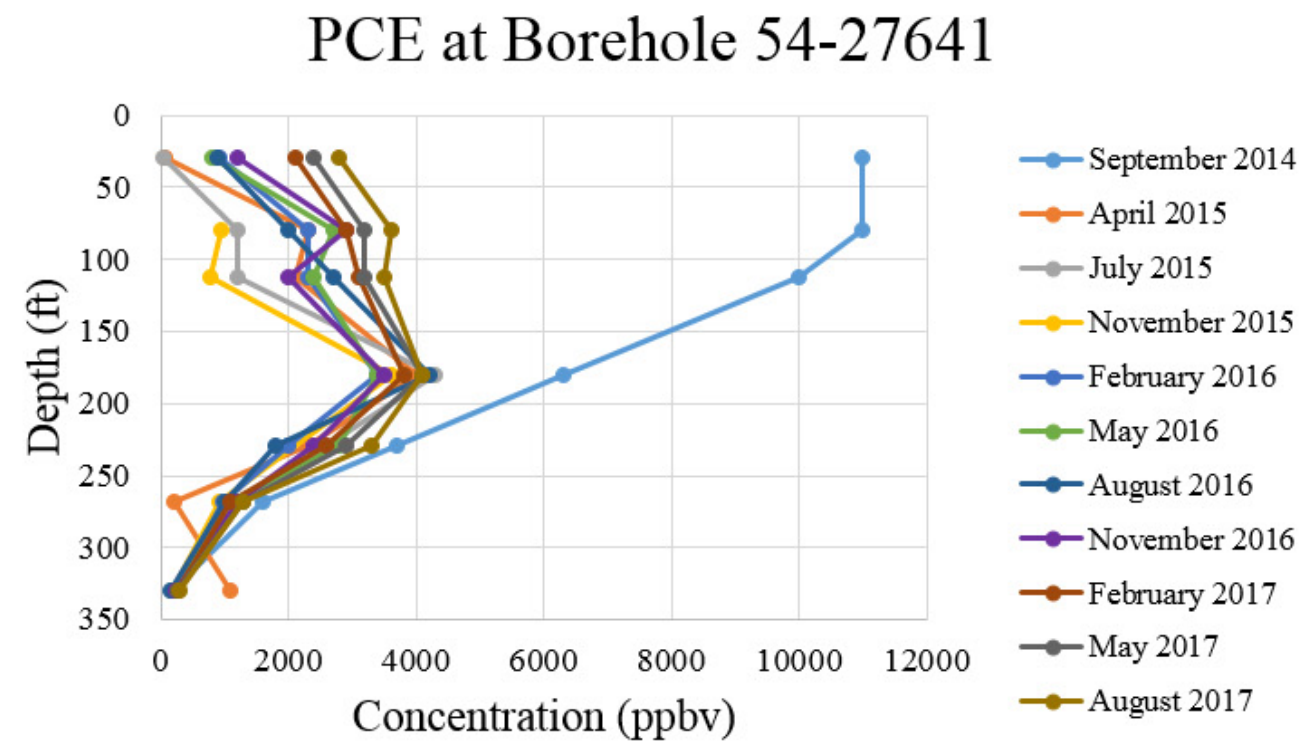
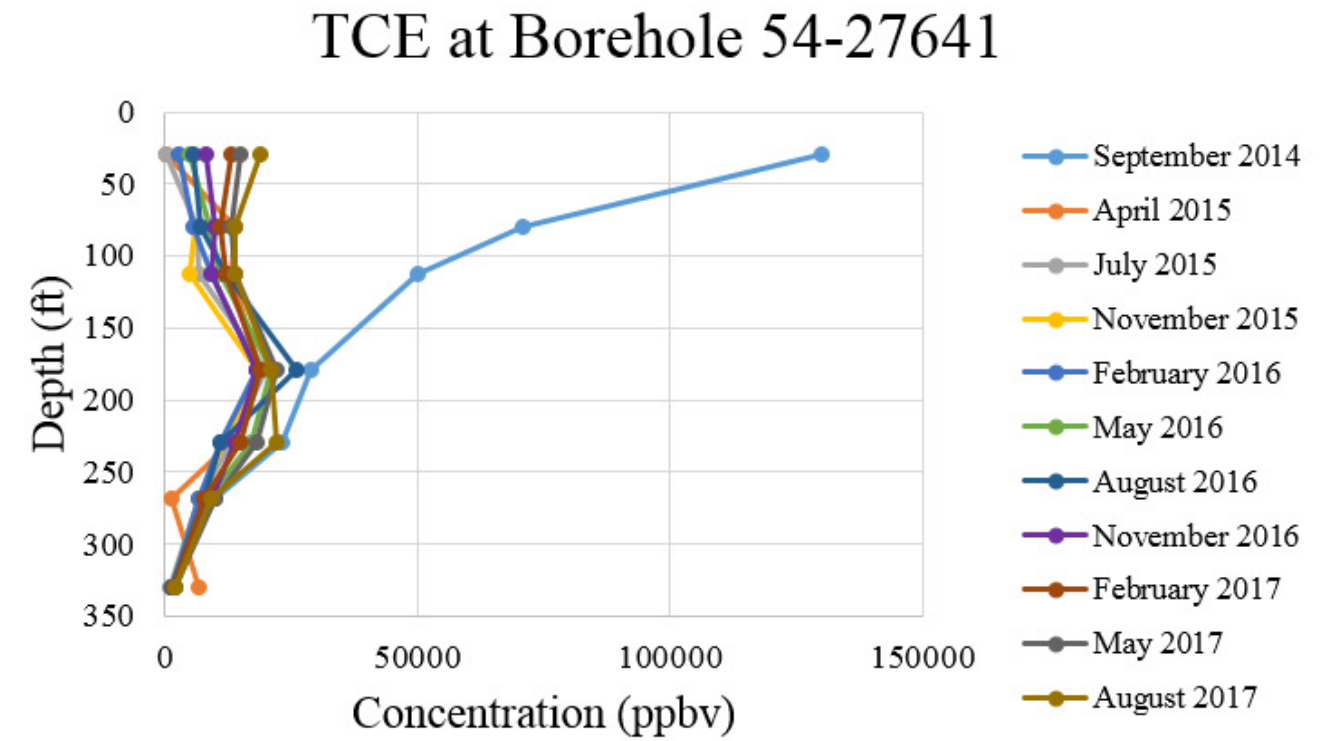
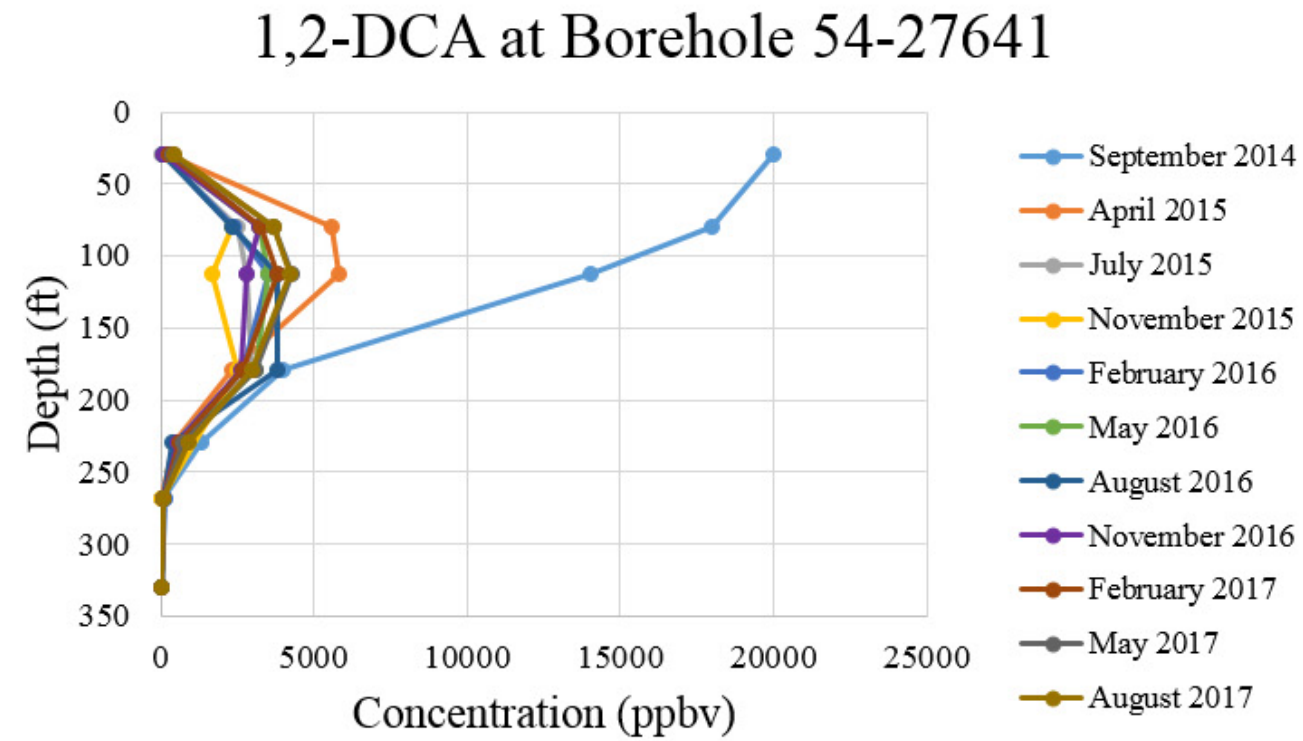
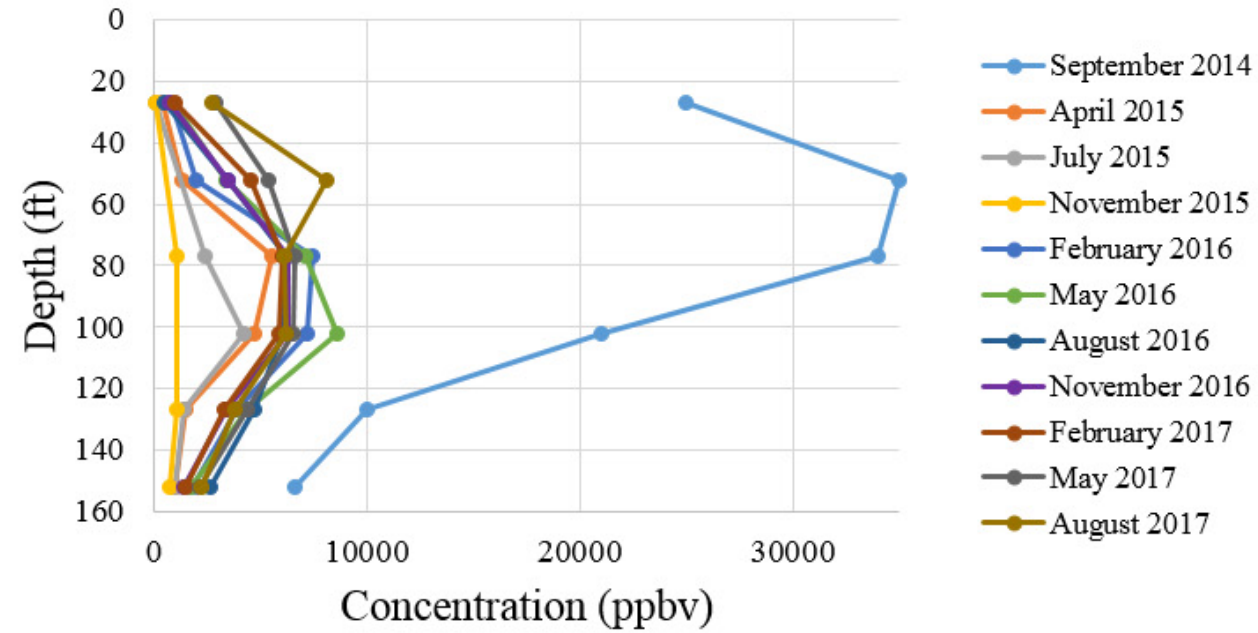
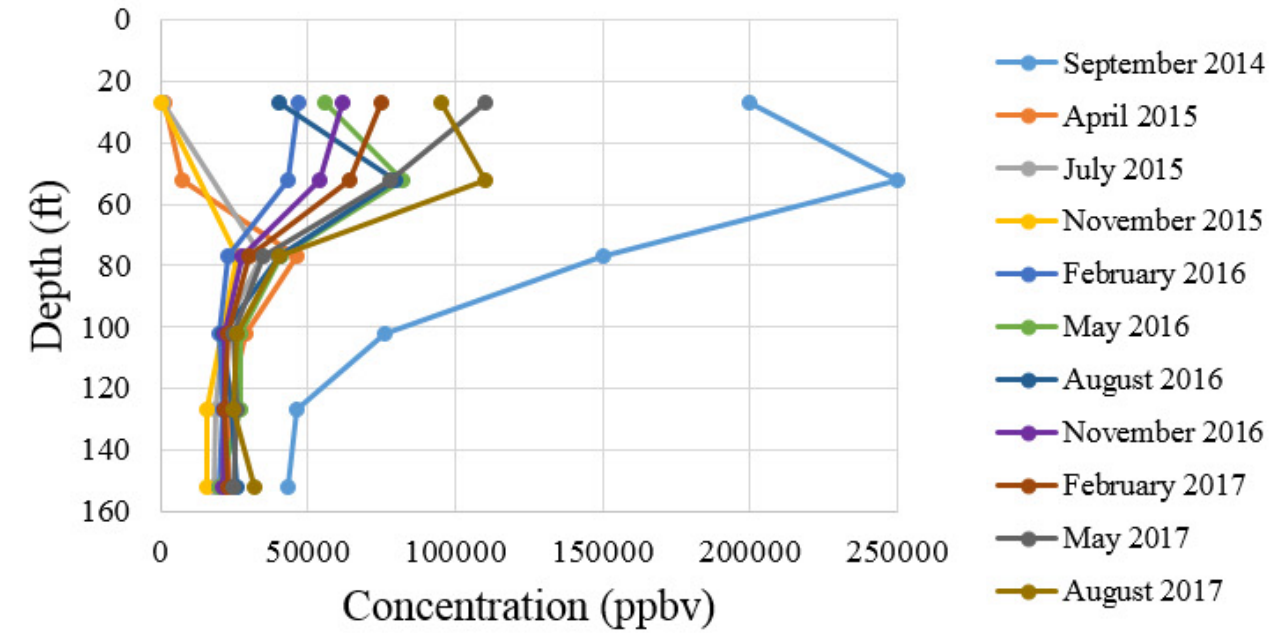


Figure 4.3-7 DCA[1,2], TCE, PCE, and 1,1,1-TCA concentration data for borehole 54-27641

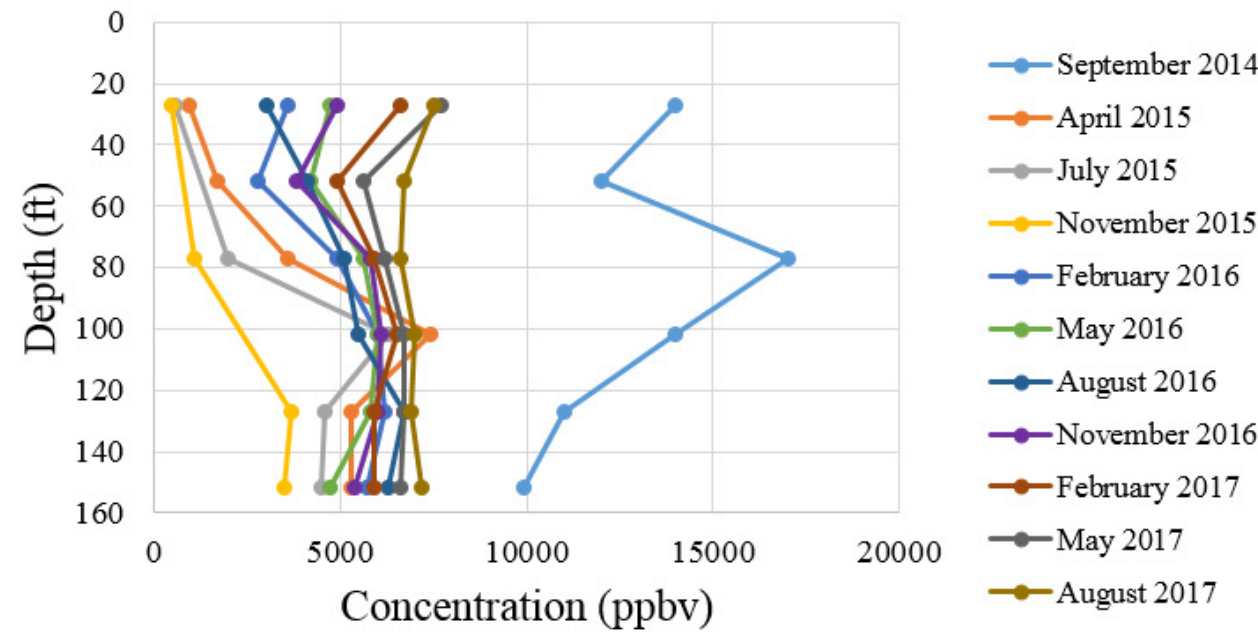
1,2-DCA at Borehole 54-24240



TCE at Borehole 54-24240



PCE at Borehole 54-24240



1,1,1-TCA at Borehole 54-24240

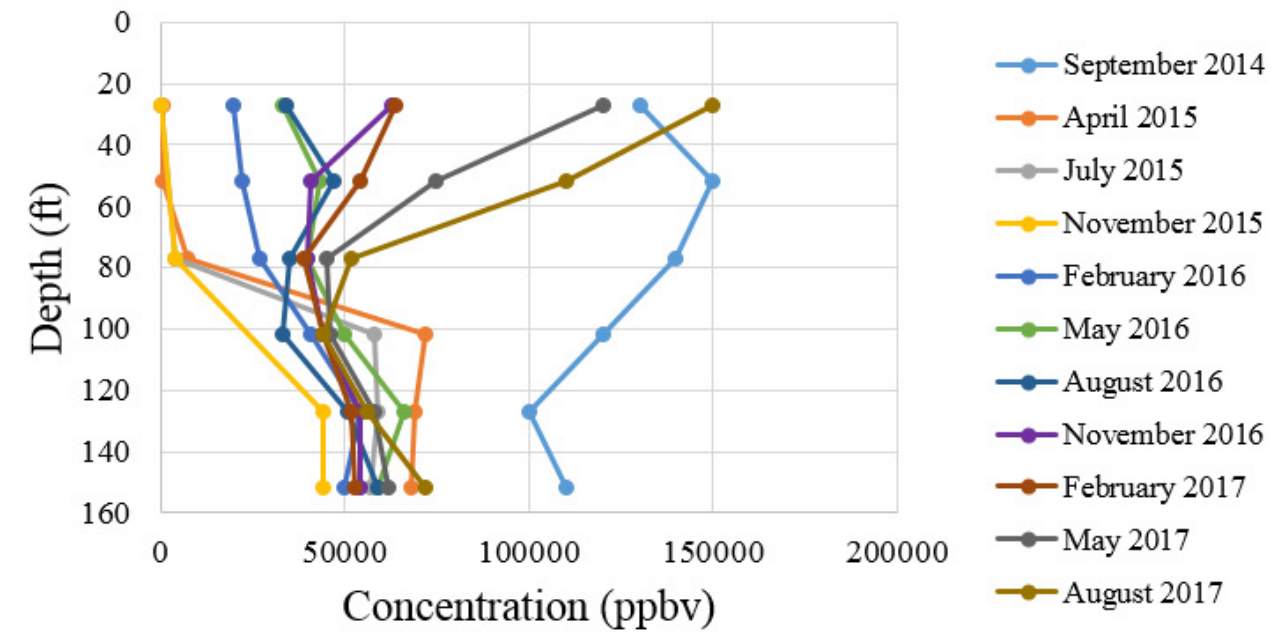
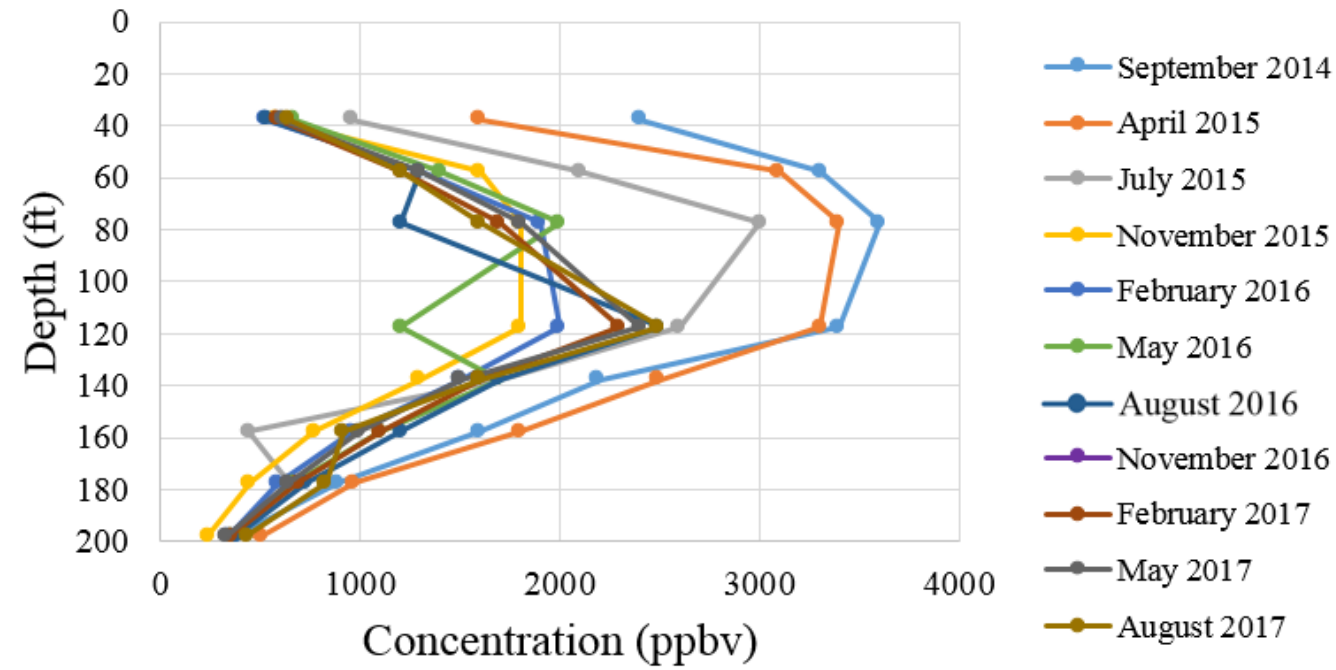
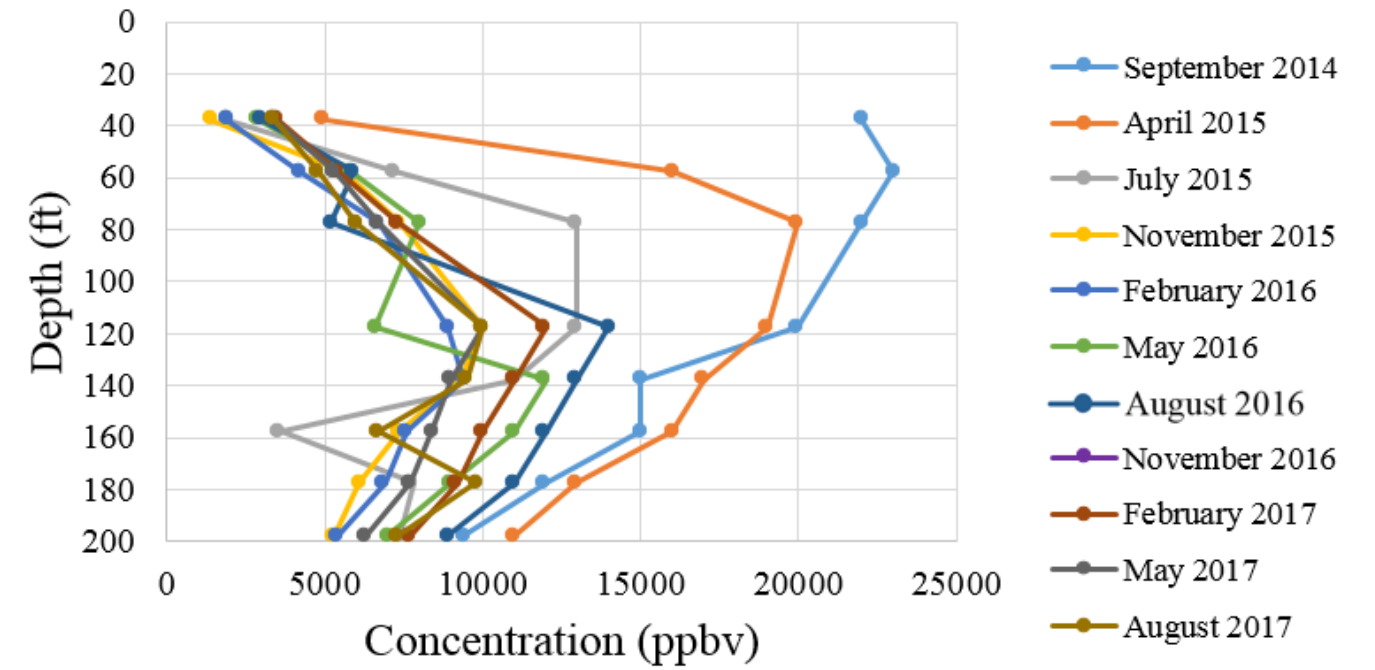


Figure 4.3-8 DCA[1,2], TCE, PCE, and 1,1,1-TCA concentration data for borehole 54-24240

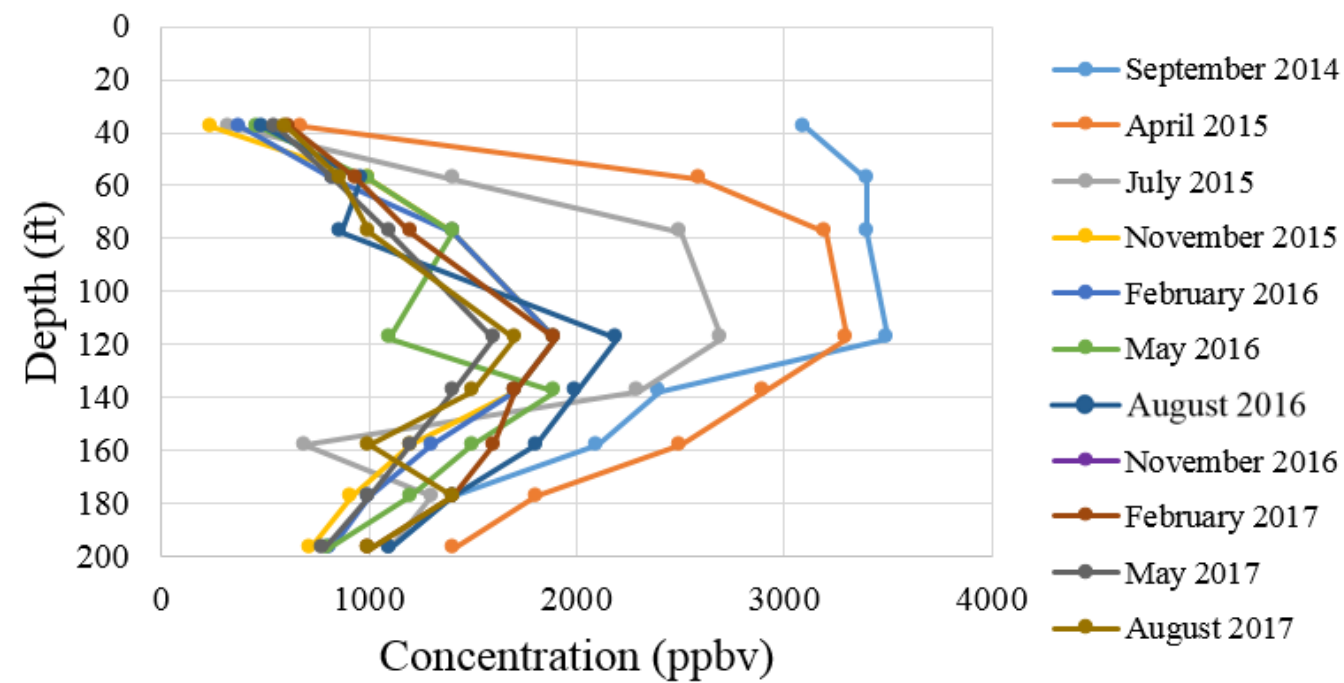
1,2-DCA at Borehole 54-02022



TCE at Borehole 54-02022



PCE at Borehole 54-02022



1,1,1-TCA at Borehole 54-02022

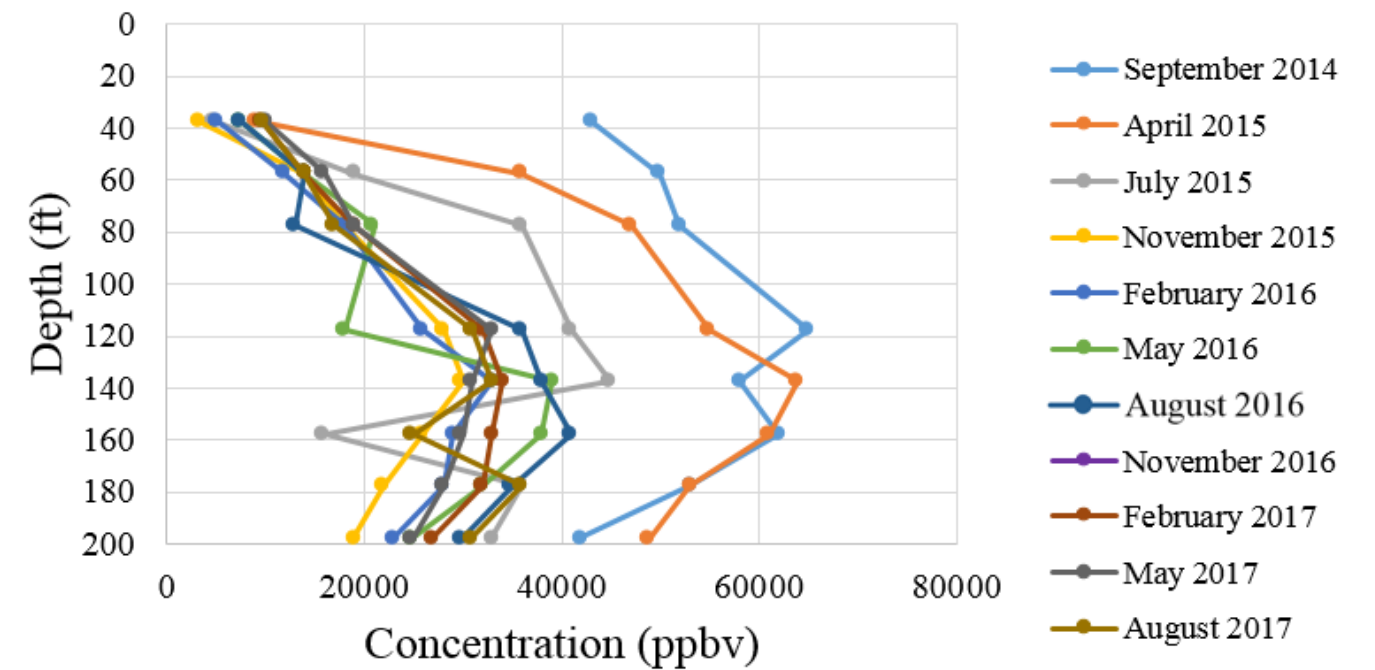
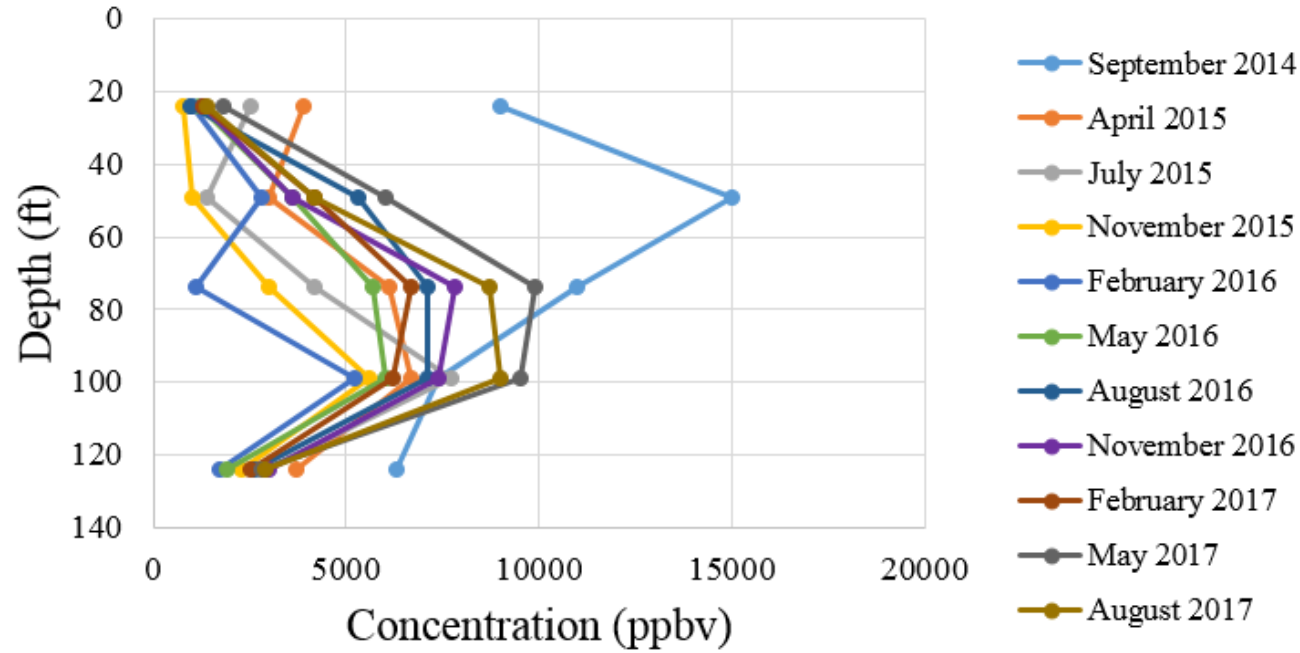
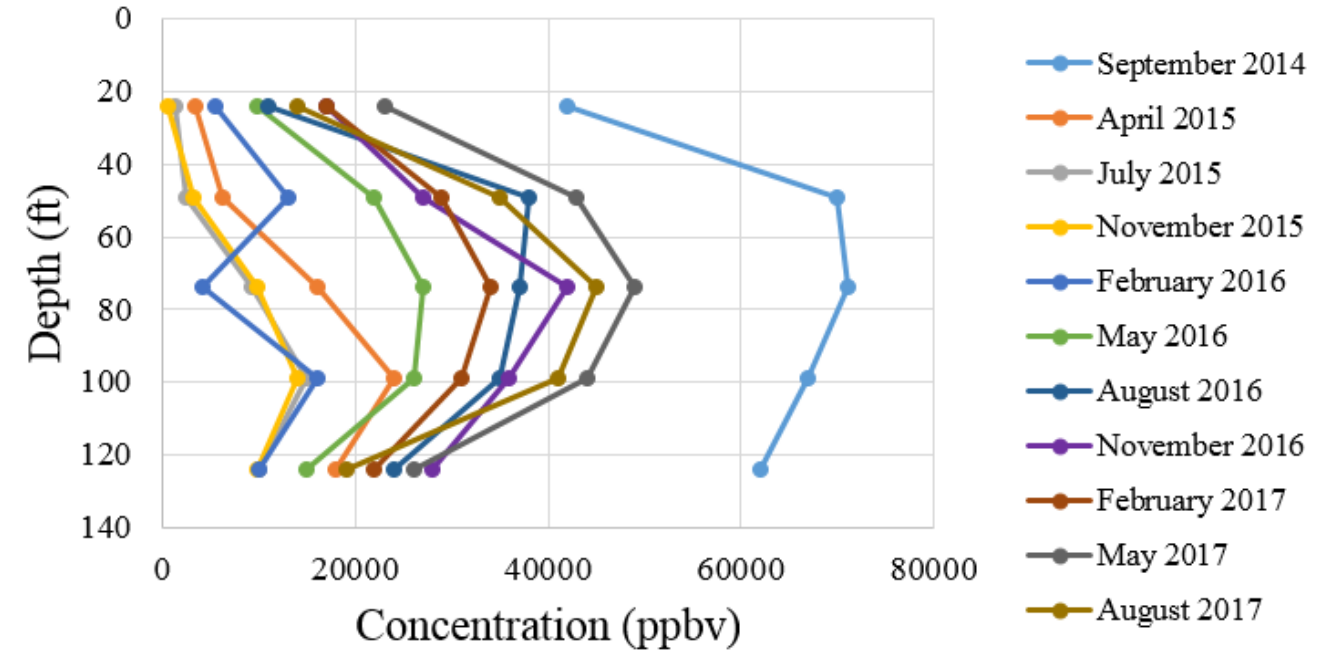


Figure 4.3-9 DCA[1,2], TCE, PCE, and 1,1,1-TCA concentration data for borehole 54-02022

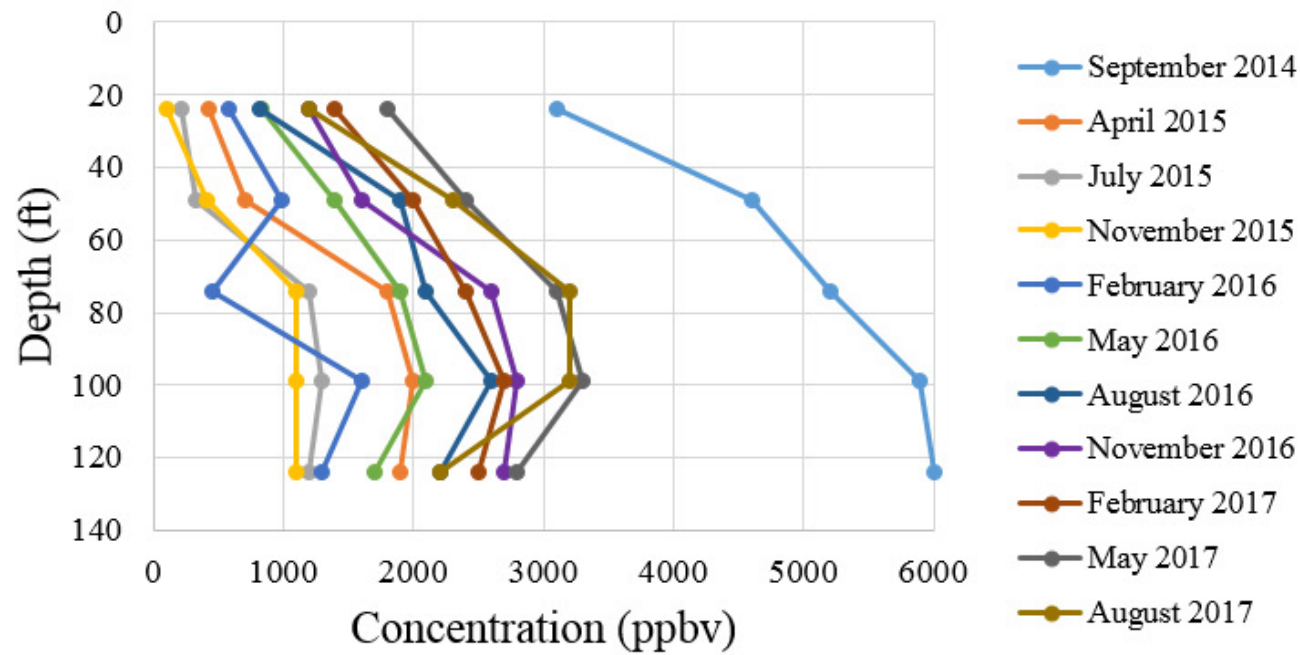
1,2-DCA at Borehole 54-24243



TCE at Borehole 54-24243



PCE at Borehole 54-24243



1,1,1-TCA at Borehole 54-24243

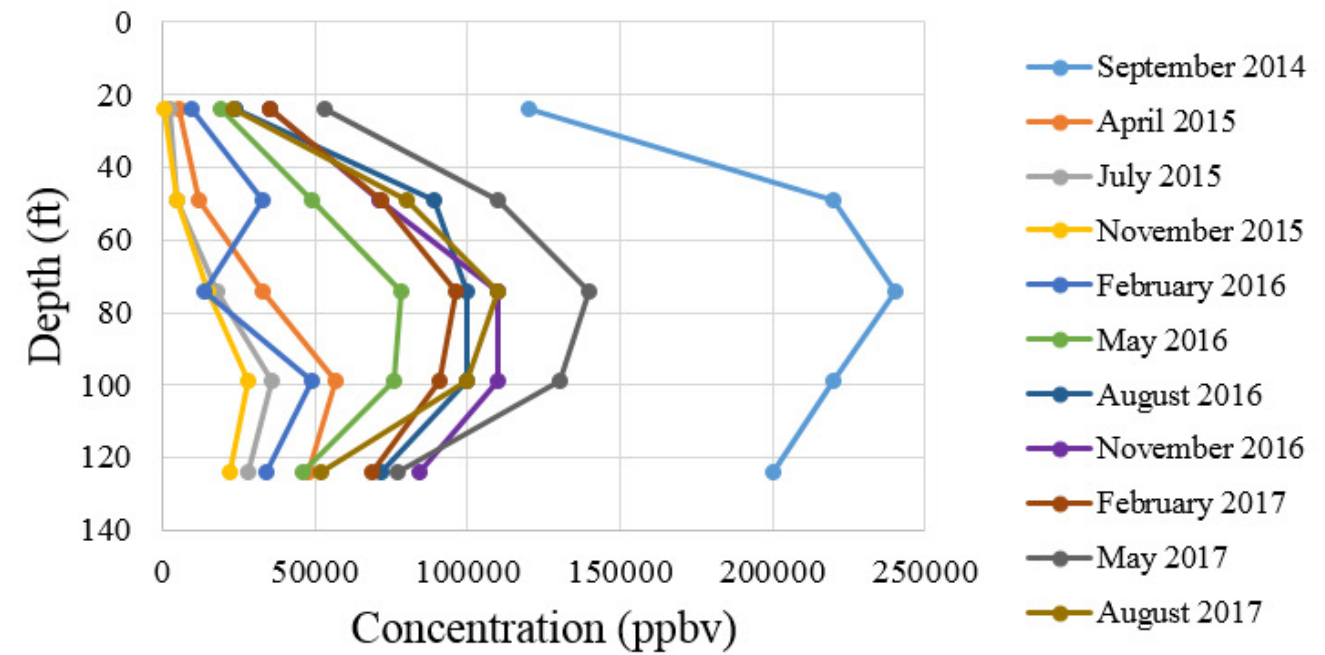
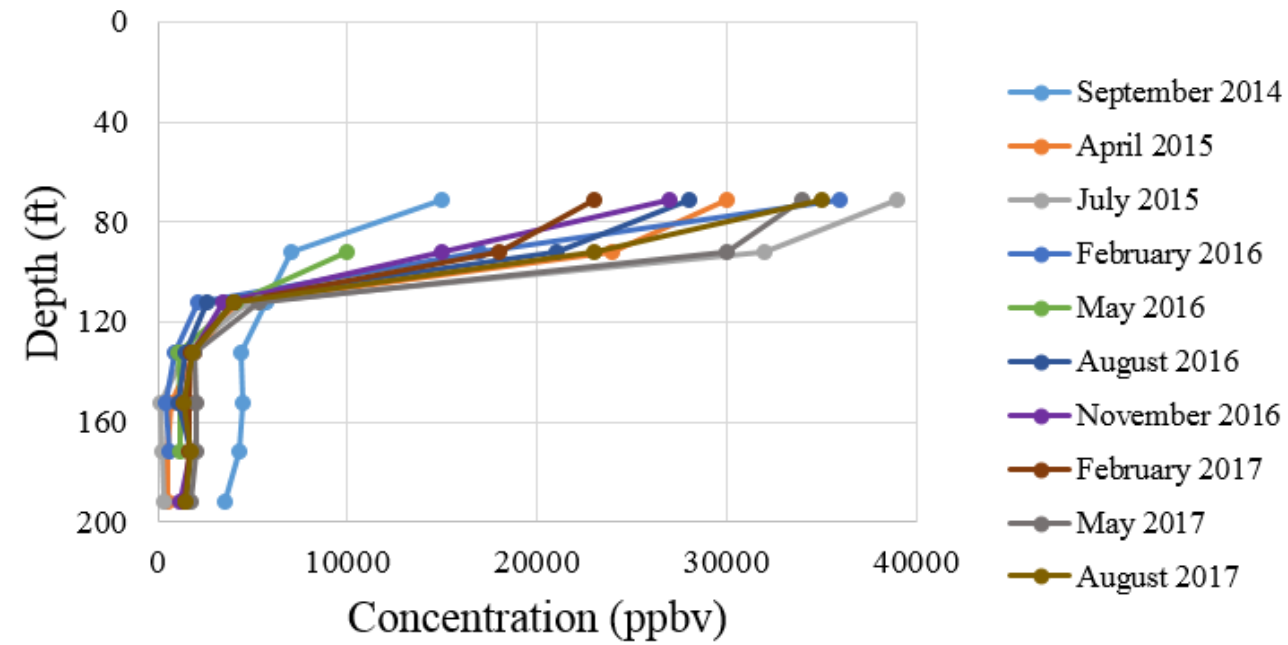
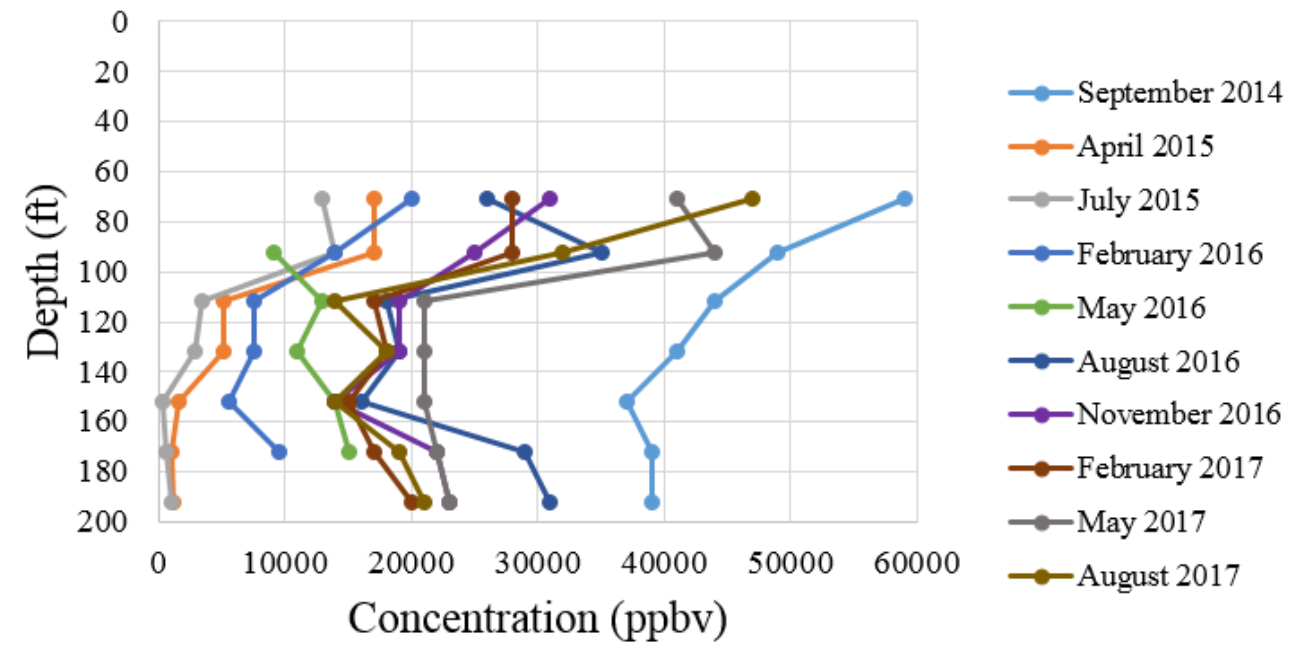


Figure 4.3-10 DCA[1,2], TCE, PCE, and 1,1,1-TCA concentration data for borehole 54-24243

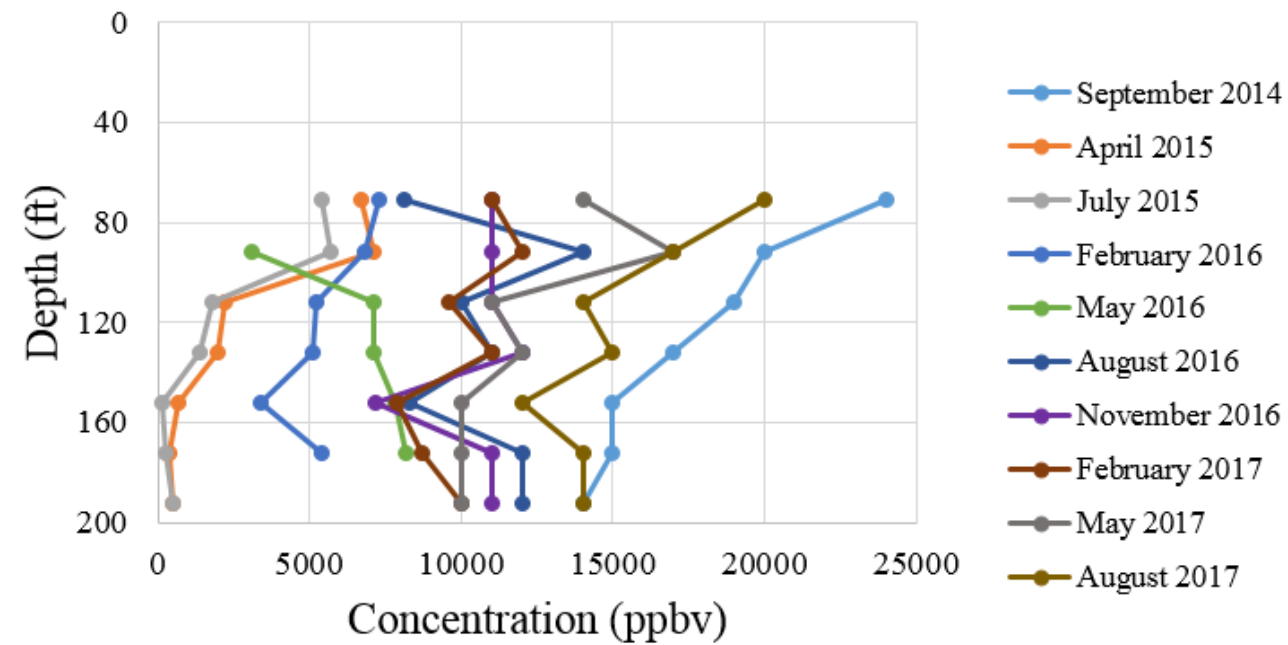
1,2-DCA at Borehole 54-24241



TCE at Borehole 54-24241



PCE at Borehole 54-24241



1,1,1-TCA at Borehole 54-24241

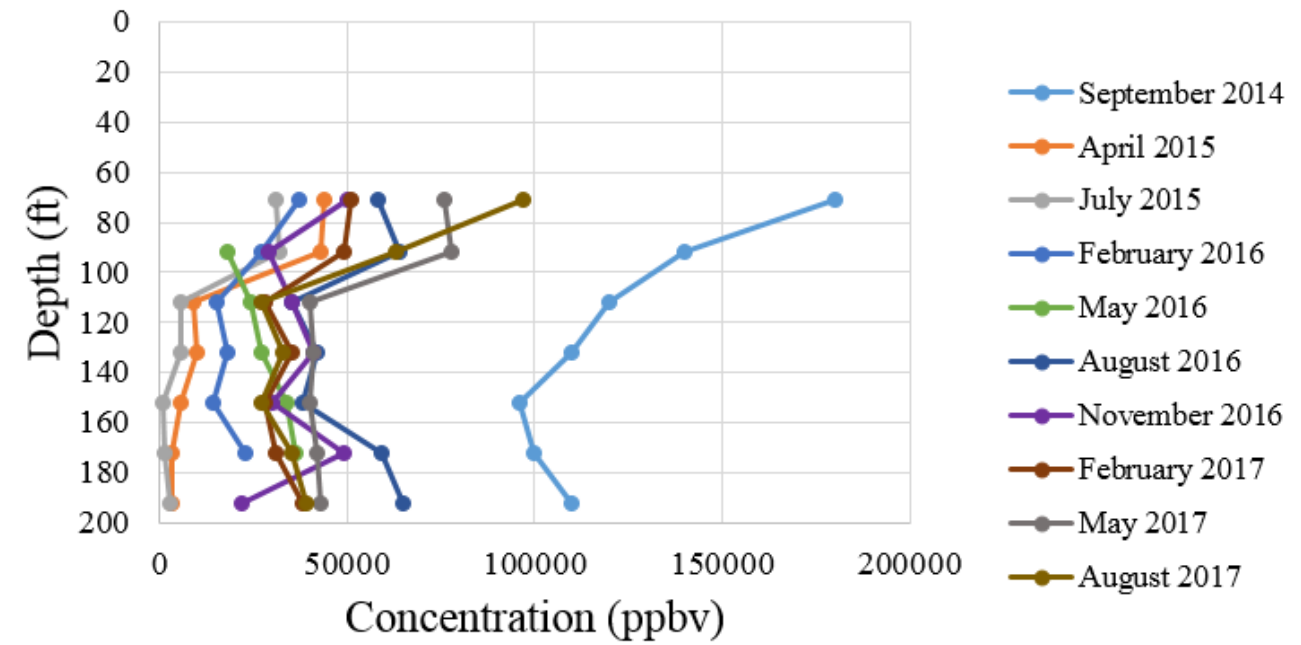
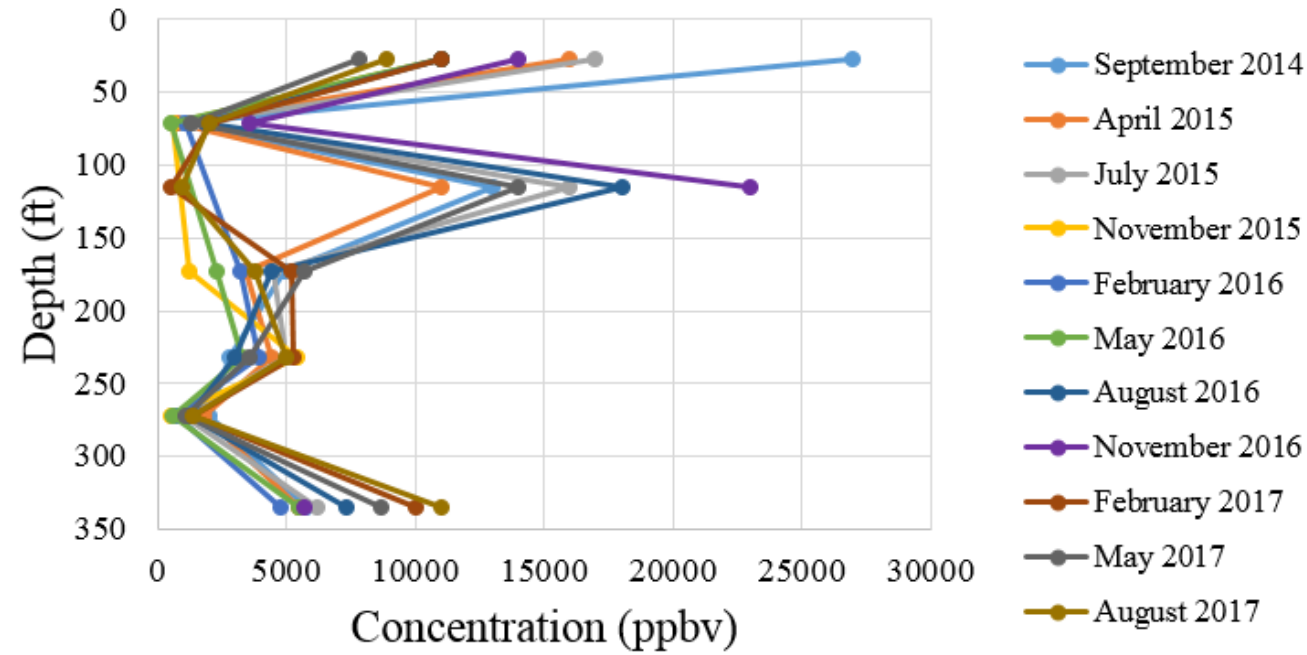
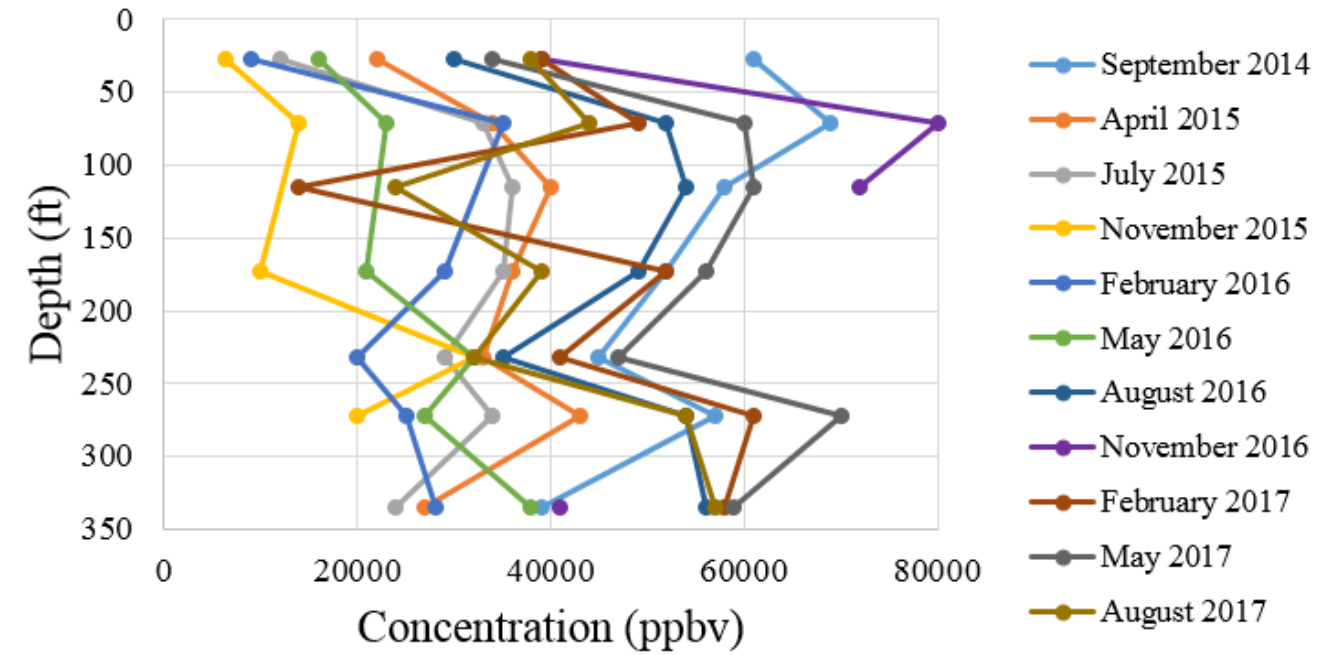


Figure 4.3-11 DCA[1,2], TCE, PCE, and 1,1,1-TCA concentration data for borehole 54-24241

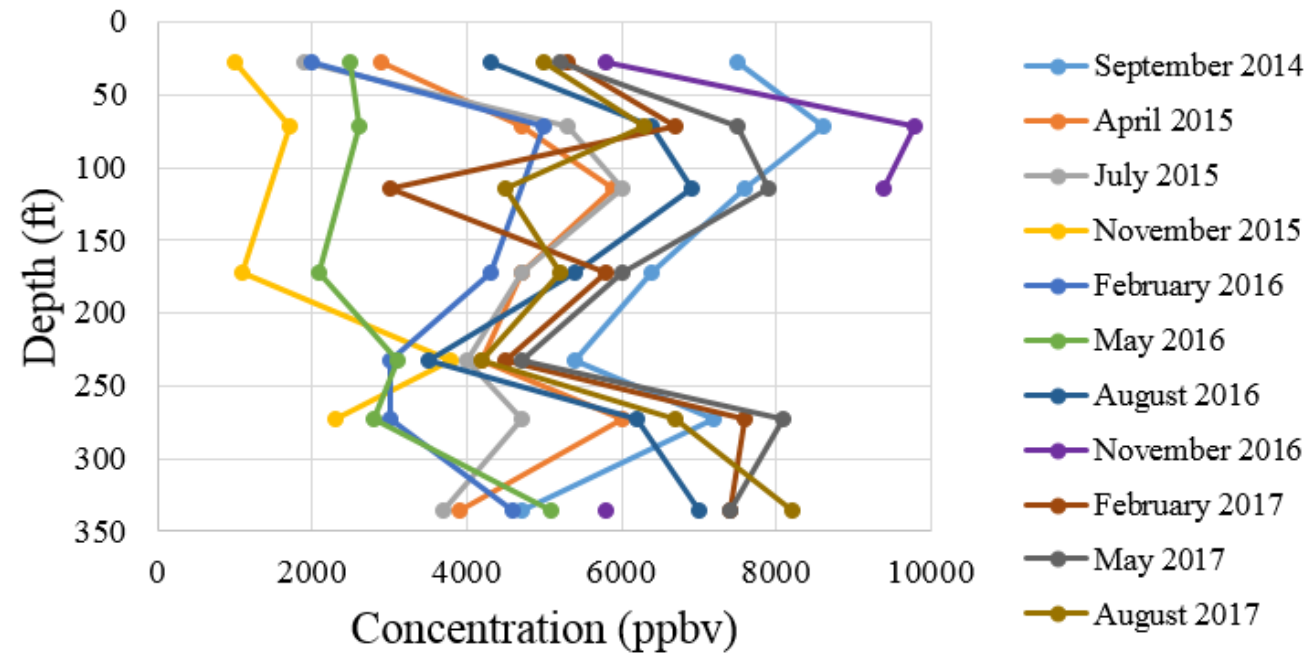
1,2-DCA at Borehole 54-27642



TCE at Borehole 54-27642



PCE at Borehole 54-27642



1,1,1-TCA at Borehole 54-27642

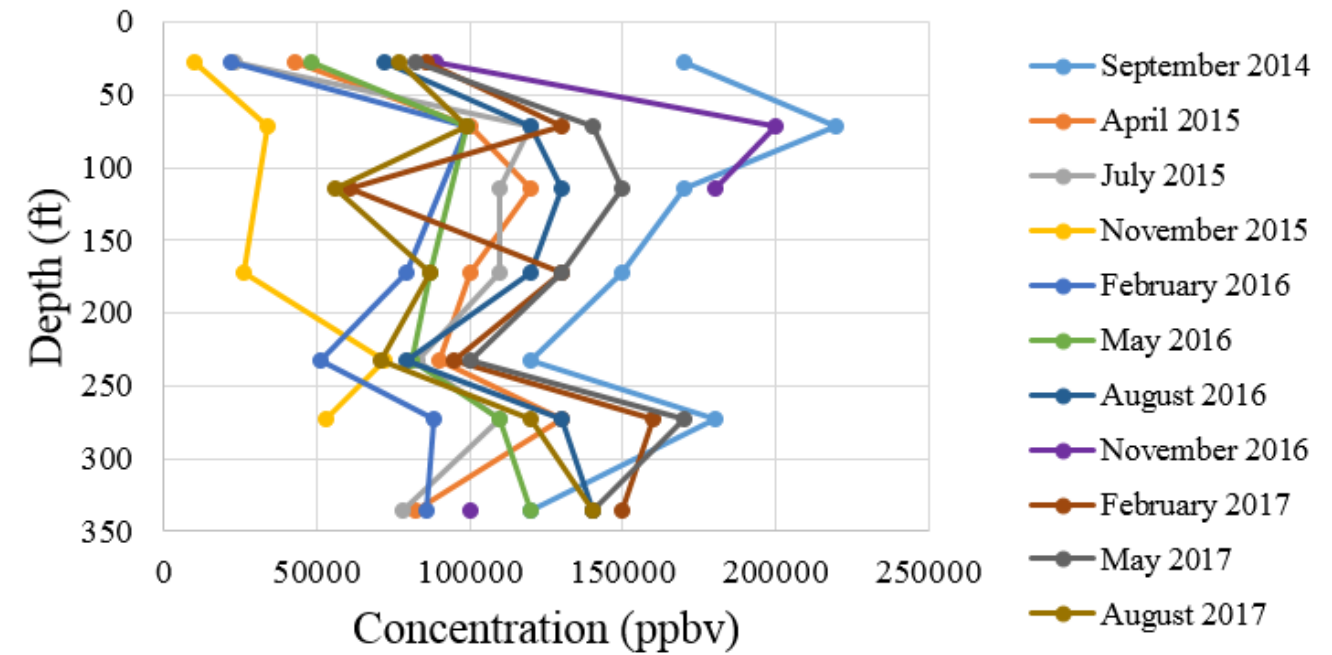
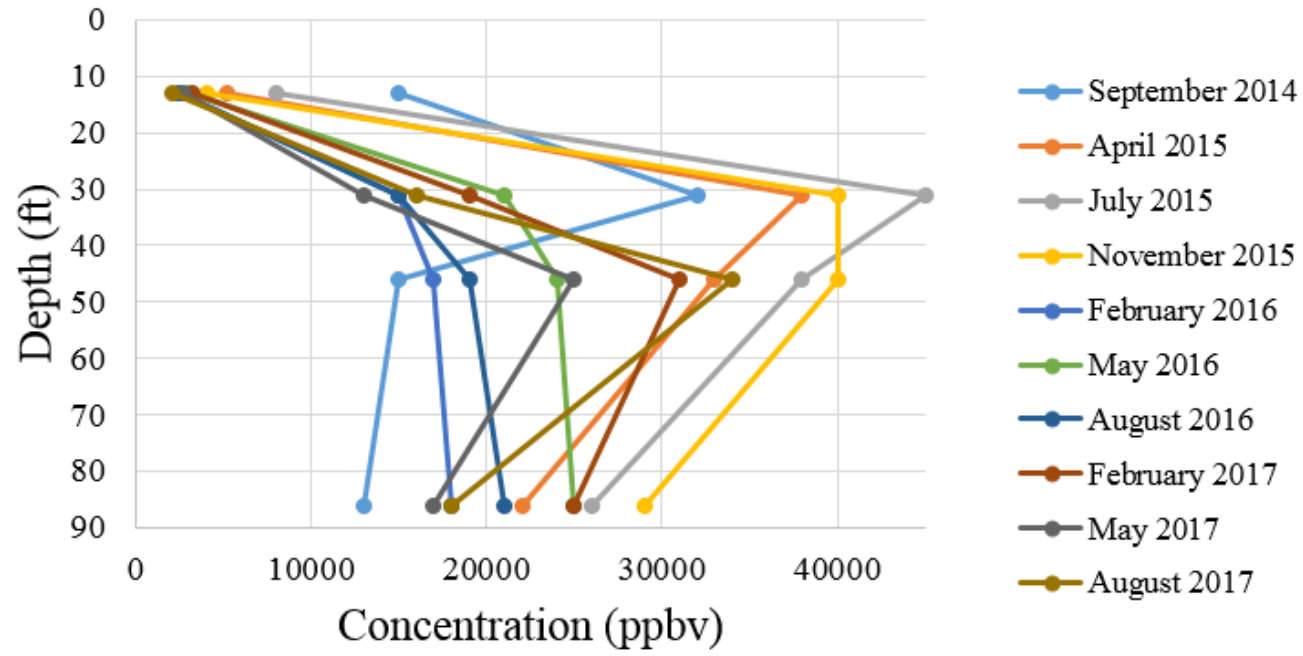
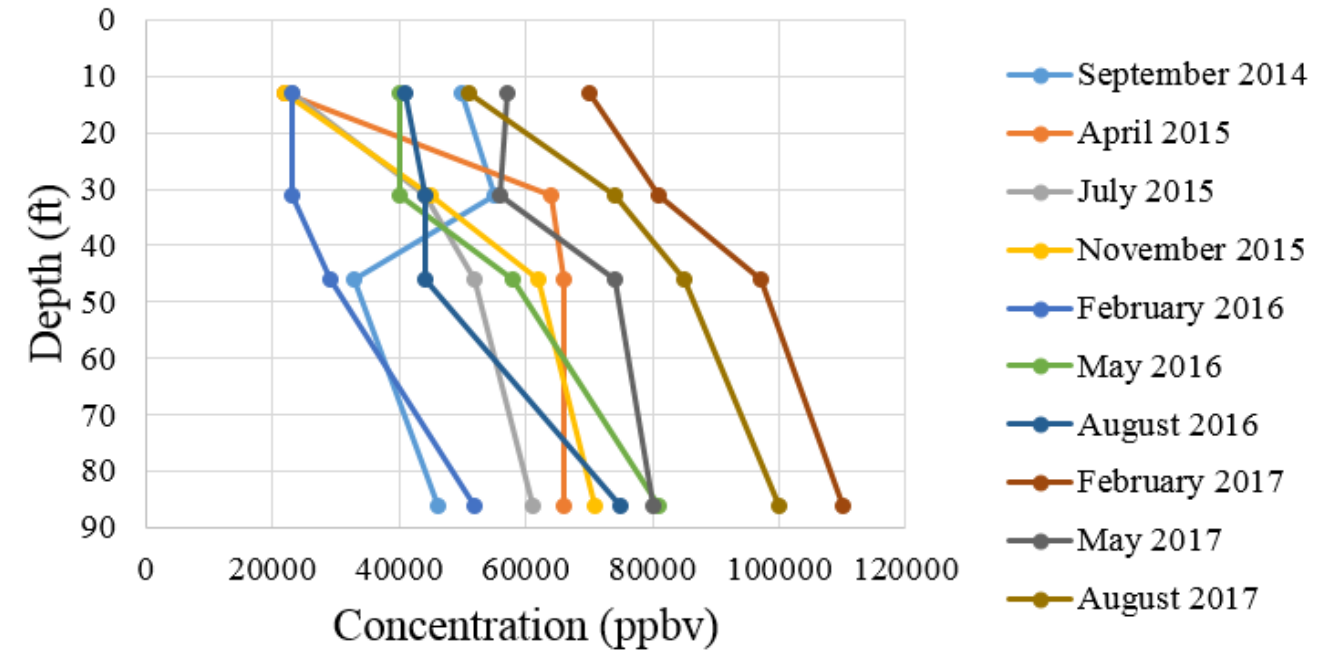


Figure 4.3-12 DCA[1,2], TCE, PCE, and 1,1,1-TCA concentration data for borehole 54-27642

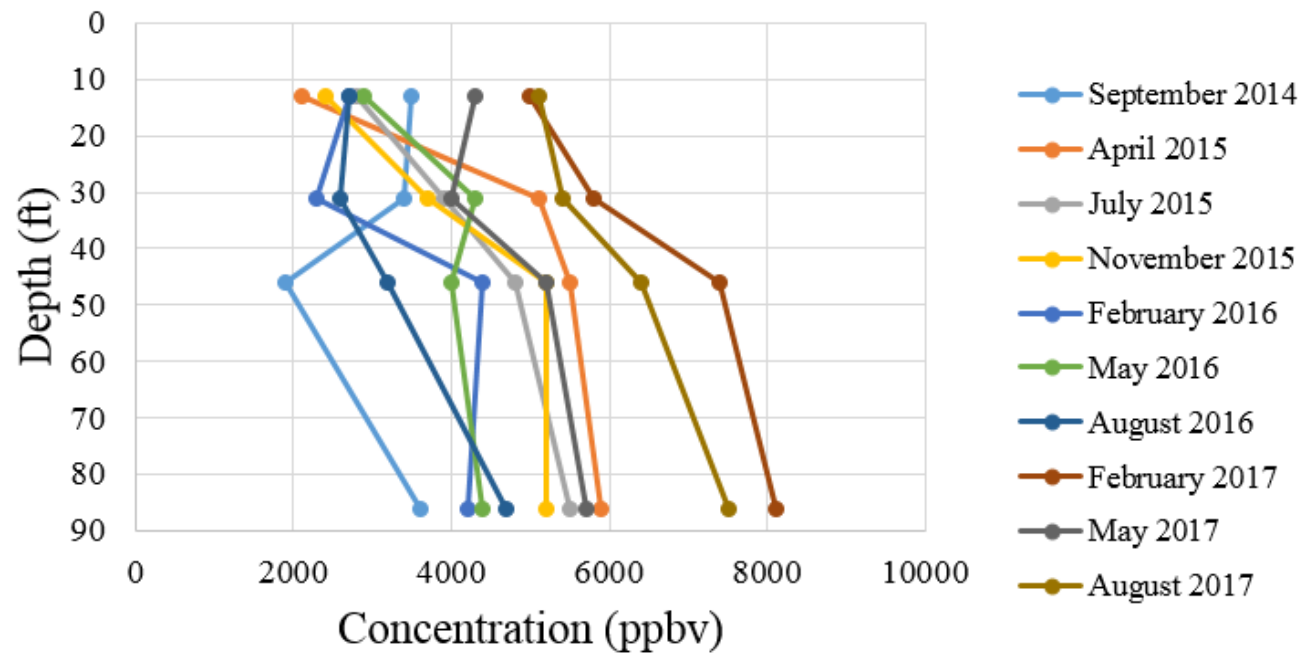
1,2-DCA at Borehole 54-02089



TCE at Borehole 54-02089



PCE at Borehole 54-02089



1,1,1-TCA at Borehole 54-02089

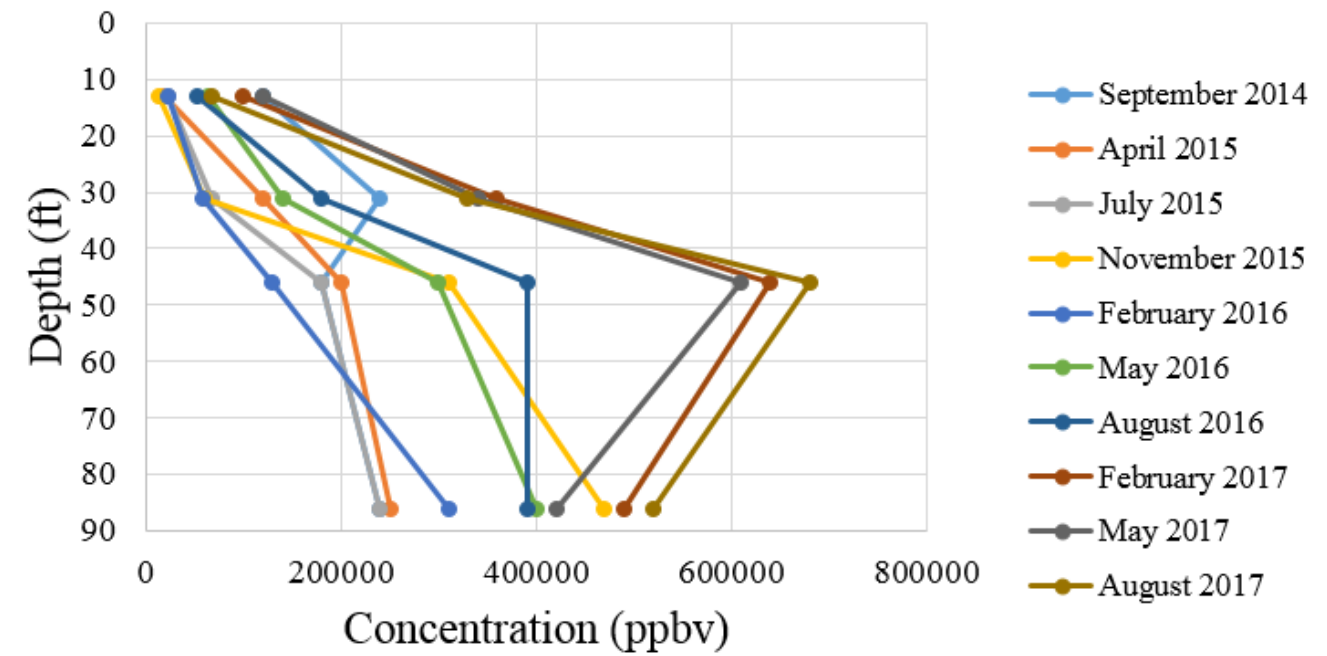
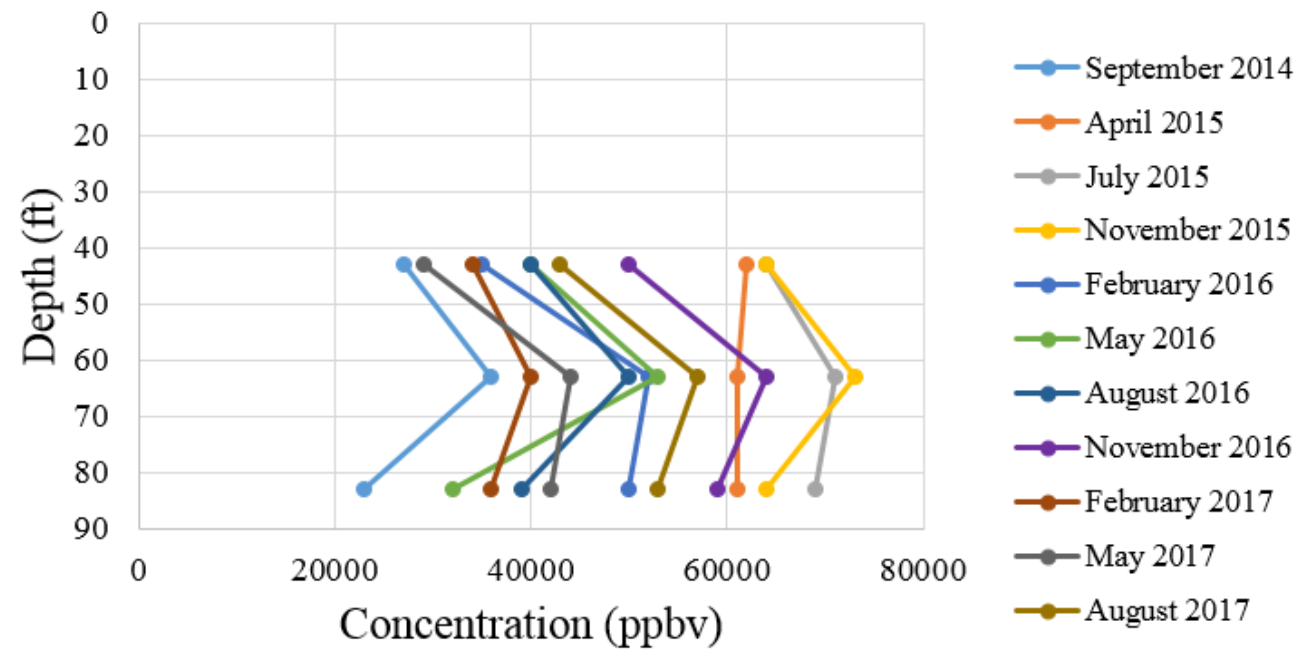
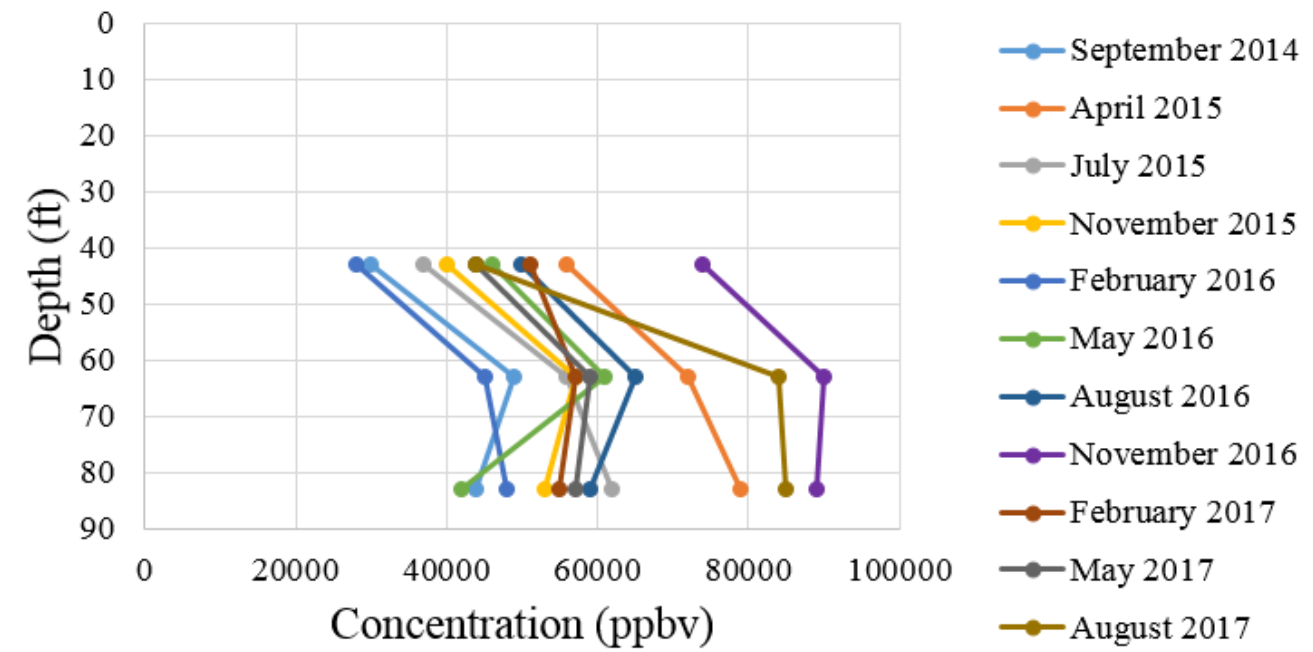


Figure 4.3-13 DCA[1,2], TCE, PCE, and 1,1,1-TCA concentration data for borehole 54-02089

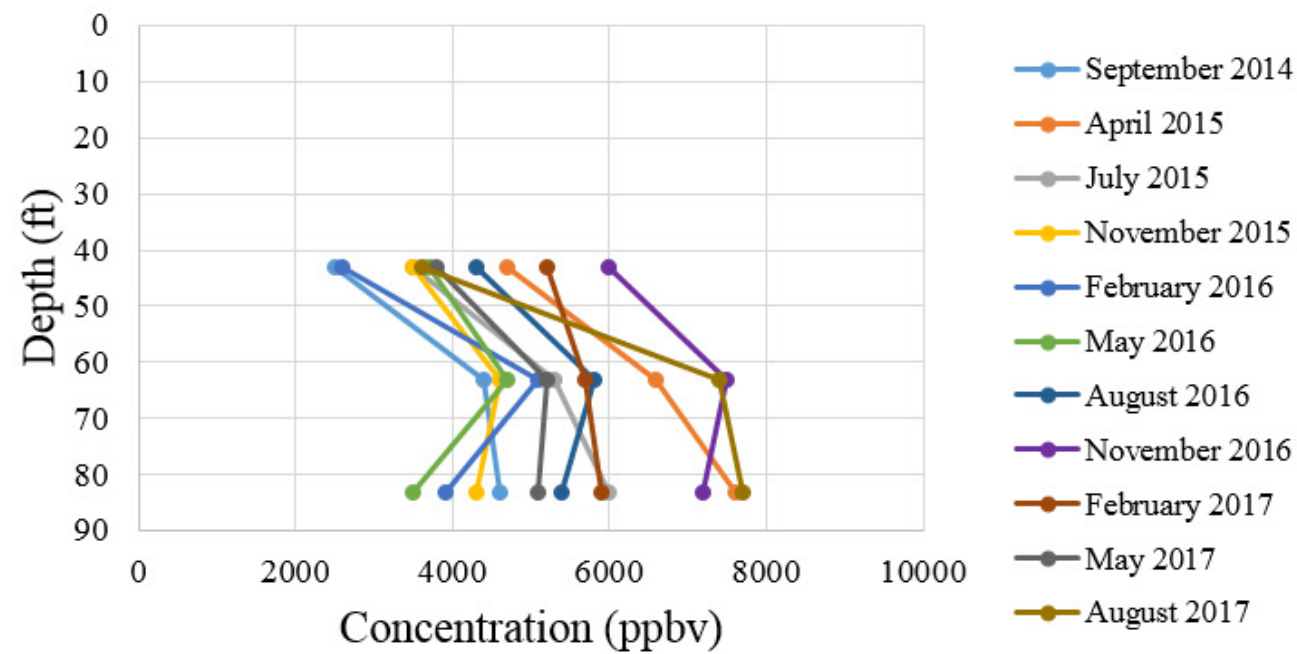
1,2-DCA at Borehole 54-24238



TCE at Borehole 54-24238



PCE at Borehole 54-24238



1,1,1-TCA at Borehole 54-24238

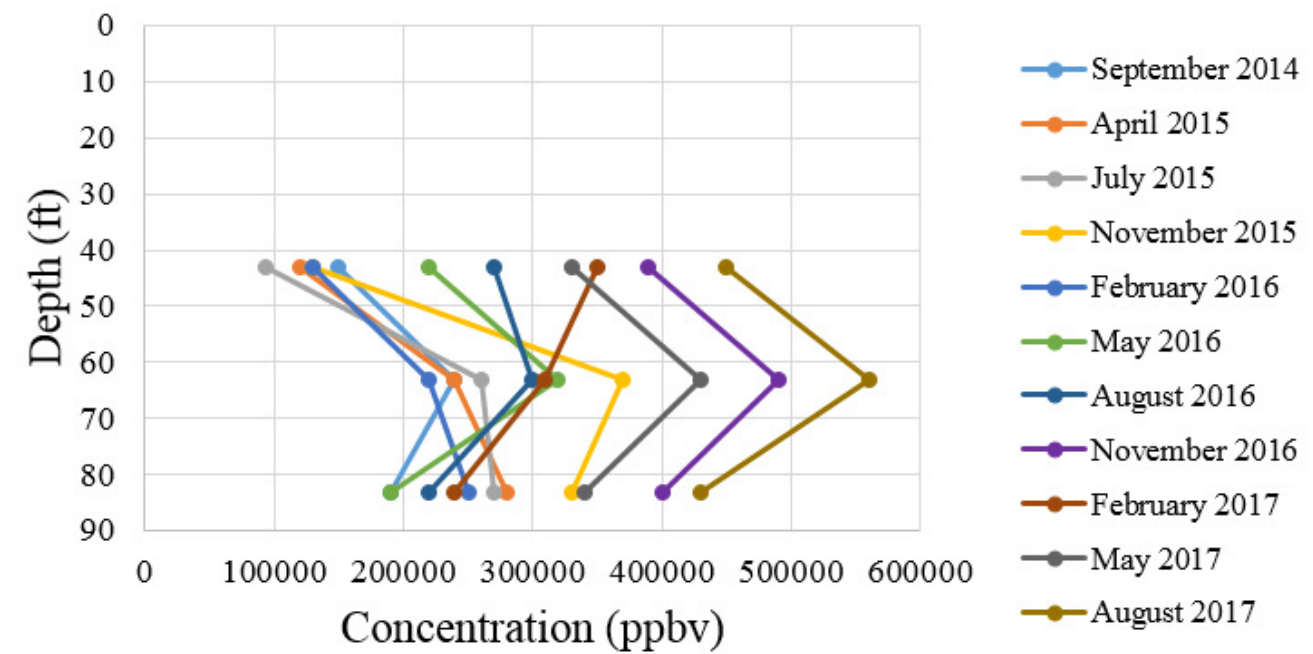


Figure 4.3-14 DCA[1,2], TCE, PCE, and 1,1,1-TCA concentration data for borehole 54-24238

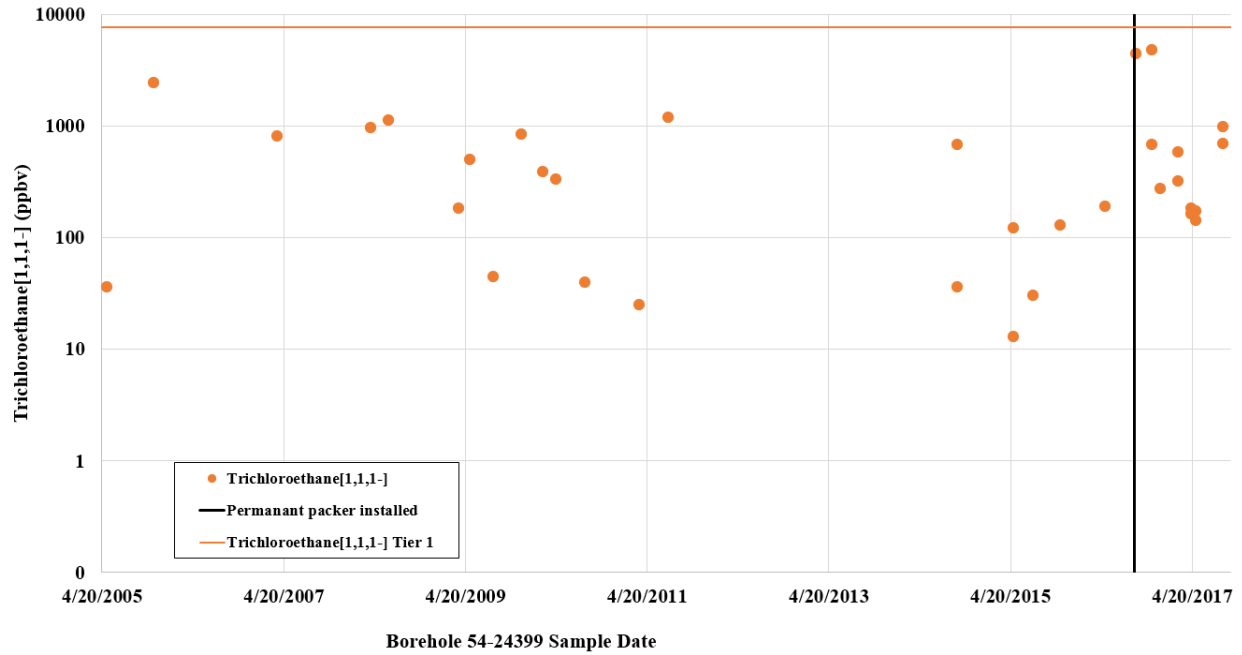


Figure 4.4-1 TCA[1,1,1] in borehole 54-24399 sampled using SUMMA canisters, relative to the Tier 1 screening level

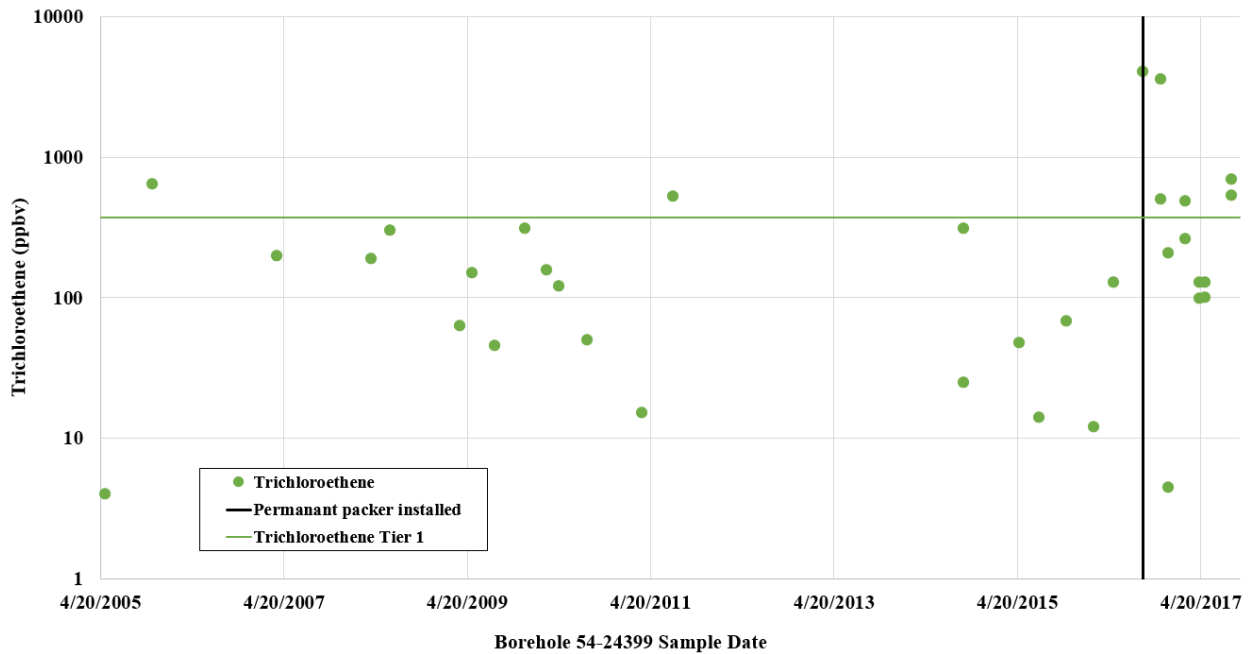


Figure 4.4-2 TCE in borehole 54-24399 sampled using SUMMA canisters, relative to the Tier 1 screening level

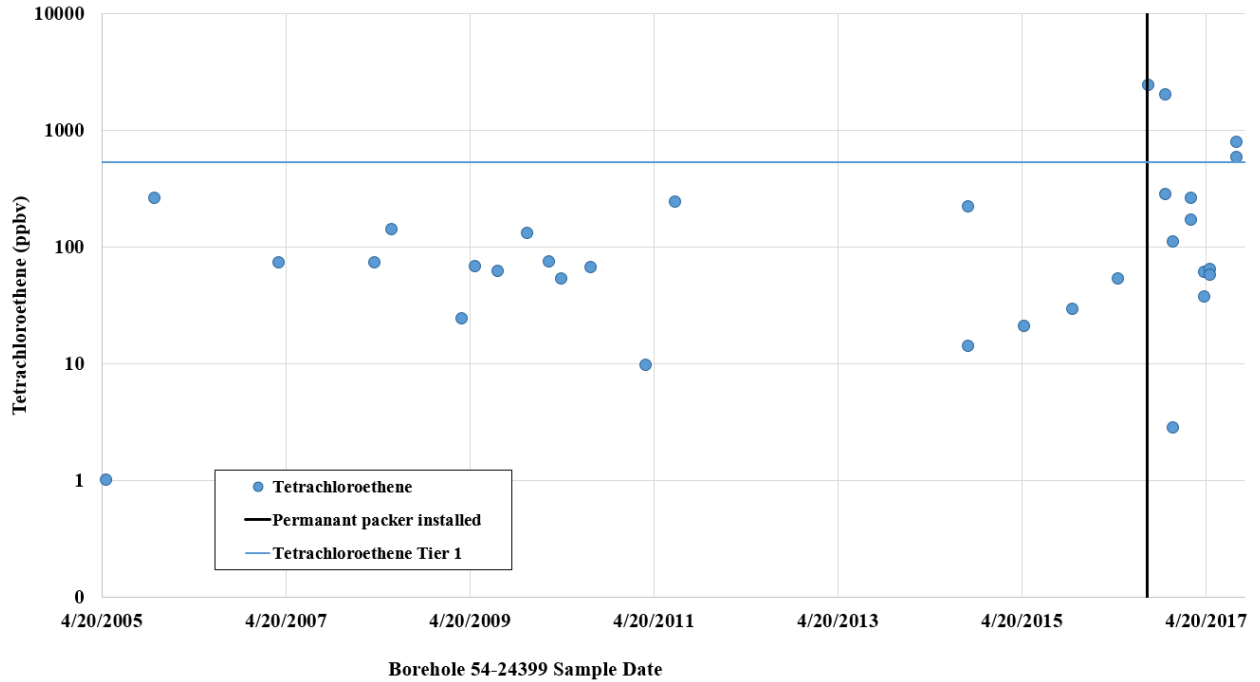


Figure 4.4-3 PCE in borehole 54-24399 sampled using SUMMA canisters, relative to the Tier 1 screening level

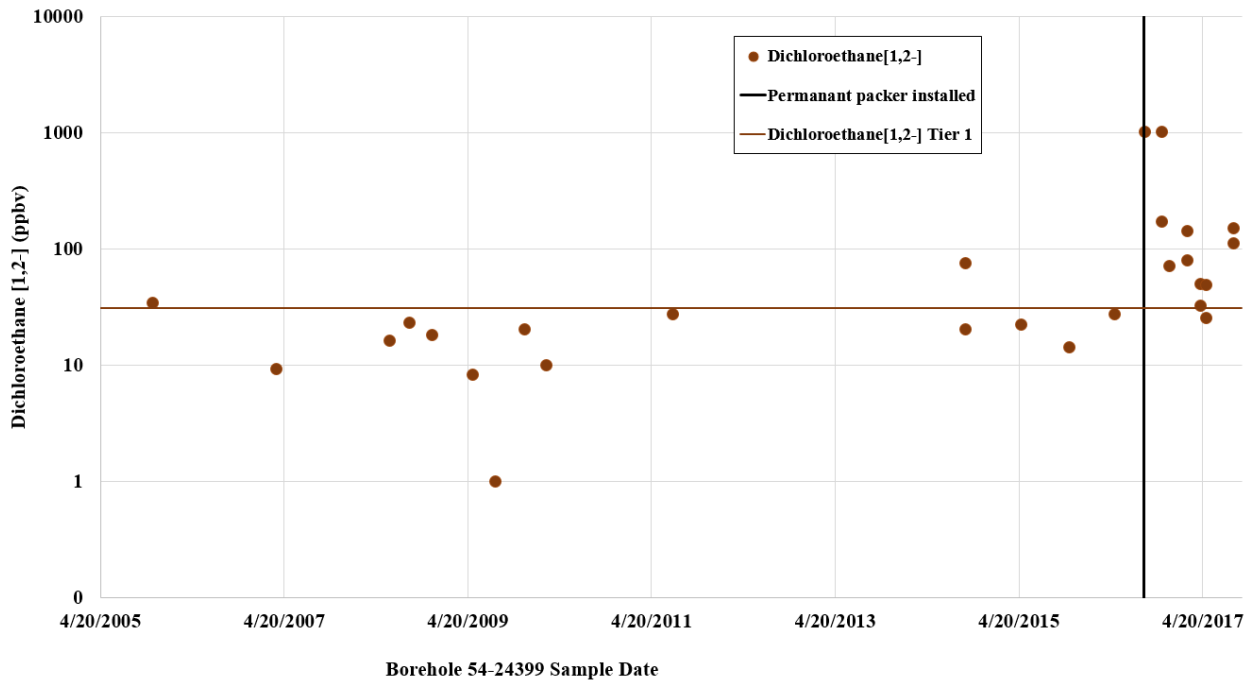


Figure 4.4-4 DCA[1,2] in borehole 54-24399 sampled using SUMMA canisters, relative to the Tier 1 screening level

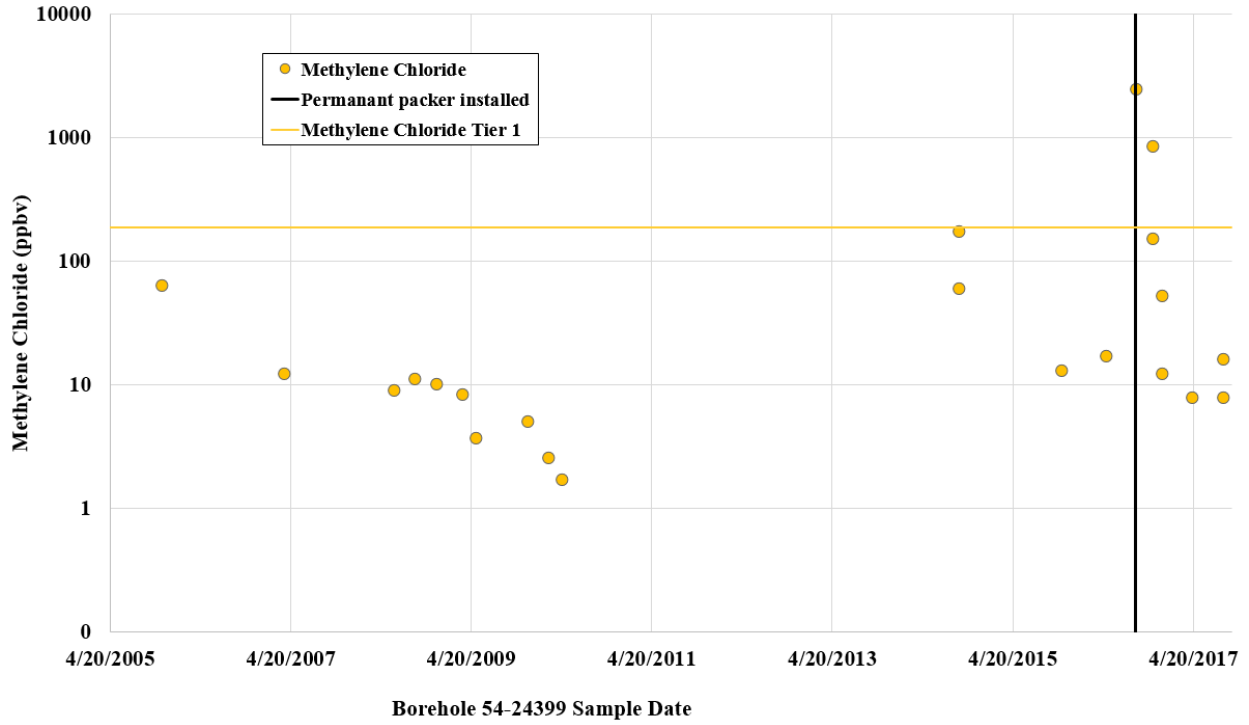


Figure 4.4-5 Methylene chloride in borehole 54-24399 sampled using SUMMA canisters, relative to the Tier 1 screening level

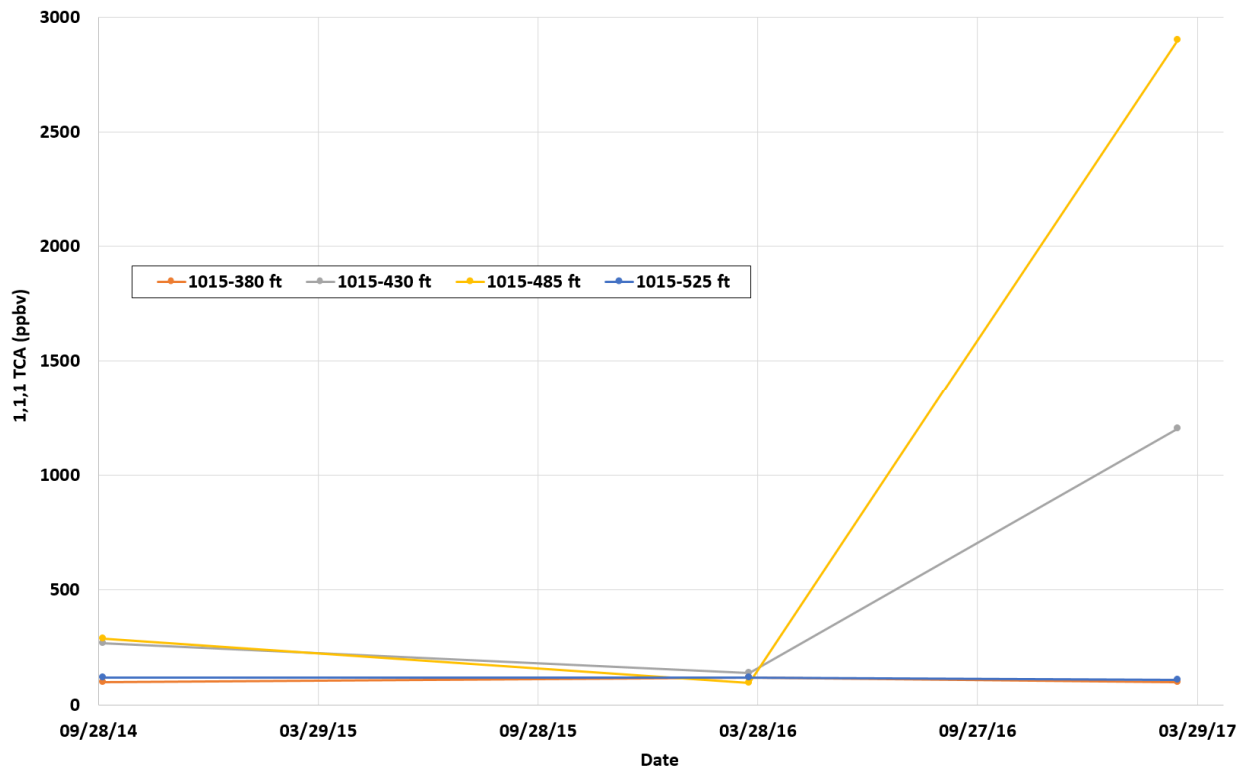


Figure 4.4-6 Concentration of 1,1,1-TCA in borehole 54-01015

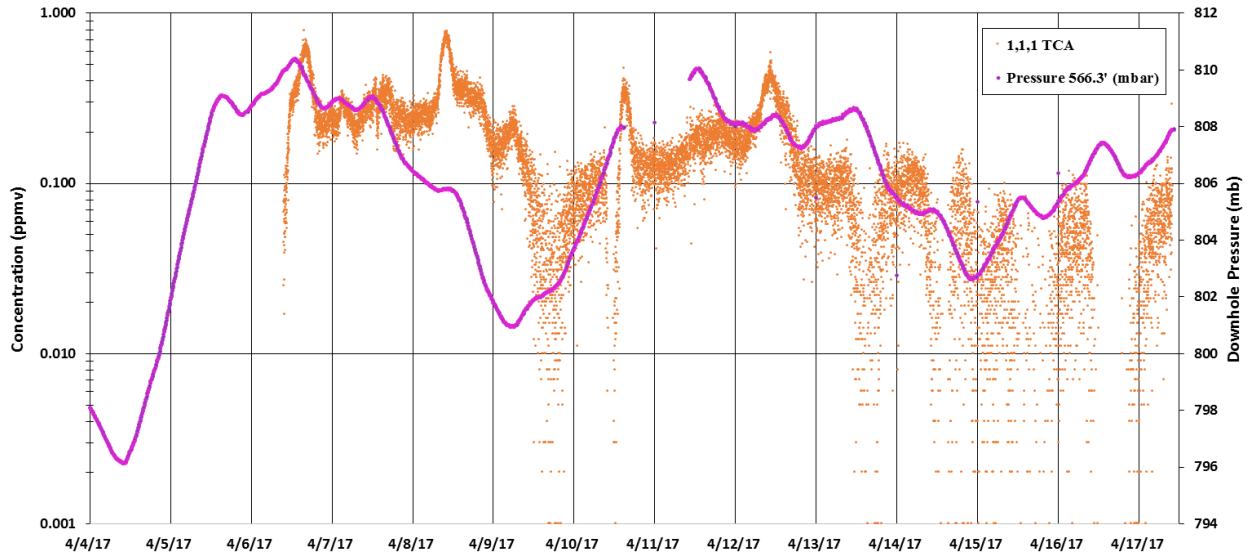


Figure 4.4-7 LumaSense Photoacoustic Gas Monitor measurements of 1,1,1-TCA from borehole 54-24399 during 12 d in April 2017. Pressure measured beneath the packer is also shown.

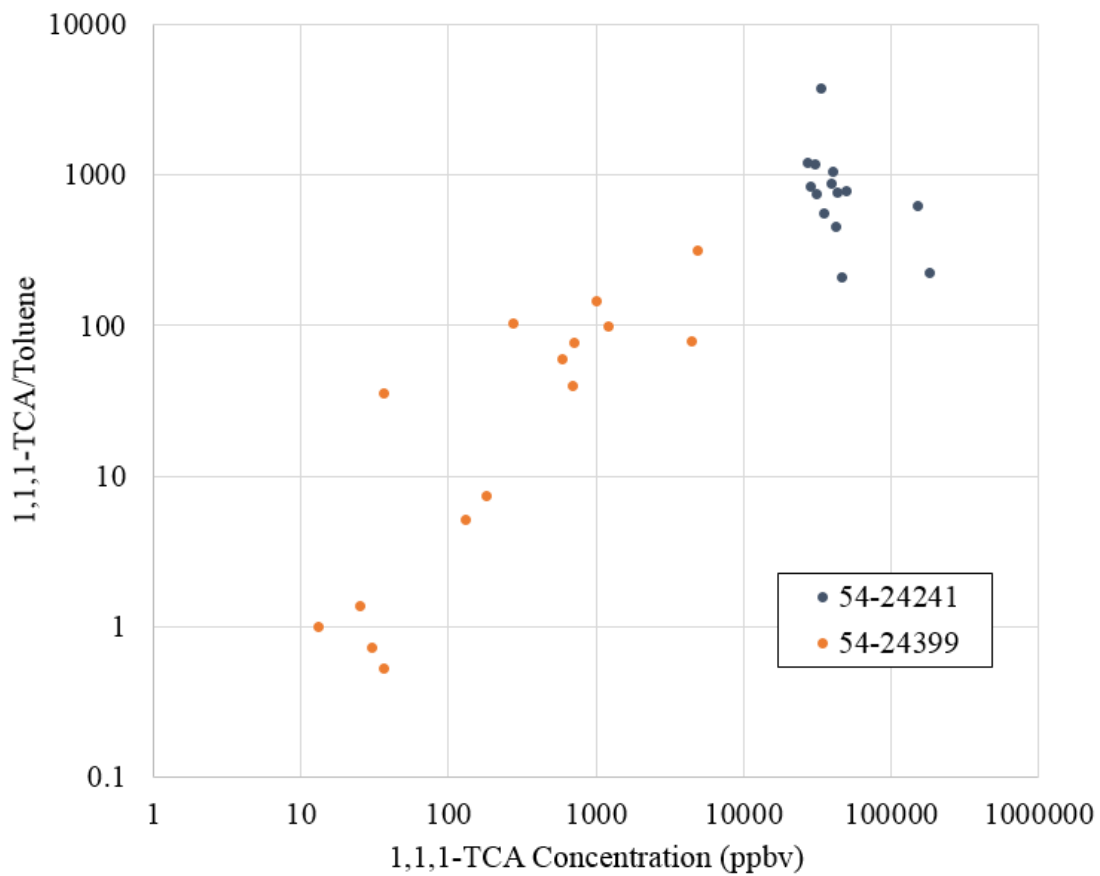


Figure 4.4-8 Ratio of 1,1,1-TCA to toluene plotted versus 1,1,1-TCA concentration comparing borehole 54-24399 with borehole 54-24241

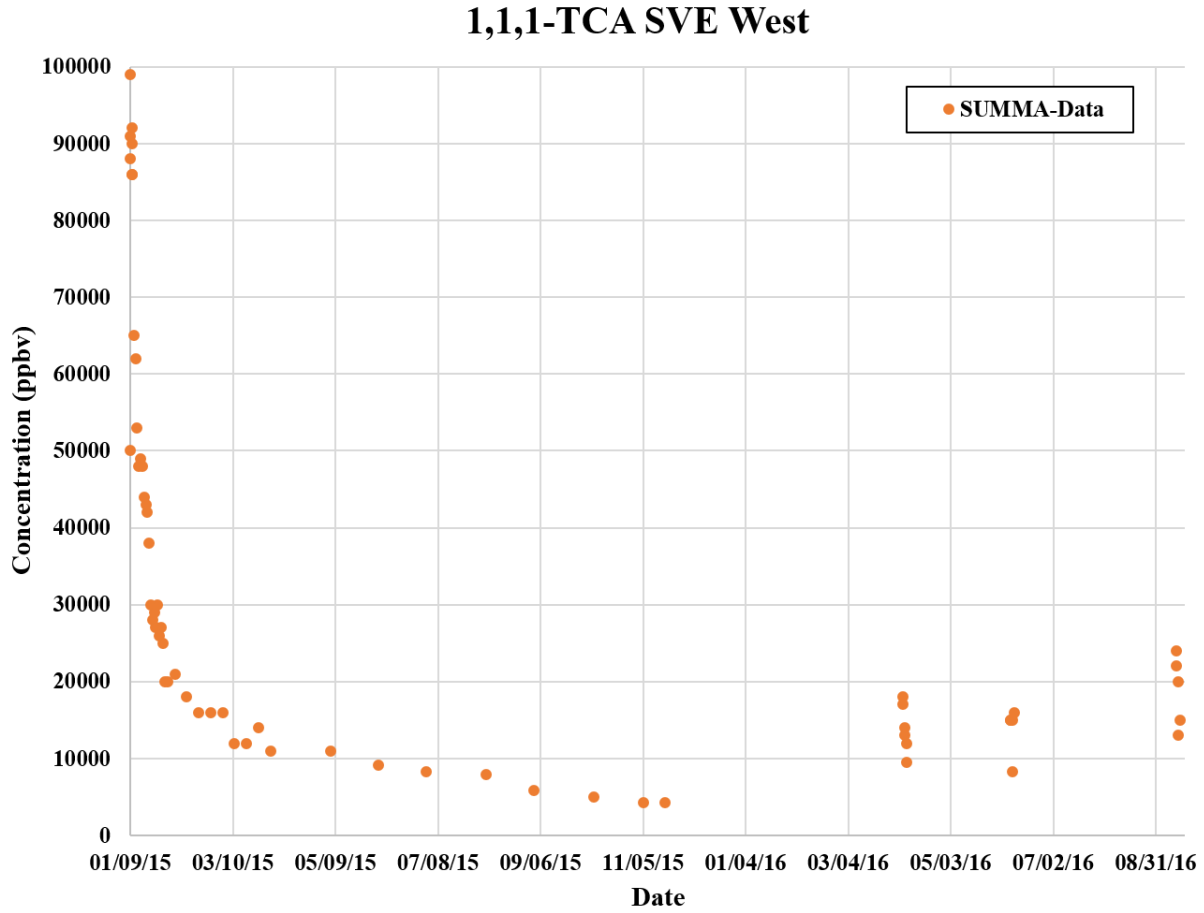


Figure 4.6-1 TCA[1,1,1] concentrations in effluent from SVE-West versus time including three short duration (2-d) rebound tests in 2016

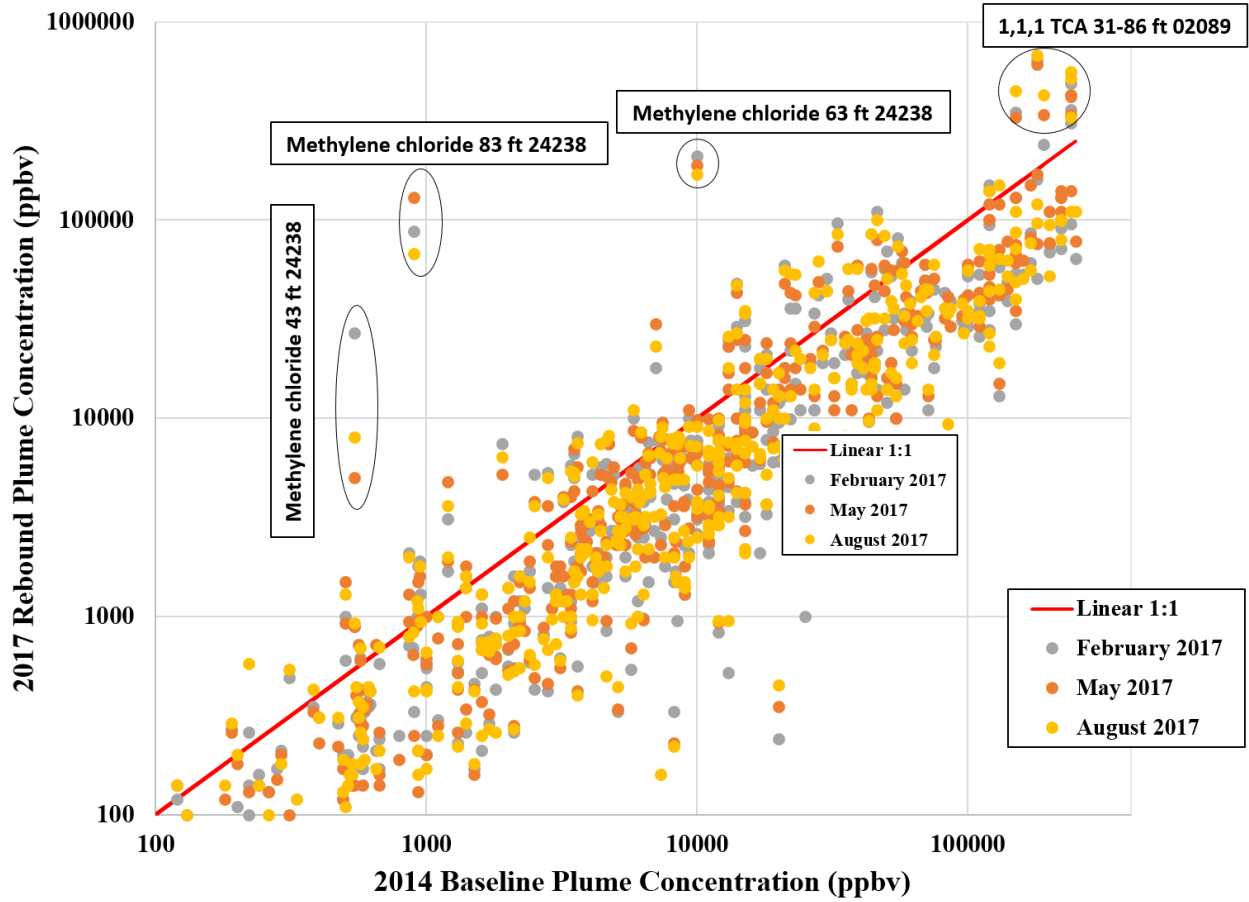


Figure 4.6-3 Subsurface plume concentrations in 2017 versus baseline (2014) concentrations for seven analytes

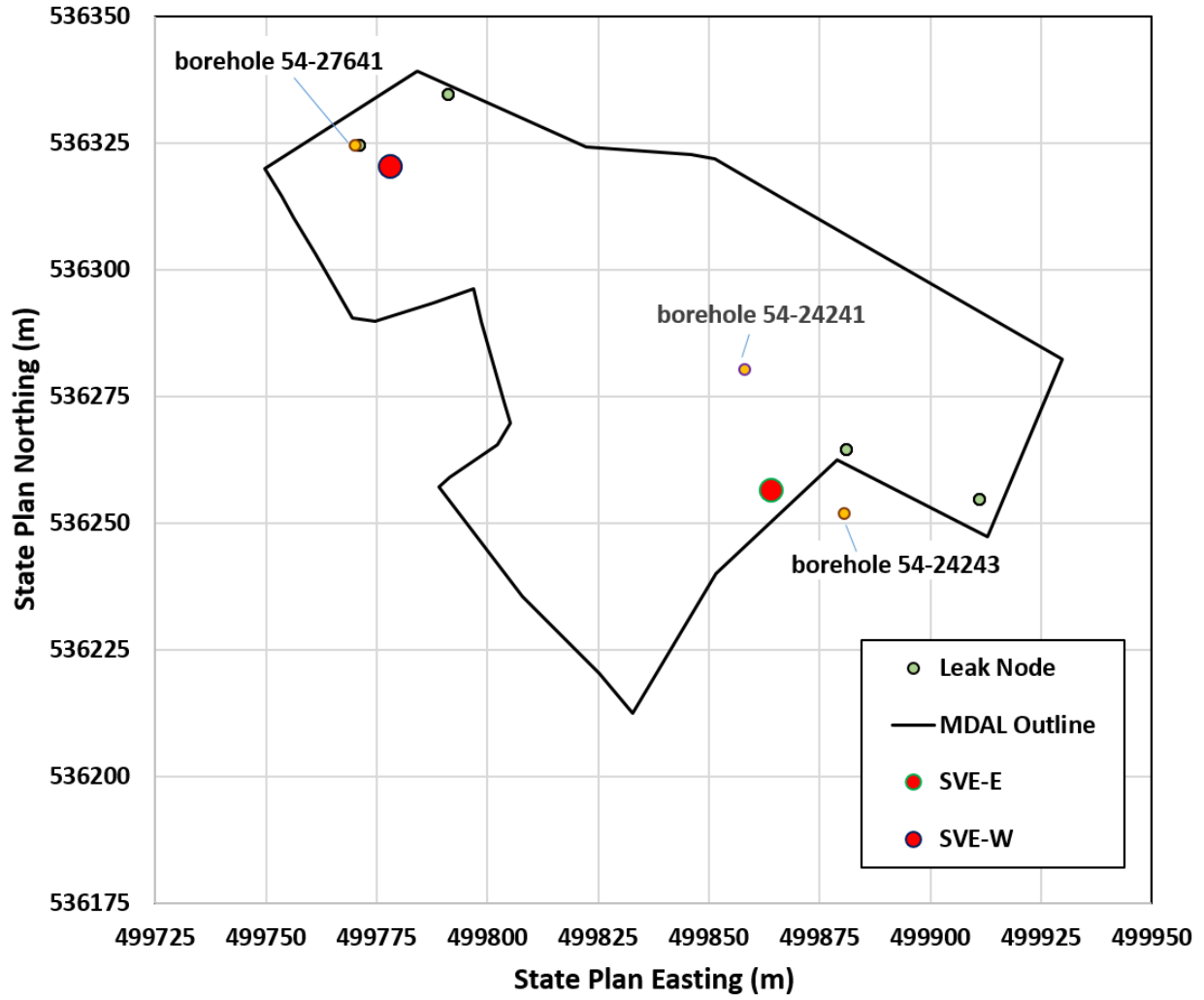


Figure 5.1-1 Locations of the MDA L outline, example monitoring boreholes, SVE units, and simulated leaking subsurface sources

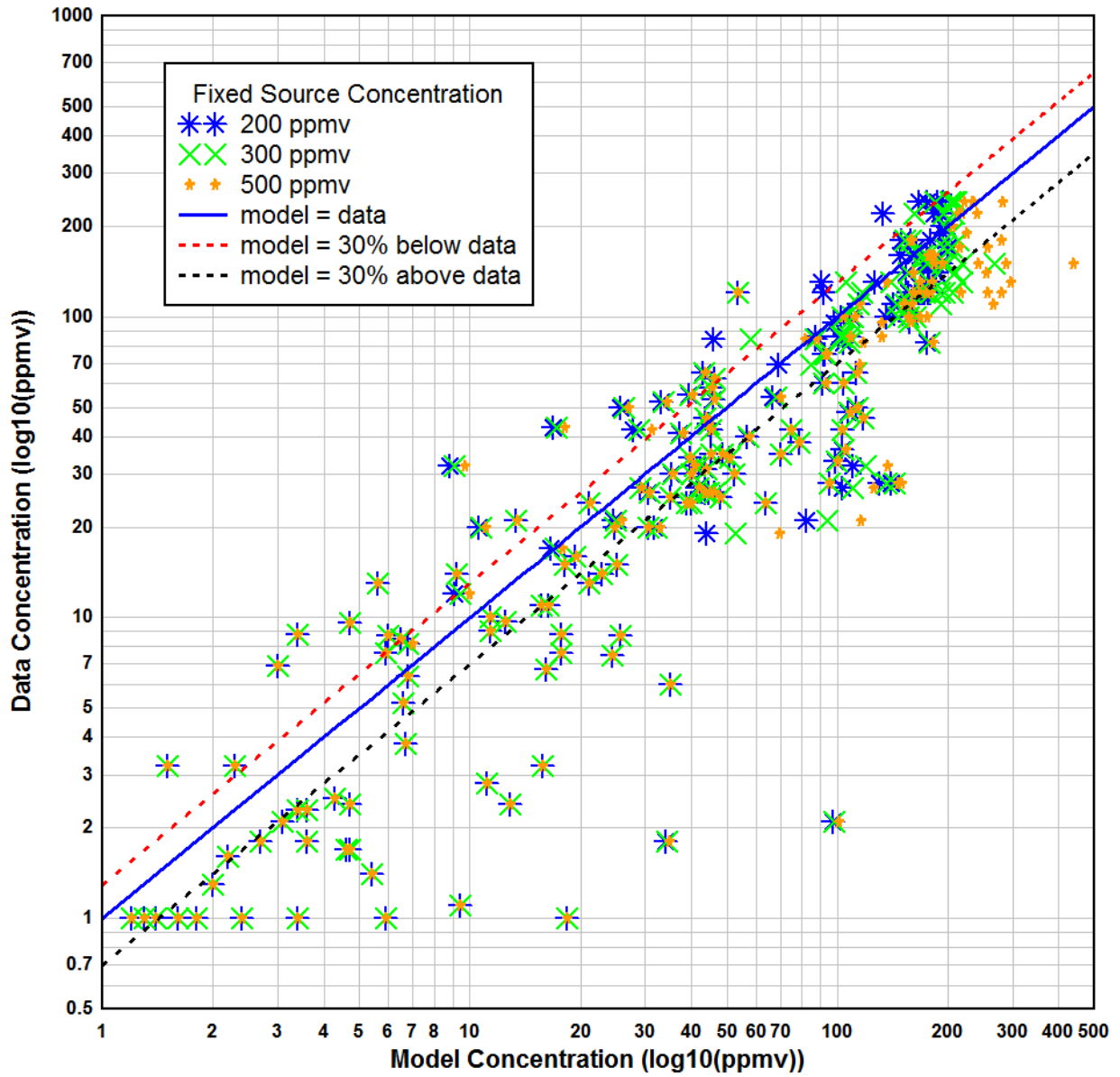
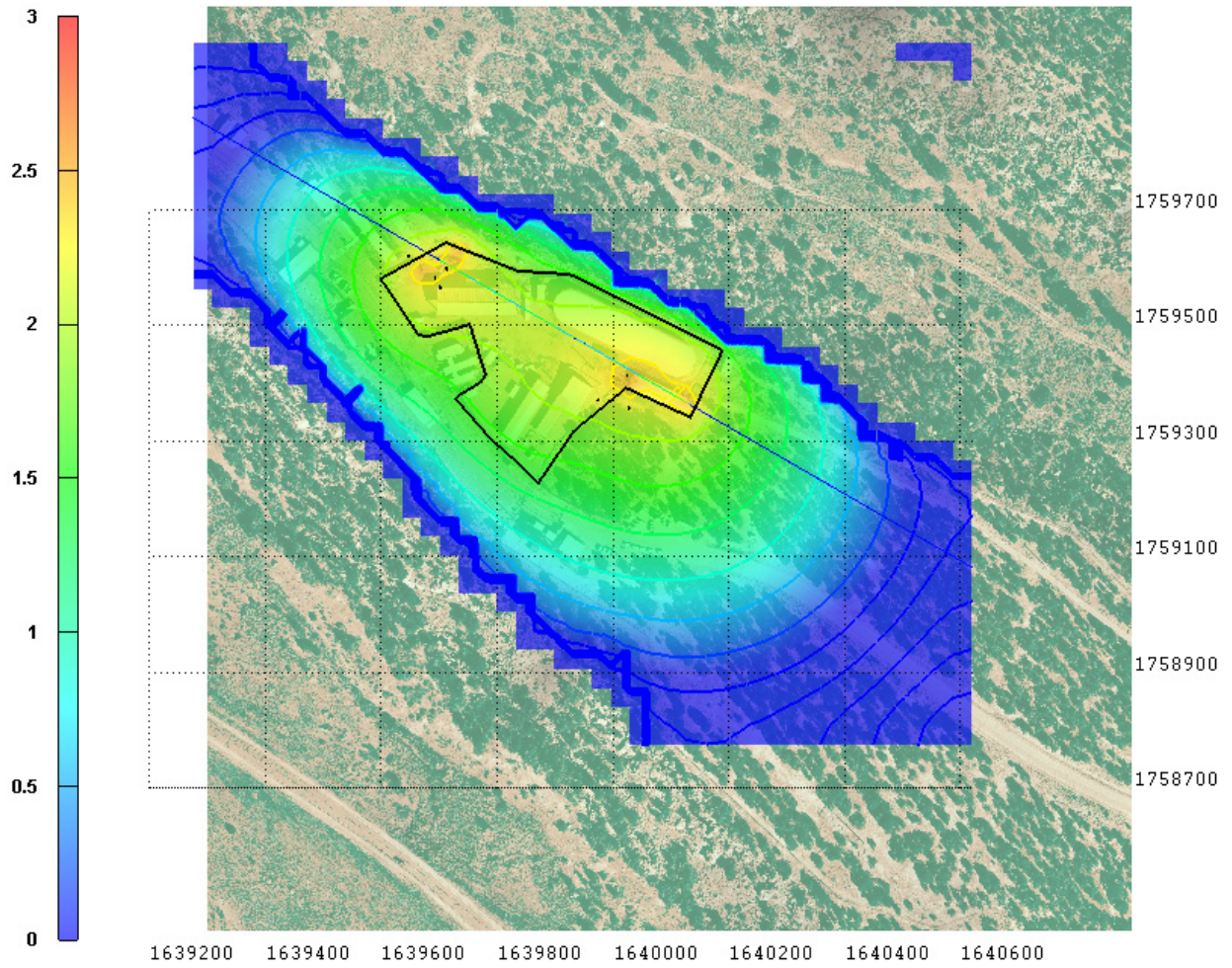


Figure 5.2-1 Simulated 1,1,1-TCA concentration compared with data for the 2014 baseline pre-SVE initial state



Note: X-Y units are State Plan feet while the legend shows log₁₀ (ppmv).

Figure 5.2-2 Simulated 1,1,1-TCA concentration on a plane 60 ft below the ground surface of MDA L

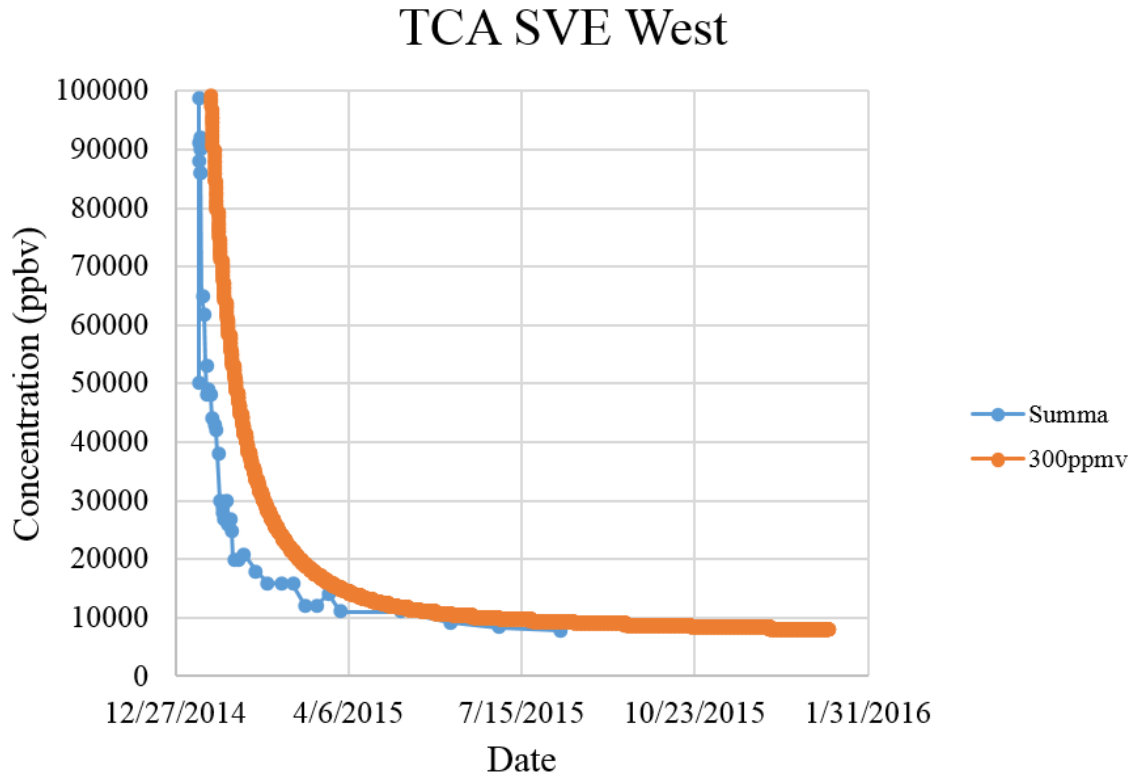


Figure 5.3-1 Predicted versus measured concentrations of 1,1,1-TCA at SVE-West

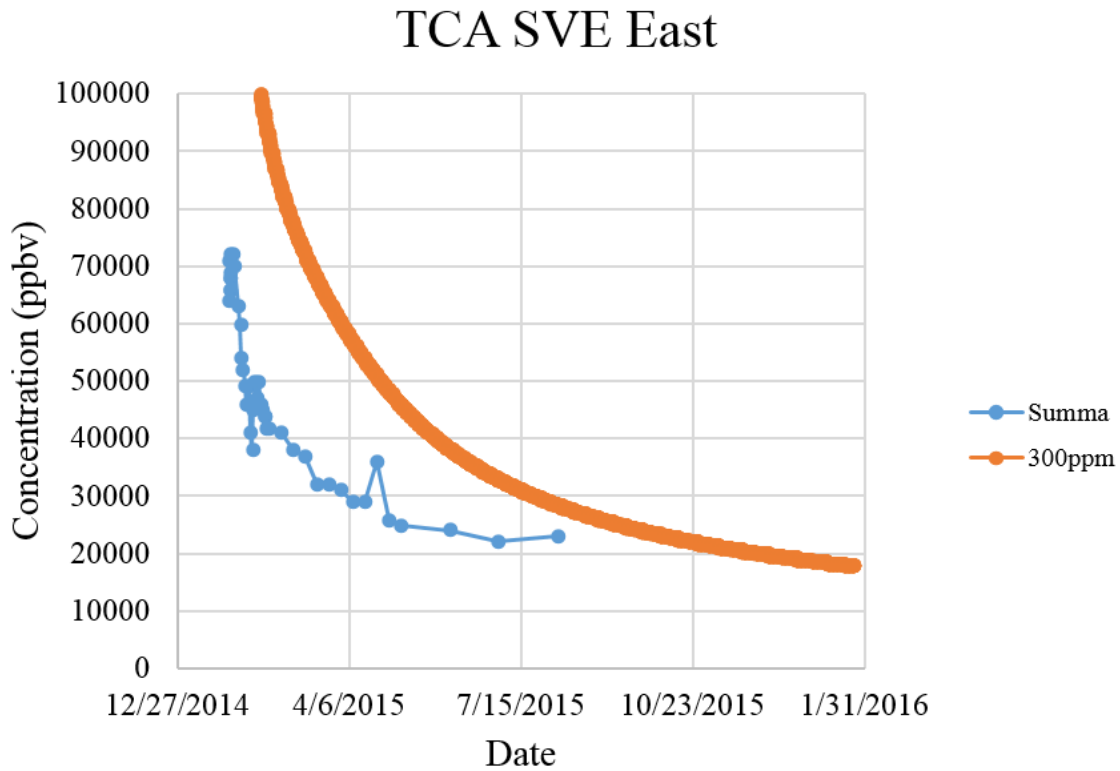


Figure 5.3-2 Predicted versus measured 1,1,1-TCA concentrations at SVE-East

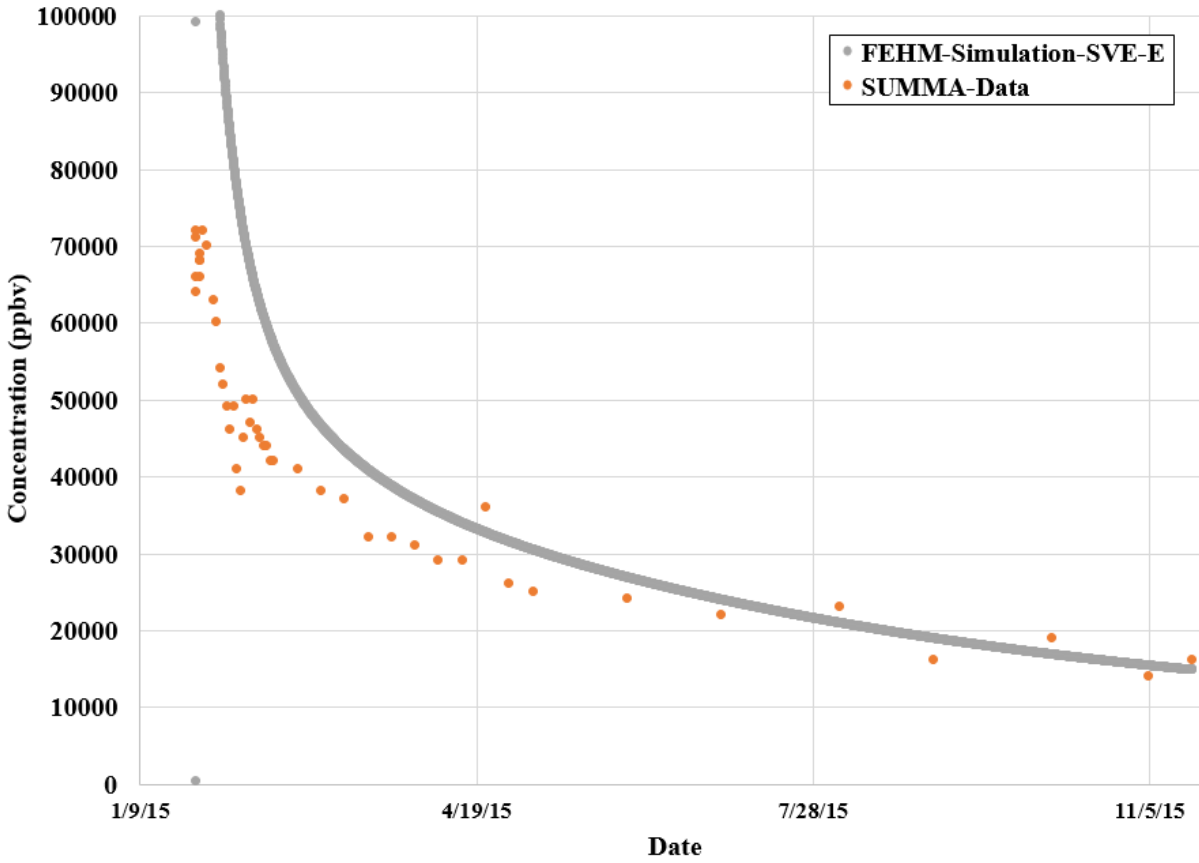


Figure 5.3-3 Predicted versus measured 1,1,1-TCA concentrations at SVE-East for the recalibrated simulation

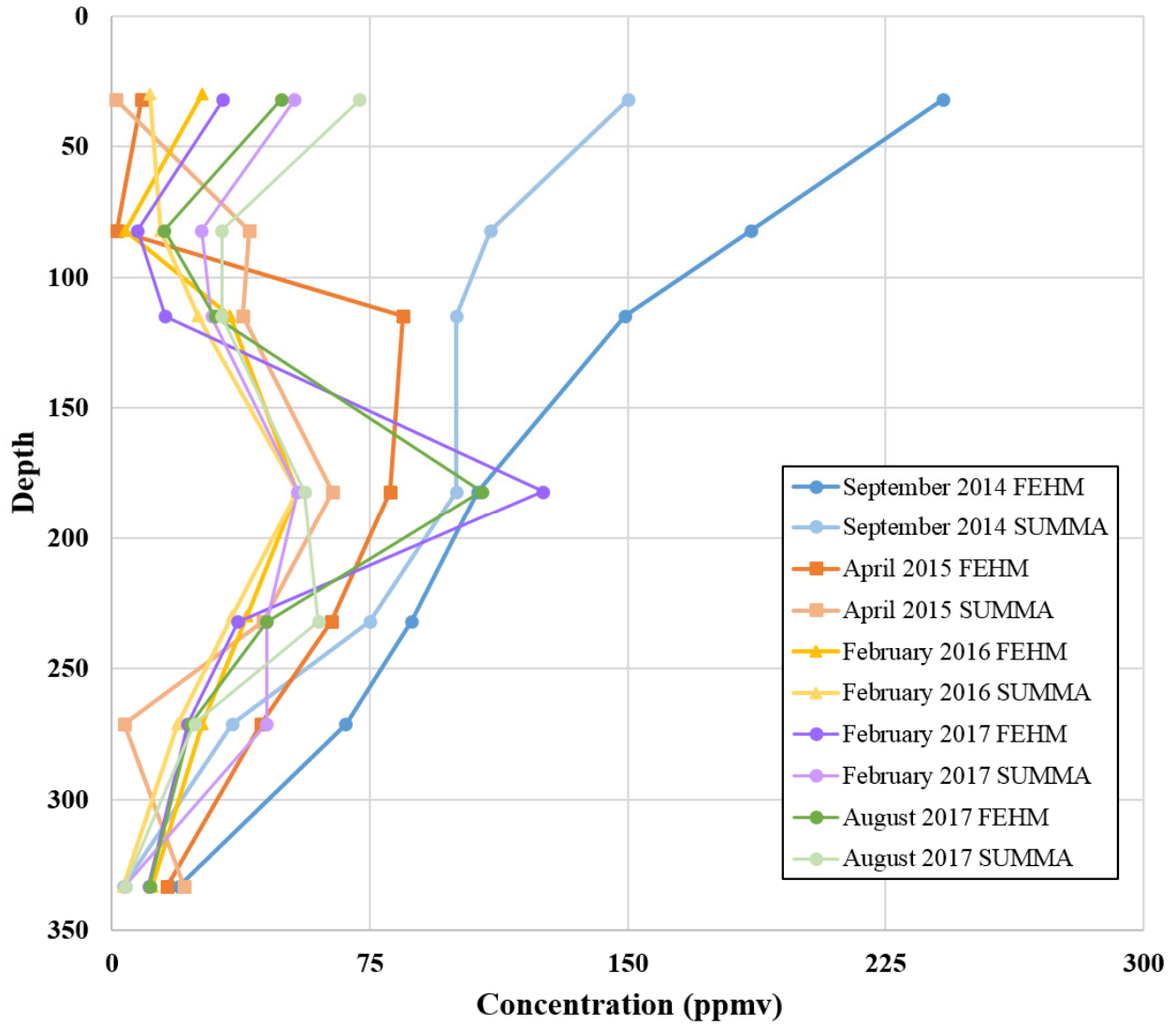


Figure 5.4-1 Simulated versus measured 1,1,1-TCA concentration in borehole 54-27641

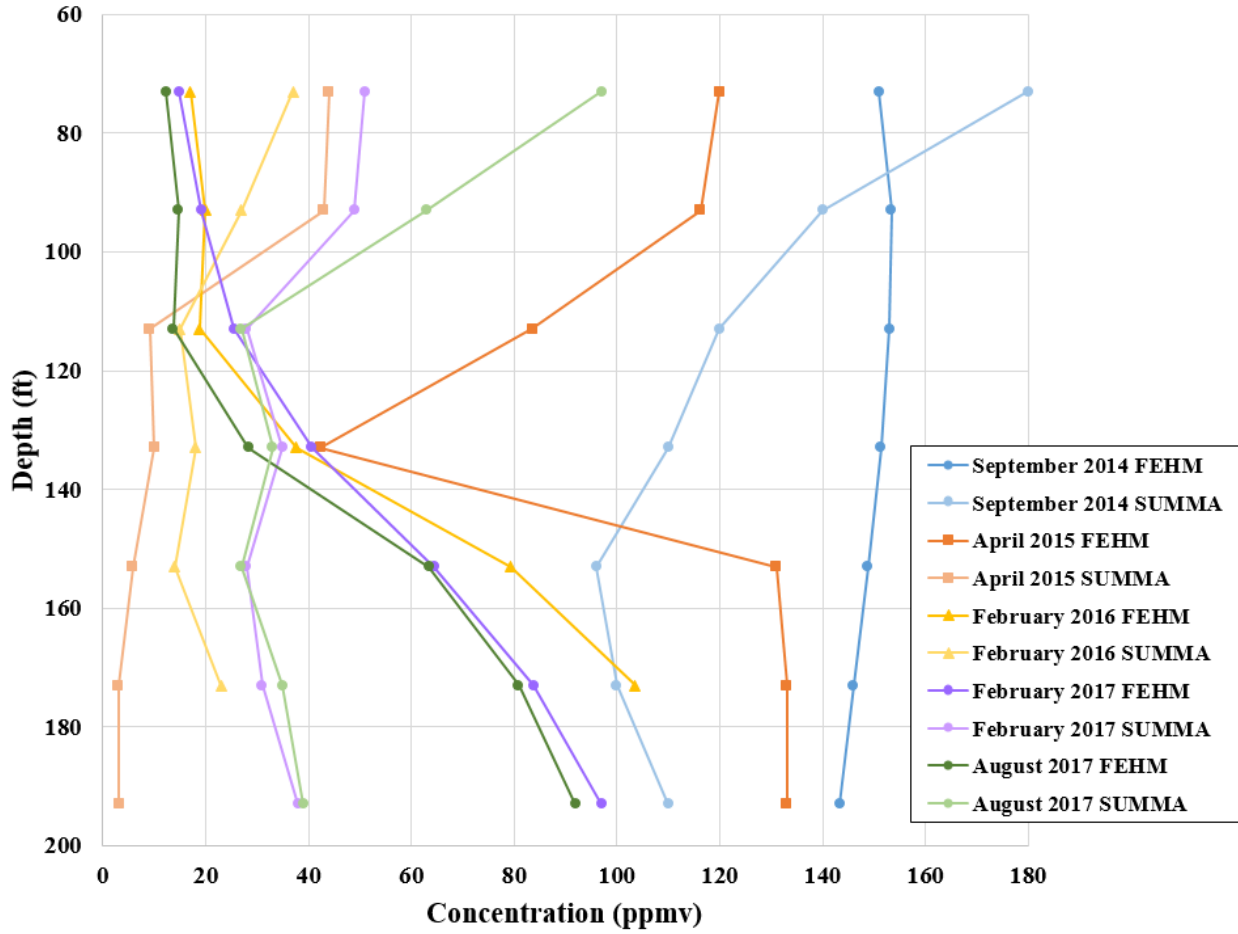


Figure 5.4-2 Simulated versus measured 1,1,1-TCA concentration in borehole 54-24241

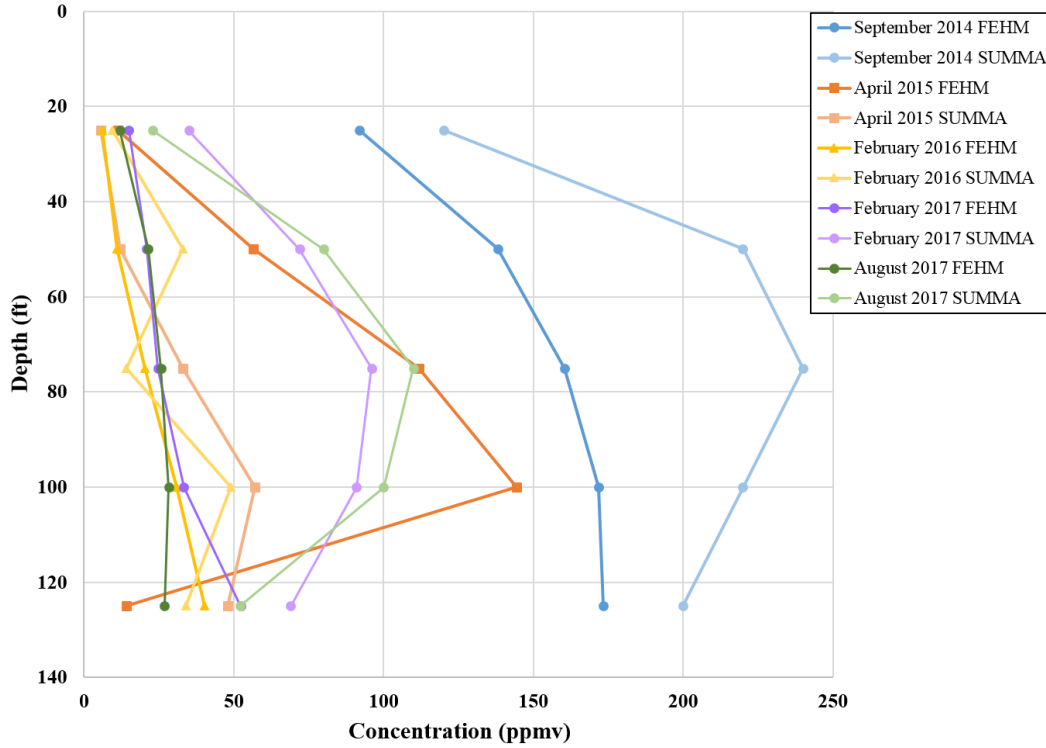


Figure 5.4-3 Simulated versus measured 1,1,1-TCA concentration in borehole 54-24243

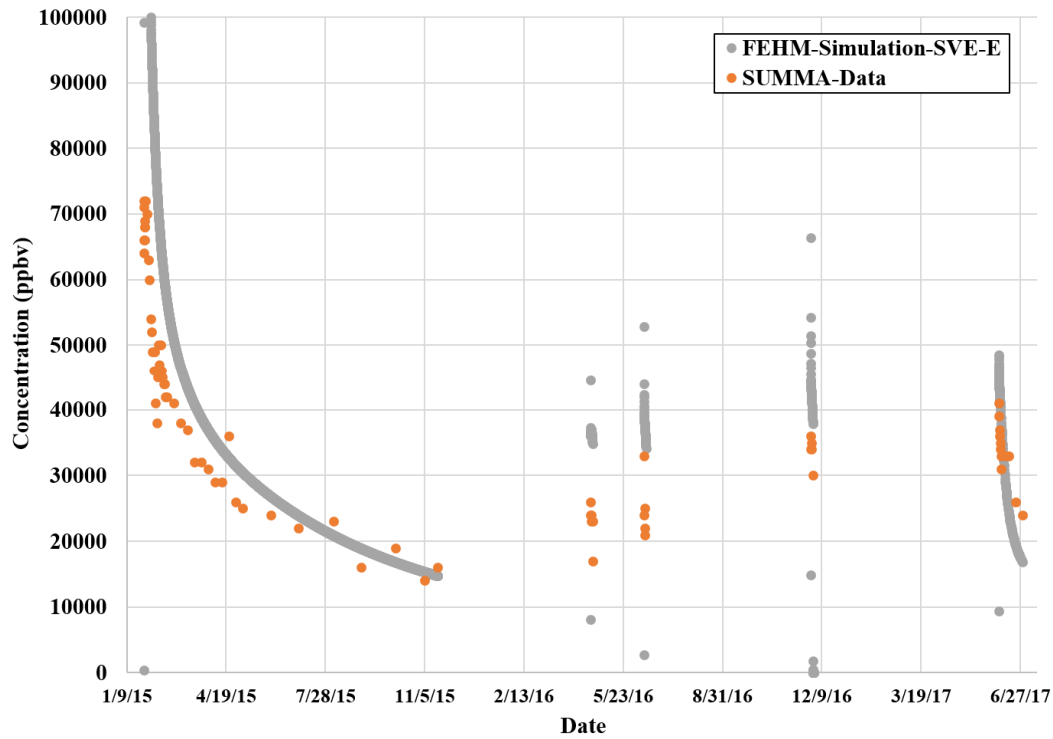


Figure 5.5-1 Simulated rebound for SVE-East compared with measured SUMMA data from SVE-East effluent

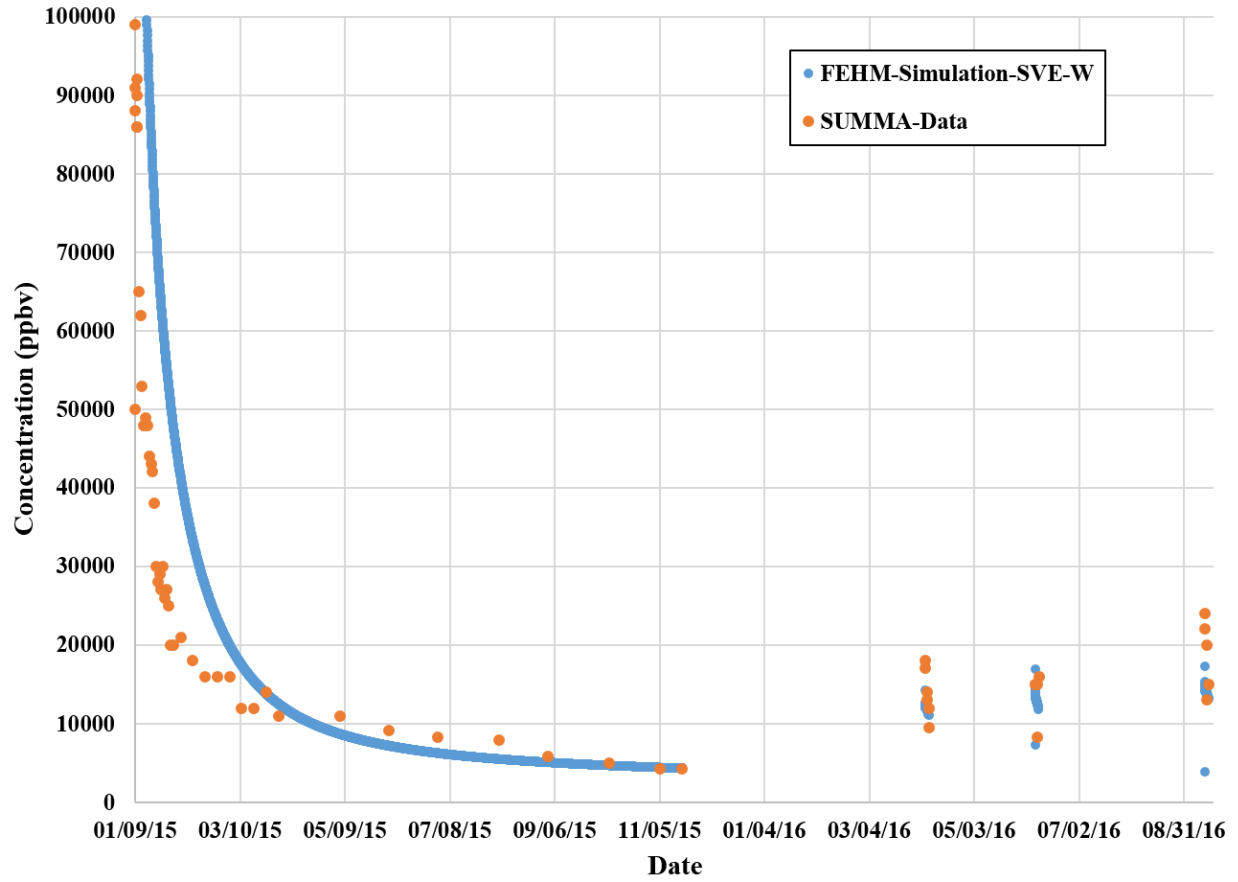


Figure 5.5-2 Simulated active extraction concentrations and rebound for SVE-West compared with measured SUMMA data

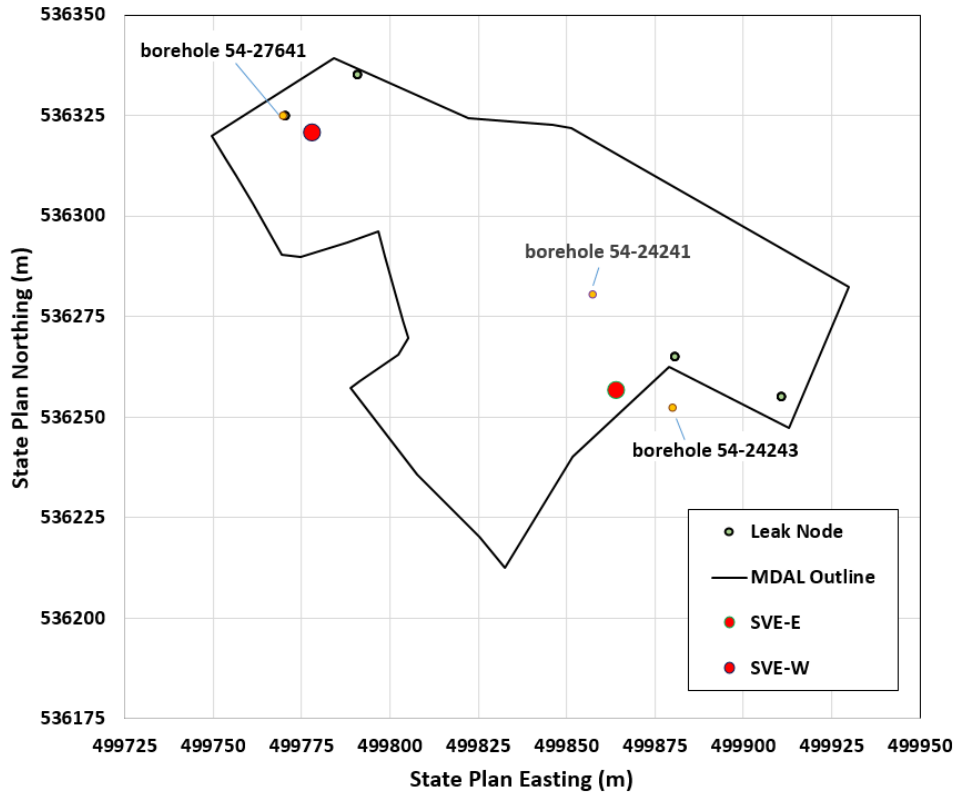


Figure 5.6-1 Location of sudden drum failure and three existing monitoring wells

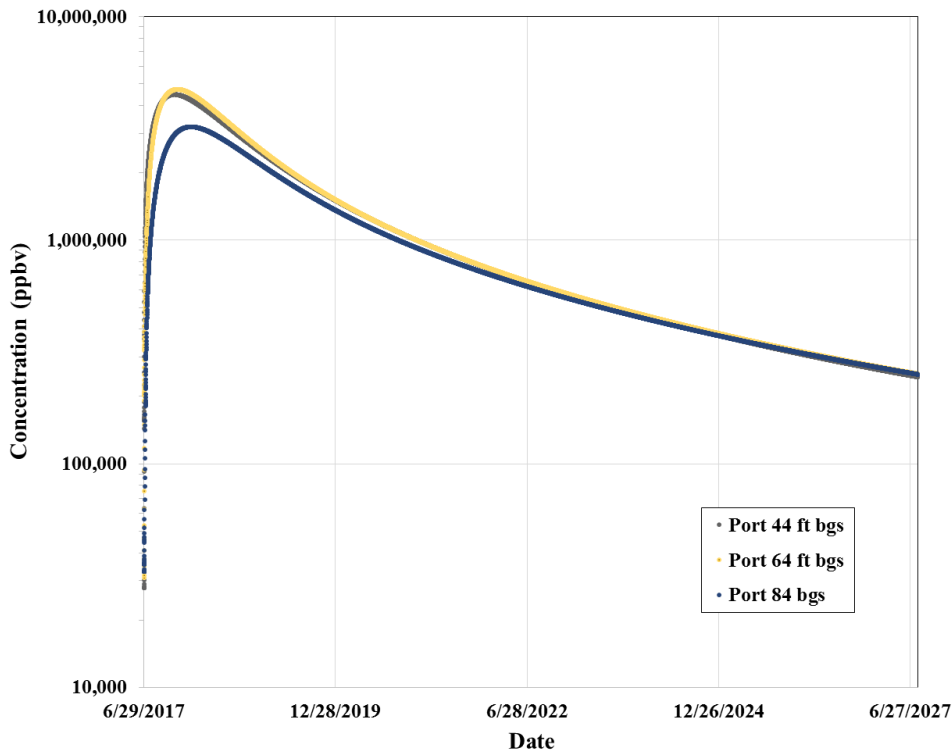


Figure 5.6-2 Borehole 54-24238 response to sudden release of 1 drum (200 L) of 1,1,1-TCA

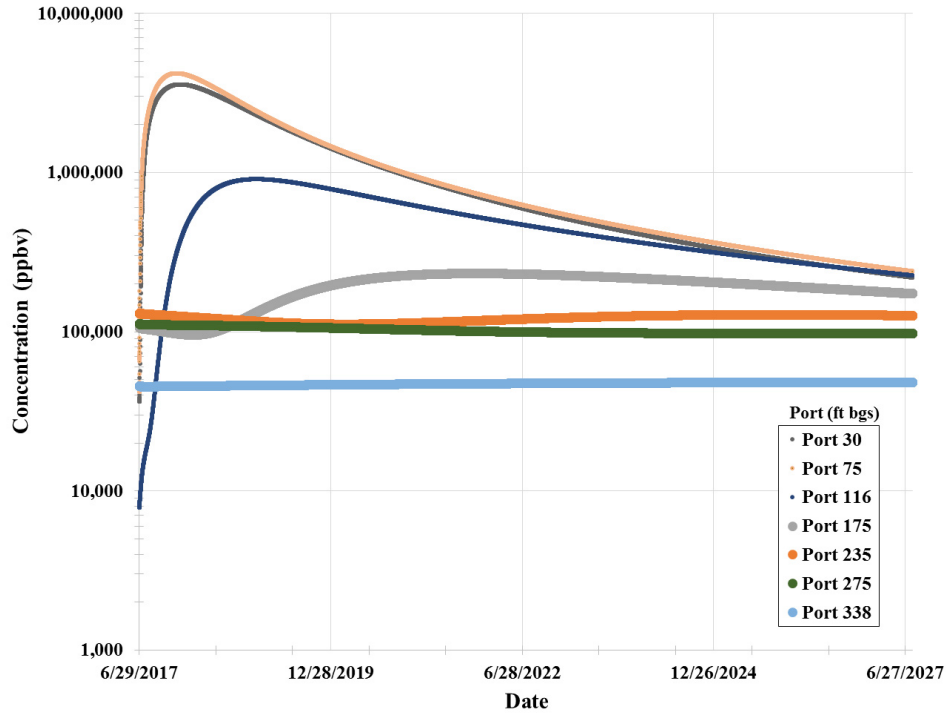


Figure 5.6-3 Borehole 54-27642 response to sudden release of 1 drum (200 L) of 1,1,1-TCA

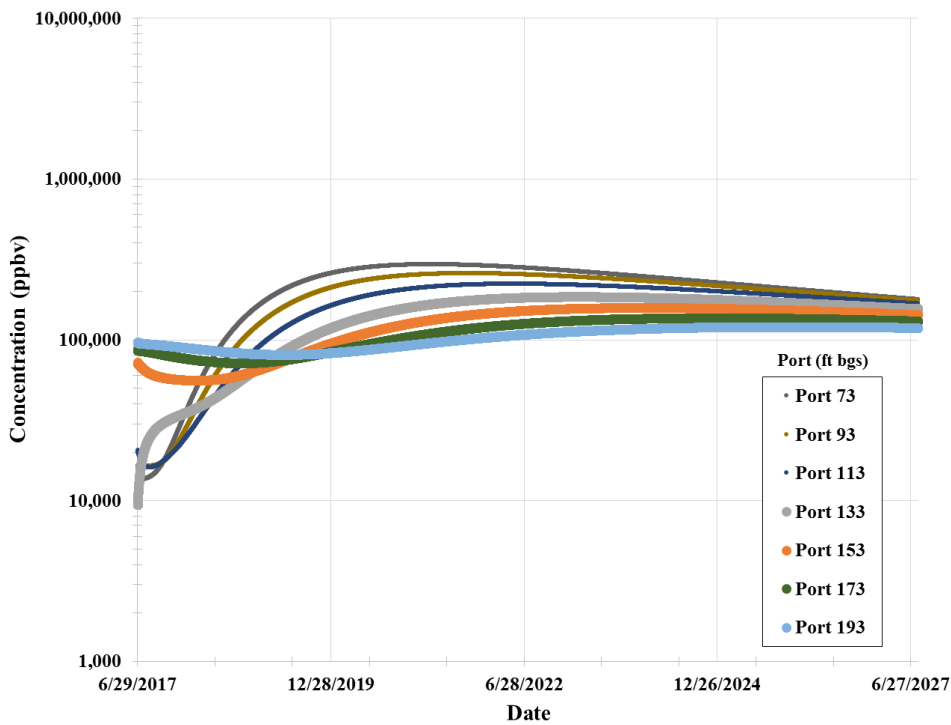


Figure 5.6-4 Borehole 54-24241 response to sudden release of 1 drum (200 L) of 1,1,1-TCA

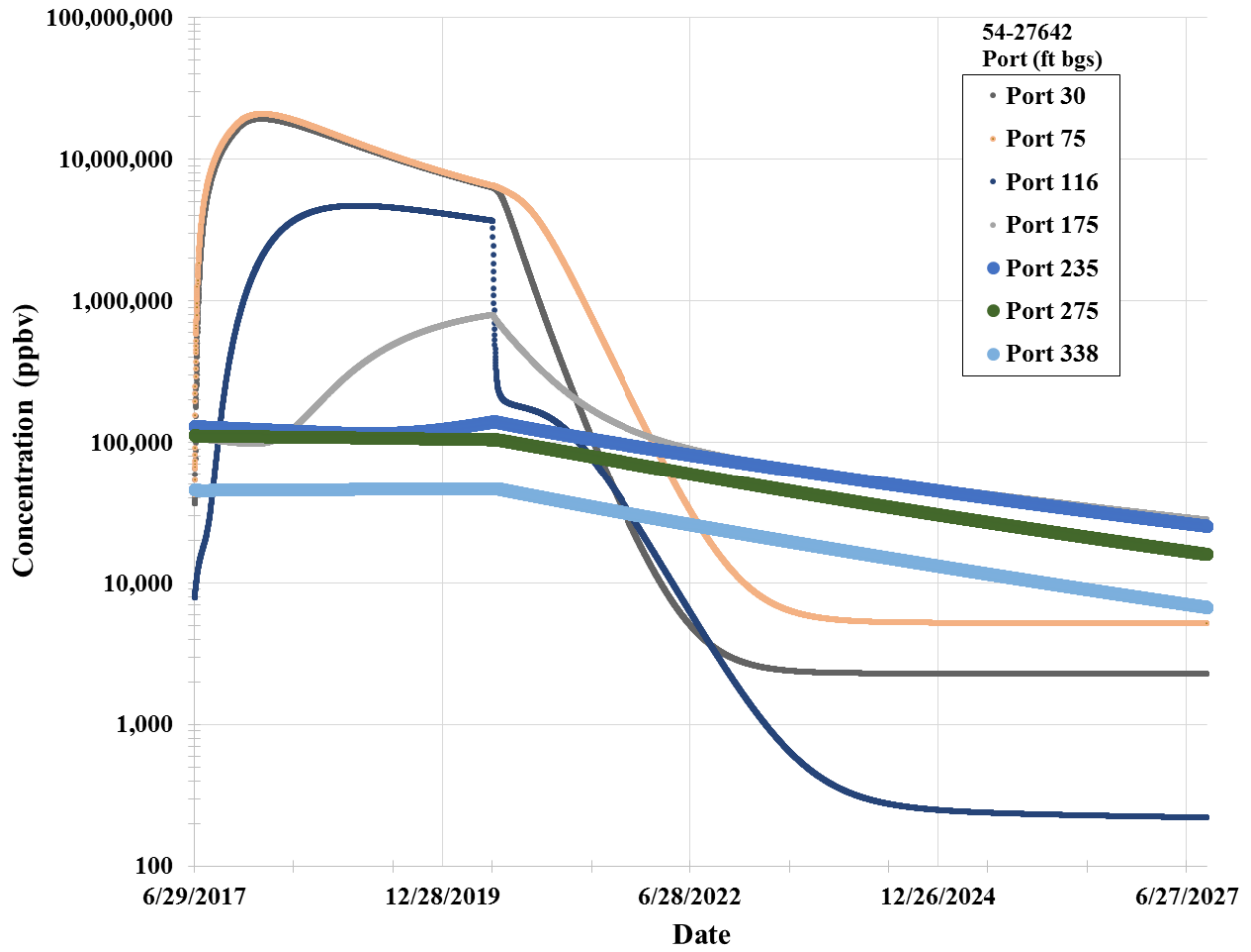


Figure 5.6-5 Concentrations in monitoring borehole 54-27642 for a simulated five-drum sudden failure of TCA followed by 7 yr of SVE

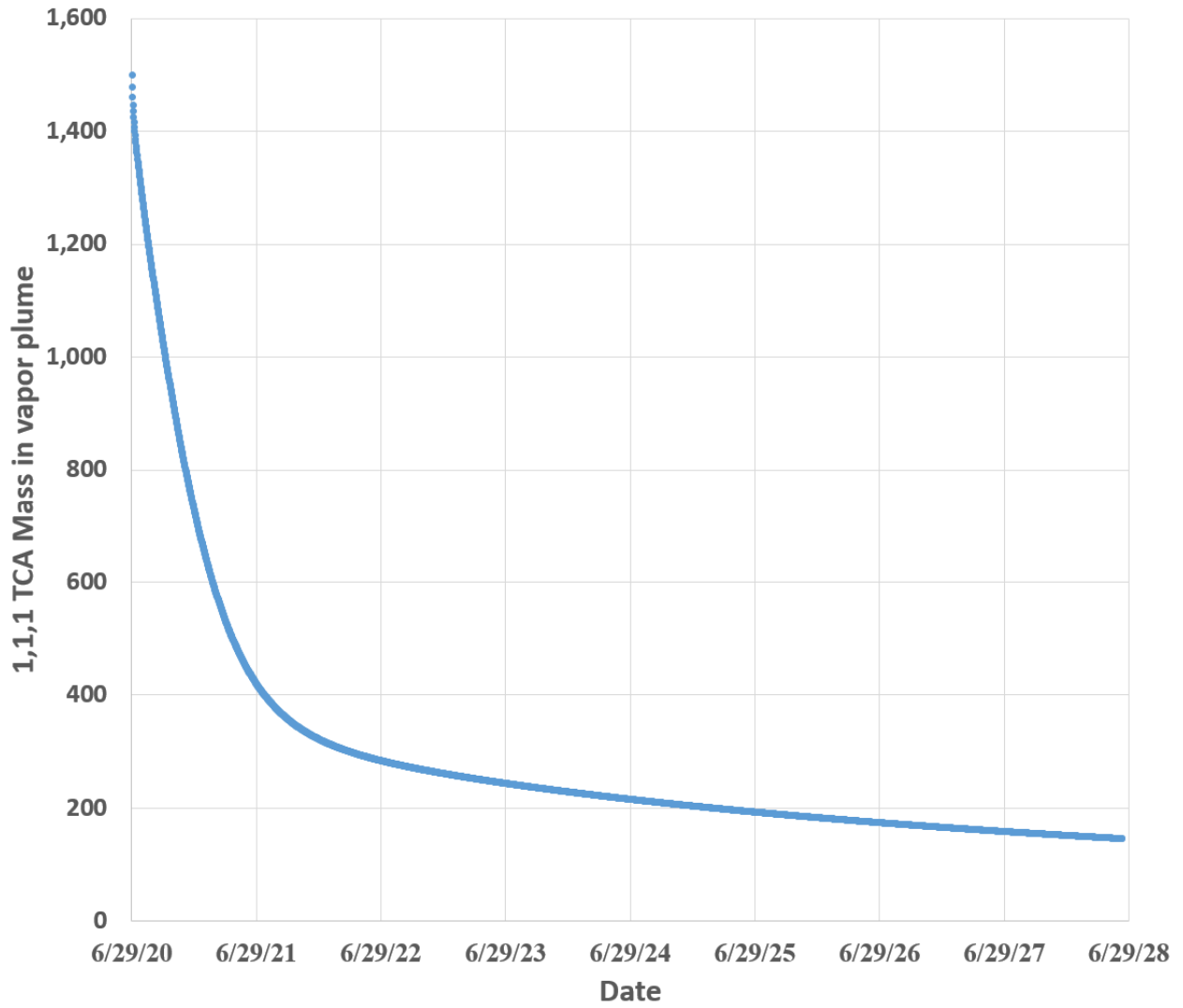


Figure 5.6-6 Mass removal by active SVE of 1,1,1-TCA versus time for the five-drum case

Table 2.2-1
List of 62 Organic Compounds Analyzed
by EPA Method TO-15 during SVE Operations

Acetone	Dioxane[1,4-]
Benzene	Ethanol
Benzyl Chloride	Ethylbenzene
Bromodichloromethane	Ethyltoluene[4-]
Bromoform	Hexachlorobutadiene
Bromomethane	Hexane
Butadiene[1,3-]	Hexanone[2-]
Butanone[2-]	Isooctane
Carbon Disulfide	Isopropylbenzene
Carbon Tetrachloride	Methyl tert-Butyl Ether
Chloro-1-propene[3-]	Methyl-2-pentanone[4-]
Chlorobenzene	Methylene Chloride
Chlorodibromomethane	n-Heptane
Chloroethane	Propanol[2-]
Chloroform	Propylbenzene[1-]
Chloromethane	Styrene
Cyclohexane	Tetrachloroethane[1,1,2,2-]
Dibromoethane[1,2-]	Tetrachloroethene
Dichloro-1,1,2,2-tetrafluoroethane[1,2-]	Tetrahydrofuran
Dichlorobenzene[1,2-]	Toluene
Dichlorobenzene[1,3-]	Trichloro-1,2,2-trifluoroethane[1,1,2-]
Dichlorobenzene[1,4-]	Trichlorobenzene[1,2,4-]
Dichlorodifluoromethane	Trichloroethane[1,1,1-]
Dichloroethane[1,1-]	Trichloroethane[1,1,2-]
Dichloroethane[1,2-]	Trichloroethene
Dichloroethene[1,1-]	Trichlorofluoromethane
Dichloroethene[cis-1,2-]	Trimethylbenzene[1,2,4-]
Dichloroethene[trans-1,2-]	Trimethylbenzene[1,3,5-]
Dichloropropane[1,2-]	Vinyl Chloride
Dichloropropene[cis-1,3-]	Xylene[1,2-]
Dichloropropene[trans-1,3-]	Xylene[1,3-]+Xylene[1,4-]

Table 2.2-2
Subsurface Vapor-Monitoring Locations, Port Depths, and
Corresponding Sampling Intervals Used for Baseline and Annual Monitoring

MDA L Well	Port Depth (ft bgs)	Sampling Interval (ft length along borehole)	Status
54-01015 ^a	37.6	36–46	S
54-01015 ^a	165.4	182–192	S
54-01015 ^a	308.3	340–352	S
54-01015 ^a	333.3	375–385	S
54-01015 ^a	377.7	425–435	S
54-01015 ^a	426.5	480–490	S
54-01015 ^a	462.1	520–530	S
54-01016 ^a	30.8	30–40	S
54-01016 ^a	162.2	178–190	S
54-01016 ^a	274.7	318–324	S
54-01016 ^a	336.3	386–396	S
54-01016 ^a	414.3	473–483	RfP
54-01016 ^a	459.5	530–540	RfP
54-01016 ^a	517.6	592–602	S
54-02001	20	17.5–22.5	S
54-02001	40	37.5–42.5	S
54-02001	60	57.5–62.5	RfP
54-02001	80	77.5–82.5	S
54-02001	100	97.5–102.5	S
54-02001	120	117.5–122.5	S
54-02001	140	137.5–142.5	S
54-02001	160	157.5–162.5	RfP
54-02001	180	177.5–182.5	S
54-02001	200	197.5–202.5	RfP
54-02002	20	17.5–22.5	RfP
54-02002	40	37.5–42.5	S
54-02002	60	57.5–62.5	S
54-02002	80	77.5–82.5	RfP
54-02002	100	97.5–102.5	RfP
54-02002	120	117.5–122.5	S
54-02002	140	137.5–142.5	RfP
54-02002	157/160	154.5–159.5	RfP
54-02002	180	177.5–182.5	S
54-02002	200	197.5–202.5	S
54-02016	18	15.5–20.5	RfP
54-02016	31	28.5–33.5	S
54-02016	82	79.5–84.5	RfP

Table 2.2-2 (continued)

MDA L Borehole	Port Depth (ft bgs)	Sampling Interval (ft length along borehole)	Status
54-02020	20	10–30	S
54-02020	40	30–50	S
54-02020	60	50–70	S
54-02020	80	70–90	S
54-02020	95	90–110	S
54-02020	120	110–130	S
54-02020	140	130–150	S
54-02020	160	150–170	S
54-02020	180	170–190	S
54-02020	200	190–210	S
54-02021	20	10–30	S
54-02021	40	30–50	RfP
54-02021	60	50–70	RfP
54-02021	80	70–90	RfP
54-02021	100	90–110	RfP
54-02021	120	110–130	RfP
54-02021	140	130–150	S
54-02021	160	150–170	S
54-02021	180	170–190	S
54-02021	198	190–210	S
54-02022	20	17.5–22.5	RfP
54-02022	40	37.5–42.5	S
54-02022	60	57.5–62.5	S
54-02022	80	77.5–82.5	S
54-02022	100	97.5–102.5	RfP
54-02022	120	117.5–122.5	S
54-02022	140	137.5–142.5	S
54-02022	160	157.5–162.5	S
54-02022	180	177.5–182.5	S
54-02022	200	197.5–202.5	S
54-02023	20	10–30	S
54-02023	40	30–50	S
54-02023	60	50–70	S
54-02023	80	70–90	S
54-02023	100	90–110	S
54-02023	120	110–130	RfP
54-02023	140	130–149	RfP
54-02023	159	149–169	S
54-02023	180	170–190	RfP
54-02023	200	190–210	S

Table 2.2-2 (continued)

MDA L Borehole	Port Depth (ft bgs)	Sampling Interval (ft length along borehole)	Status
54-02024	20	10–30	S
54-02024	40	30–50	S
54-02024	60	50–70	S
54-02024	80	70–90	S
54-02024	100	90–110	S
54-02024	120	110–130	RfP
54-02024	140	130–150	S
54-02024	160	150–170	S
54-02024	180	170–190	S
54-02024	200	190–210	S
54-02025	20	20	S
54-02025	60	60	S
54-02025	100	100	S
54-02025	160	160	S
54-02025	190	190	S
54-02026	20	20	S
54-02026	60	60	S
54-02026	100	100	S
54-02026	160	160	S
54-02026	200	200	S
54-02026	215	215	S
54-02027	20	20	S
54-02027	60	60	S
54-02027	100	100	S
54-02027	160	160	S
54-02027	200	200	S
54-02027	220	220	S
54-02027	250	250	S
54-02028	20	20	S
54-02028	60	60	S
54-02028	100	100	S
54-02028	160	160	S
54-02028	200	200	S
54-02028	220	220	S
54-02028	250	250	S
54-02031	20	20	S
54-02031	60	60	S
54-02031	100	100	S
54-02031	160	160	S
54-02031	200	200	S
54-02031	220	220	S
54-02031	260	260	S

Table 2.2-2 (continued)

MDA L Borehole	Port Depth (ft bgs)	Sampling Interval (ft length along borehole)	Status
54-02034	20	20	S
54-02034	60	60	S
54-02034	100	100	S
54-02034	160	160	S
54-02034	200	200	S
54-02034	220	220	S
54-02034	260	260	S
54-02034	300	300	S
54-02089	13	13	S
54-02089	31	31	S
54-02089	46	46	S
54-02089	86	86	S
54-24238	44	43–45	S
54-24238	64	63–65	S
54-24238	84	83–85	S
54-24239	25	24–26	S
54-24239	50	49–51	S
54-24239	75	74–76	S
54-24239	99.5	98.5–100.5	S
54-24240	28	27–29	S
54-24240	53	52–54	S
54-24240	78	77–79	S
54-24240	103	102–104	S
54-24240	128	127–129	S
54-24240	153	152–154	S
54-24241	73	71–74	S
54-24241	93	92–94	S
54-24241	113	112–114	S
54-24241	133	132–134	S
54-24241	153	152–154	S
54-24241	173	172–174	S
54-24241	193	192–194	S
54-24242	25	24–26	S
54-24242	50	49–51	S
54-24242	75	74–76	S
54-24242	100	99–101	S
54-24242	110.5	109.5–111.5	S
54-24243	25	24–26	S
54-24243	50	49–51	S
54-24243	75	74–76	S
54-24243	100	99–101	S
54-24243	125	124–126	S

Table 2.2-2 (continued)

MDA L Borehole	Port Depth (ft bgs)	Sampling Interval (ft length along borehole)	Status
54-24399 ^b	568	568	RfP
54-24399 ^b	568	568-569	RfP
54-24399 ^{b, c}	567 ^c	567	S
54-24399 ^{b, c}	588	588	S
54-27641	32	29.5–34.5	S
54-27641	82	79.5–84.5	S
54-27641	115	112.5–117.5	S
54-27641	182	179.5–184.5	S
54-27641	232	229.5–234.5	S
54-27641	271	268.5–273.5	S
54-27641	332.5	330–335	S
54-27642	30	27.5–32.5	S
54-27642	75	71.5–76.5	S
54-27642	116	114.5–119.5	S
54-27642	175	172.5–177.5	S
54-27642	235	232.5–237.5	S
54-27642	275	272.5–277.5	S
54-27642	338	335.5–340.5	S
54-27643	30	27.5–32.5	S
54-27643	74	71.5–76.5	S
54-27643	117	114.5–119.5	S
54-27643	167	164.5–169.5	S
54-27643	235	232.5–237.5	S
54-27643	275	272.5–277.5	S
54-27643	354	351.5–356.5	S
54-610786 ^d	25	22.5–27.5	S
54-610786 ^d	50	47.5–52.5	S
54-610786 ^d	75	72.5–77.5	S
54-610786 ^d	100	97.5–102.5	S
54-610786 ^d	118.5	116–121	S

Notes: S = Sampled; RfP = Removed from plan.

^a Vapor-monitoring borehole angled. Port depth is depth below ground surface. Port-depth interval is length along borehole.

^b Open borehole below 566.7 ft bgs.

^c Permanent packer installed August 2016.

^d Drilled in December 2009.

Table 2.2-3
Subsurface Vapor-Monitoring Locations, Port Depths, and Corresponding
Sampling Intervals Used for Quarterly Sampling within 150-ft Radius of the SVE Units

MDA L Well	Port depth (ft bgs)	Sampling Interval (ft length along borehole)	Apr-15	Jul-15	Nov-15	Feb-16	May-16	Aug-16	Nov-16	Feb-17	May-17	Aug-17	Status
54-02001	20	17.5-22.5	S	S	NS-RS	S	S	S	S	S	S	S	S
54-02001	40	37.5-42.5	S	S	NS-RS	S-PB	S	S	S	S	S	S	S
54-02001	60	57.5-62.5	NS-B	NS-B	NS	NS	NS	NS	NS	NS	NS	NS	RfP
54-02001	80	77.5-82.5	S	S	NS-RS	S	S	S	S	S	S	S	S
54-02001	100	97.5-102.5	S	S	NS-RS	S	S	S	S	S	S	S	S
54-02001	120	117.5-122.5	S	S	NS-RS	S	S	S	S	S	S	S	S
54-02001	140	137.5-142.5	S	S	NS-RS	S-PB	NS-B	S-PB	S	S	S	S	S
54-02001	160	157.5-162.5	NS-B	NS-B	NS	NS	NS	NS	NS	NS	NS	NS	RfP
54-02001	180	177.5-182.5	S	S	NS-RS	S	S	S	S	S	S	S	S
54-02001	200	197.5-202.5	NS-B	S-PB	NS-B	NS-B	NS-B	NS-B	NS-B	NS-B	NS-B	NS-B	RfP
54-02002	20	17.5-22.5	NS-B	NS-B	NS	NS	NS	NS	NS	NS	NS	NS	RfP
54-02002	40	37.5-42.5	S	S	S	S	S	S	S	S	S	S	S
54-02002	60	57.5-62.5	S	S	S	S	S	S	S	S	S	S	S
54-02002	80	77.5-82.5	S-PB	S-PB	NS	NS	NS	NS	NS	NS	NS	NS	RfP
54-02002	100	97.5-102.5	NS-B	NS-B	NS	NS	NS	NS	NS	NS	NS	NS	RfP
54-02002	120	117.5-122.5	S	S	S	S	S	S	S	S	S	S	S
54-02002	140	137.5-142.5	S-PB	S-PB	NS-B	NS-B	NS-B	NS-B	NS-B	NS-B	NS-B	NS-B	RfP
54-02002	157/160	154.5-159.5	S-PB	S-PB	NS	NS	NS	NS	NS	NS	NS	NS	RfP
54-02002	180	177.5-182.5	S	S	S	S	S	S	S	S	S	S	S
54-02002	200	197.5-202.5	S	S	S	S	S	S	S	S	S	S	S
54-02016	18	15.5-20.5	NS-B	NS-B	NS-B	NS-B	NS-B	NS-B	NS-B	NS-B	NS-B	NS-B	RfP
54-02016	31	28.5-33.5	S	S	S	S	S	S	S	S	S	S	S
54-02016	82	79.5-84.5	NS-B	NS-B	NS-B	NS-B	NS-B	NS-B	NS-B	NS-B	NS-B	NS-B	RfP

Table 2.2-3 (continued)

MDA L Well	Port depth (ft bgs)	Sampling Interval (ft length along borehole)	Apr-15	Jul-15	Nov-15	Feb-16	May-16	Aug-16	Nov-16	Feb-17	May-17	Aug-17	Status
54-02021	20	10-30	S	S	S	S	S	S	S	S	S	S	S
54-02021	40	30-50	S-PB	S-PB	NS	NS	NS	NS	NS	NS	NS	NS	RfP
54-02021	60	50-70	S	S-PB	NS	NS	NS	NS	NS	NS	NS	NS	RfP
54-02021	80	70-90	S-PB	S-PB	NS	NS	NS	NS	NS	NS	NS	NS	RfP
54-02021	100	90-110	S-PB	S-PB	NS	NS	NS	NS	NS	NS	NS	NS	RfP
54-02021	120	110-130	S-PB	S-PB	NS	NS	NS	NS	NS	NS	NS	NS	RfP
54-02021	140	130-150	S	S	S	S	S	S	S	S	S	S	S
54-02021	160	150-170	S	S	S	S	S	S	S	S	S	S	S
54-02021	180	170-190	S	S	S	S	S	S	S	S	S	S	S
54-02021	198	190-210	S	S	S	S	S	S	S	S	S	S	S
54-02022	20	17.5-22.5	NS-B	S-PB	NS	NS	NS	NS	NS	NS	NS	NS	RfP
54-02022	40	37.5-42.5	S	S	S	S	S	S	S	S	S	S	S
54-02022	60	57.5-62.5	S	S	S	S	S	S	S	S	S	S	S
54-02022	80	77.5-82.5	S	S	S	S	S	S	S	S	S	S	S
54-02022	100	97.5-102.5	NS-B	S-PB	NS	NS	NS	NS	NS	NS	NS	NS	RfP
54-02022	120	117.5-122.5	S	S	S	S	S	S	S	S	S	S	S
54-02022	140	137.5-142.5	S	S	S	S	S	S	S	S	S	S	S
54-02022	160	157.5-162.5	S	S	S	S	S	S	S	S	S	S	S
54-02022	180	177.5-182.5	S	S	S	S	S	S	S	S	S	S	S
54-02022	200	197.5-202.5	S	S	S	S	S	S	S	S	S	S	S
54-02089	13	13	S	S	S	S	S	S	S	S	S	S	S
54-02089	31	31	S	S	S	S	S	S	S	S	S	S	S
54-02089	46	46	S	S	S	S	S	S	S	S	S	S	S
54-02089	86	86	S	S	S	S	S	S	S	S	S	S	S

Table 2.2-3 (continued)

MDA L Well	Port depth (ft bgs)	Sampling Interval (ft length along borehole)	Apr-15	Jul-15	Nov-15	Feb-16	May-16	Aug-16	Nov-16	Feb-17	May-17	Aug-17	Status
54-24238	44	43-45	S	S	S	S	S	S	S	S	S	S	S
54-24238	64	63-65	S	S	S	S	S	S	S	S	S	S	S
54-24238	84	83-85	S	S	S	S	S	S	S	S	S	S	S
54-24239	25	24-26	S	S	S	S	S	S	S	S	S	S	S
54-24239	50	49-51	S	S	S	S	S	S	S	S	S	S	S
54-24239	75	74-76	S	S	S	S	S	S	S	S	S	S	S
54-24239	99.5	98.5-100.5	S	S	S	S	S	S	S	S	S	S	S
54-24240	28	27-29	S	S	S	S	S	S	S	S	S	S	S
54-24240	53	52-54	S	S	S	S	S	S	S	S	S	S	S
54-24240	78	77-79	S	S	S	S	S	S	S	S	S	S	S
54-24240	103	102-104	S	S	NS-FV	S	S	S	S	S	S	S	S
54-24240	128	127-129	S	S	S	S	S	S	S	S	S	S	S
54-24240	153	152-154	S	S	S	S	S	S	S	S	S	S	S
54-24241	73	71-74	S	S	NS-RS	S	NS-B	S	S	S	S	S	S
54-24241	93	92-94	S	S	NS-RS	S	S	S	S	S	S	S	S
54-24241	113	112-114	S	S	NS-RS	S	S	S	S	S	S	S	S
54-24241	133	132-134	S	S	NS-RS	S	S	S	S	S	S	S	S
54-24241	153	152-154	S	S	NS-RS	S	S	S	S	S	S	S	S
54-24241	173	172-174	S	S	NS-RS	S	S	S	S	S	S	S	S
54-24241	193	192-194	S	S	NS-RS	NS-B	NS-B	S	S	S	S	S	S
54-24243	25	24-26	S	S	S	S	S	S	S	S	S	S	S
54-24243	50	49-51	S	S	S	S	S	S	S	S	S	S	S
54-24243	75	74-76	S	S	S	S	S	S	S	S	S	S	S
54-24243	100	99-101	S	S	S	S	S	S	S	S	S	S	S
54-24243	125	124-126	S	S	S	S	S	S	S	S	S	S	S

Table 2.2-3 (continued)

MDA L Well	Port depth (ft bgs)	Sampling Interval (ft length along borehole)	Apr-15	Jul-15	Nov-15	Feb-16	May-16	Aug-16	Nov-16	Feb-17	May-17	Aug-17	Status
54-24399 ^a	568	568	S	S	S	S	S	NS	NS	NS	NS	NS	RfP
54-24399 ^a	568	568-569	S	S	NS	NS	NS	NS	NS	NS	NS	NS	RfP
54-24399 ^{a,b}	567	567	n/a ^c	n/a	n/a	n/a	n/a	n/a	S	S	S	S	S
54-24399 ^{a,b}	588	588	n/a	n/a	n/a	n/a	n/a	S	S	S	S	S	S
54-27641	32	29.5-34.5	S	S	NS-RS	S	S	S	S	S	S	S	S
54-27641	82	79.5-84.5	S	S	S	S	S	S	S	S	S	S	S
54-27641	115	112.5-117.5	S	S	S	S	S	S	S	S	S	S	S
54-27641	182	179.5-184.5	S	S	S	S	S	S	S	S	S	S	S
54-27641	232	229.5-234.5	S	S	NS-RS	S	S	S	S	S	S	S	S
54-27641	271	268.5-273.5	S	S	S	S	S	S	S	S	S	S	S
54-27641	332.5	330-335	S	S	S	S	S	S	S	S	S	S	S
54-27642	30	27.5-32.5	S	S	S	S	S	S	S	S	S	S	S
54-27642	75	71.5-76.5	S	S	S	S	S	S	S	S	S	S	S
54-27642	116	114.5-119.5	S	S	NS-RS	NS-B	NS-B	S	S	S	S	S	S
54-27642	175	172.5-177.5	S	S	S	S	S	S	S	S	S	S	S
54-27642	235	232.5-237.5	S	S	S	S	S	S	S	S	S	S	S
54-27642	275	272.5-277.5	S	S	S	S	S	S	S	S	S	S	S
54-27642	338	335.5-340.5	S	S	NS-RS	S	S	S	S	S	S	S	S

Notes: S (green) = Sampled; S-PB (light blue) = Sample partially blocked; NS-B (yellow) = Not sampled because port blocked; NS-RS (orange) = Not sampled because of radiological screening; NS (purple) = Not sampled; NS-FV (dark blue) = Not sampled because valve faulty; RfP (pink) = Removed from plan.

^a Open borehole below 566.7 ft bgs.

^b Permanent packer installed August 2016.

^c n/a = Not applicable since these ports did not exist before August 2016.

**Table 4.1-1
Mass Removed for Detected Organic Compounds during SVE Operation**

Parameter Name	Cumulative Total Pounds through 2/18/2015 10:53:00 AM	Cumulative Total Pounds through 3/18/2015 10:53:00 AM	Cumulative Total Pounds through 4/18/2015 10:53:00 AM	Cumulative Total Pounds through 5/18/2015 10:53:00 AM	Cumulative Total Pounds through 6/18/2015 10:53:00 AM
Acetone	0.01	0.01	0.01	0.01	0.01
Benzene	0.12	0.22	0.31	0.39	0.48
Carbon Tetrachloride	0.58	0.92	1.22	1.49	1.72
Chlorobenzene	0.00	0.00	0.00	0.01	0.02
Chloroform	5.39	8.51	11.19	13.53	15.65
Dichlorodifluoromethane	0.48	0.74	0.96	1.15	1.33
Dichloroethane[1,1-]	4.16	6.36	8.29	9.97	11.47
Dichloroethane[1,2-]	12.16	17.48	22.52	27.03	31.06
Dichloroethene[1,1-]	5.84	9.73	13.30	16.50	19.82
Dichloropropane[1,2-]	4.13	8.08	11.50	14.62	17.50
Dioxane[1,4-]	0.22	0.60	1.15	1.73	2.39
Ethanol	0.01	0.01	0.03	0.05	0.05
Hexane	0.05	0.05	0.05	0.05	0.05
Isooctane	0.02	0.13	0.13	0.14	0.17
Methylene Chloride	2.52	4.63	6.64	8.51	10.27
n-Heptane	0.02	0.02	0.02	0.02	0.02
Tetrachloroethene	20.10	33.02	45.67	57.13	67.95
Tetrahydrofuran	0.11	0.24	0.35	0.47	0.61
Toluene	0.20	0.43	0.66	0.88	1.11
Trichloro-1,2,2-trifluoroethane[1,1,2-]	21.40	37.13	50.75	62.63	73.57
Trichloroethane[1,1,1-]	116.25	187.31	250.50	305.43	354.80
Trichloroethene	65.87	97.69	125.95	150.78	173.69
Trichlorofluoromethane	1.24	2.13	2.94	3.65	4.27
Xylene[1,3-]+Xylene[1,4-]	0.02	0.03	0.05	0.06	0.07
Total VOCs	260.88	415.49	554.20	676.23	788.08

Table 4.1-1 (continued)

Parameter Name	Cumulative Total Pounds through 7/18/2015	Cumulative Total Pounds through 8/18/2015	Cumulative Total Pounds through 9/18/2015	Cumulative Total Pounds through 10/18/2015	Cumulative Total Pounds through 11/18/2015
Acetone	0.01	0.01	0.01	0.01	0.01
Benzene	0.56	0.64	0.71	0.78	0.85
Carbon Tetrachloride	1.92	2.10	2.27	2.42	2.56
Chlorobenzene	0.03	0.05	0.06	0.06	0.07
Chloroform	17.59	19.47	21.12	22.62	24.12
Dichlorodifluoromethane	1.50	1.67	1.82	1.95	2.06
Dichloroethane[1,1-]	12.75	13.94	15.00	16.00	16.98
Dichloroethane[1,2-]	34.66	38.12	41.05	43.63	46.19
Dichloroethene[1,1-]	23.11	26.27	28.85	31.15	34.00
Dichloropropane[1,2-]	20.00	22.35	24.51	26.61	28.70
Dioxane[1,4-]	3.04	3.67	4.24	4.79	5.38
Ethanol	0.05	0.05	0.11	0.23	0.31
Hexane	0.06	0.08	0.09	0.09	0.09
Isooctane	0.19	0.19	0.19	0.19	0.19
Methylene Chloride	11.83	13.33	14.72	16.05	17.41
n-Heptane	0.04	0.07	0.09	0.09	0.09
Tetrachloroethene	77.26	85.97	94.19	102.16	110.63
Tetrahydrofuran	0.74	0.86	1.00	1.13	1.25
Toluene	1.29	1.44	1.61	1.79	1.97
Trichloro-1,2,2-trifluoroethane[1,1,2-]	83.64	93.00	101.17	109.01	117.16
Trichloroethane[1,1,1-]	399.42	441.79	477.93	510.09	540.98
Trichloroethene	193.45	211.32	227.65	243.63	259.45
Trichlorofluoromethane	4.86	5.43	5.93	6.38	6.82
Xylene[1,3-]+Xylene[1,4-]	0.11	0.16	0.20	0.21	0.21
Total VOCs	888.08	981.99	1064.50	1141.05	1217.49

**Table 4.1-2
Flow Rate Data for SVE-West**

Date	Time	Flow Rate (scfm)
1/9/2015	12:55	0.0
1/9/2015	12:56	99.9
1/9/2015	12:59	99.9
1/9/2015	13:01	99.9
1/9/2015	13:02	99.9
1/9/2015	13:05	99.9
1/9/2015	13:07	99.9
1/9/2015	13:09	99.9
1/9/2015	13:11	99.9
1/9/2015	13:32	99.9
1/9/2015	13:36	99.9
1/9/2015	13:37	99.9
1/9/2015	13:38	99.9
1/9/2015	13:45	99.9
1/9/2015	13:52	99.9
1/9/2015	14:01	99.9
1/9/2015	14:22	99.9
1/9/2015	14:42	99.9
1/9/2015	14:53	99.9
1/9/2015	15:05	99.9
1/9/2015	15:15	99.9
1/9/2015	15:16	99.9
1/9/2015	15:24	99.9
1/9/2015	15:34	99.9
1/9/2015	15:44	99.9
1/9/2015	15:54	99.9
1/9/2015	16:03	99.9
1/9/2015	16:05	99.9
1/9/2015	16:07	99.9
1/10/2015	9:08	99.9
1/10/2015	9:09	99.9
1/10/2015	9:10	99.9
1/10/2015	9:53	99.9
1/10/2015	9:55	99.9
1/10/2015	9:57	99.9
1/10/2015	10:41	99.9
1/10/2015	10:43	99.9

Table 4.1-2 (continued)

Date	Time	Flow Rate (scfm)
1/10/2015	10:48	99.9
1/10/2015	10:48	99.9
1/10/2015	11:35	99.9
1/10/2015	11:48	99.9
1/10/2015	11:51	99.9
1/10/2015	11:52	99.9
1/11/2015	9:02	99.9
1/11/2015	9:05	99.9
1/11/2015	9:07	99.9
1/12/2015	12:03	99.9
1/12/2015	12:05	99.9
1/12/2015	12:07	99.9
1/13/2015	8:57	99.9
1/13/2015	8:59	99.9
1/13/2015	9:00	99.9
1/14/2015	9:37	99.9
1/14/2015	9:40	99.9
1/14/2015	9:42	99.9
1/15/2015	11:36	99.9
1/15/2015	11:38	99.9
1/15/2015	11:40	99.9
1/16/2015	8:58	99.9
1/16/2015	8:59	99.9
1/16/2015	9:00	99.9
1/17/2015	9:05	99.9
1/17/2015	9:07	99.9
1/17/2015	9:09	99.9
1/18/2015	8:57	99.9
1/18/2015	8:58	99.9
1/18/2015	9:00	99.9
1/18/2015	9:02	99.9
1/19/2015	9:03	99.9
1/19/2015	9:05	99.9
1/19/2015	9:07	99.9
1/19/2015	9:09	99.9
1/20/2015	9:54	99.9
1/20/2015	9:55	99.9
1/20/2015	9:57	99.9
1/21/2015	9:54	99.9

Table 4.1-2 (continued)

Date	Time	Flow Rate (scfm)
1/21/2015	9:56	99.9
1/21/2015	9:58	99.9
1/22/2015	14:43	99.9
1/22/2015	14:44	99.9
1/22/2015	14:47	99.9
1/23/2015	9:20	100.7
1/23/2015	9:25	100.7
1/23/2015	9:28	100.7
1/24/2015	10:46	99.9
1/24/2015	10:49	99.9
1/24/2015	10:53	99.9
1/25/2015	9:40	100.3
1/25/2015	9:42	100.3
1/25/2015	9:45	100.3
1/26/2015	9:08	99.9
1/26/2015	9:11	99.9
1/26/2015	9:15	99.9
1/27/2015	10:50	99.5
1/27/2015	10:51	99.5
1/27/2015	10:52	99.5
1/28/2015	9:45	99.5
1/28/2015	9:47	99.5
1/28/2015	9:49	99.5
1/29/2015	9:02	99.6
1/29/2015	9:05	99.6
1/29/2015	9:06	99.6
1/31/2015	13:54	99.5
1/31/2015	13:55	99.5
1/31/2015	13:59	99.5
2/4/2015	10:07	99.1
2/11/2015	10:29	99.6
2/18/2015	9:58	97.8
2/25/2015	12:42	99.1
3/4/2015	9:53	100.6
3/11/2015	9:16	99.2
3/18/2015	9:05	100.1
3/25/2015	8:58	100.1
4/1/2015	10:19	99.6
4/8/2015	9:20	99.6

Table 4.1-2 (continued)

Date	Time	Flow Rate (scfm)
4/9/2015	11:43	99.2
4/14/2015	9:27	99.2
4/15/2015	9:09	99.6
4/21/2015	9:31	99.6
4/22/2015	10:33	99.6
4/28/2015	9:42	98.7
4/29/2015	9:52	99.2
5/6/2015	9:36	99.2
5/13/2015	9:58	99.7
5/20/2015	11:41	98.7
5/27/2015	9:14	98.7
6/3/2015	10:56	98.7
6/10/2015	9:23	100.0
6/17/2015	9:30	100.0
6/24/2015	11:16	100.0
7/1/2015	8:56	97.8
7/9/2015	9:48	99.5
7/15/2015	9:42	98.6
7/22/2015	9:51	97.3
7/29/2015	9:42	99.5
8/5/2015	9:45	97.3
8/12/2015	9:25	99.1
8/19/2015	15:10	98.6
8/26/2015	8:34	99.6
9/2/2015	9:17	100.0
9/9/2015	9:19	99.9
9/16/2015	11:39	99.1
9/23/2015	9:27	99.6
9/30/2015	8:56	100.1
10/7/2015	9:18	100.1
10/14/2015	8:19	100.1
10/22/2015	9:46	100.5
10/28/2015	10:55	99.7
11/5/2015	10:58	99.7
11/12/2015	9:23	101.1
11/17/2015	12:37 PM	99.7
11/18/2015	10:54	99.7

Note: Standard conditions for the orifice flow meter are 60°F and 14.7 psi (21.1°C and 101.3 kPa).

**Table 4.1-3
Flow Rate Data for SVE-East**

Date	Time	Flow Rate (scfm)
1/26/2015	10:20	0.0
1/26/2015	10:21	95.6
1/26/2015	10:25	95.6
1/26/2015	10:30	95.6
1/26/2015	10:34	95.6
1/26/2015	10:57	95.6
1/26/2015	11:01	95.6
1/26/2015	11:03	95.6
1/26/2015	11:18	95.6
1/26/2015	11:21	95.6
1/26/2015	11:27	95.6
1/26/2015	11:31	95.6
1/26/2015	11:41	95.6
1/26/2015	11:47	95.6
1/26/2015	11:55	95.6
1/26/2015	12:01	95.6
1/26/2015	12:05	95.6
1/26/2015	13:59	95.6
1/26/2015	14:06	95.6
1/26/2015	14:10	95.6
1/26/2015	14:15	95.6
1/26/2015	14:20	95.6
1/26/2015	14:24	95.6
1/26/2015	14:29	95.6
1/26/2015	14:31	95.6
1/26/2015	14:44	95.6
1/26/2015	14:47	95.6
1/26/2015	14:53	95.6
1/26/2015	15:02	95.6
1/26/2015	15:10	95.6
1/26/2015	15:17	95.6
1/26/2015	15:19	95.6
1/26/2015	15:21	95.6
1/27/2015	11:17	94.6
1/27/2015	11:19	94.6
1/27/2015	11:21	94.6
1/27/2015	12:18	94.6

Table 4.1-3 (continued)

Date	Time	Flow Rate (scfm)
1/27/2015	12:20	94.6
1/27/2015	12:22	94.6
1/27/2015	13:57	94.6
1/27/2015	13:59	94.6
1/27/2015	14:00	94.6
1/27/2015	14:55	94.6
1/27/2015	14:57	94.6
1/27/2015	14:59	94.6
1/27/2015	15:45	94.6
1/27/2015	15:50	94.6
1/27/2015	15:52	94.6
1/27/2015	15:54	94.6
1/28/2015	10:20	94.4
1/28/2015	10:21	94.4
1/28/2015	10:23	94.4
1/29/2015	10:12	94.4
1/29/2015	10:13	94.4
1/29/2015	10:15	94.4
1/31/2015	14:37	93.6
1/31/2015	14:40	93.6
1/31/2015	14:41	93.6
2/1/2015	8:51	94.1
2/1/2015	8:54	94.1
2/1/2015	8:57	94.1
2/2/2015	9:40	93.6
2/2/2015	9:42	93.6
2/2/2015	9:46	93.6
2/4/2015	10:07	93.4
2/5/2015	8:51	96.0
2/6/2015	10:23	100.6
2/7/2015	9:34	98.9
2/8/2015	9:21	98.9
2/9/2015	9:58	96.3
2/10/2015	9:34	98.0
2/11/2015	9:47	97.4
2/12/2015	9:00	97.4
2/13/2015	9:03	97.4
2/14/2015	8:58	98.0
2/15/2015	8:58	98.0

Table 4.1-3 (continued)

Date	Time	Flow Rate (scfm)
2/17/2015	9:39	98.4
2/18/2015	9:25	98.0
2/25/2015	13:18	98.2
3/4/2015	10:41	98.5
3/11/2015	9:47	98.5
3/18/2015	9:39	98.5
3/25/2015	9:21	98.5
4/1/2015	9:21	96.2
4/8/2015	9:45	97.7
4/9/2015	12:13	97.3
4/14/2015	9:55	96.6
4/15/2015	9:34	97.7
4/21/2015	9:58	96.6
4/22/2015	10:49	98.6
4/28/2015	10:05	97.3
4/29/2015	10:19	97.3
5/6/2015	10:10	97.3
5/13/2015	10:30	97.7
5/20/2015	11:59	96.8
5/27/2015	9:40	97.3
6/3/2015	11:48	98.0
6/10/2015	9:45	98.0
6/17/2015	9:45	97.3
6/24/2015	11:37	97.3
7/1/2015	9:15	97.1
7/9/2015	10:28	97.0
7/15/2015	10:02	96.6
7/22/2015	10:14	95.5
7/29/2015	10:08	98.0
8/5/2015	10:06	97.1
8/12/2015	9:47	93.4
8/19/2015	15:25	93.4
8/26/2015	8:49	96.1
9/2/2015	9:37	96.8
9/9/2015	9:36	96.4
9/16/2015	11:56	96.8
9/23/2015	9:45	97.3
9/30/2015	9:13	97.3
10/7/2015	9:49	98.4

Table 4.1-3 (continued)

Date	Time	Flow Rate (scfm)
10/14/2015	8:39	98.4
10/22/2015	10:09	98.2
10/28/2015	11:15	100.1
11/5/2015	11:30	100.3
11/12/2015	9:42	100.1
11/17/2015	13:18	102.4
11/18/2015	11:30	99.4

Note: Standard conditions for the orifice flow meter are 60°F and 14.7 psi (21.1°C and 101.3 kPa).

**Table 4.3-1
MDA L CME Tier I+II Screening Calculations**

VOC	Henry's Law Constant ^a (dimensionless)	Groundwater SL (µg/L)	Source of Groundwater SL	Tier I Pore-Gas Concentrations Corresponding to Groundwater Standard (µg/m ³)	MDA L-Specific Tier II Calculated Pore-Gas Screening Concentrations (µg/m ³)
Acetone	0.0016	22,000	EPA regional SL	35,200	104,000,000
Benzene	0.228	5	EPA MCL	1140	34,900
Butanone[2-]	0.0023	7100	EPA regional SL	16,330	553,000
Carbon Tetrachloride	1.1	5	EPA MCL	5500	74,200
Chlorobenzene	0.13	100	EPA MCL	13,000	440,000
Chloroform	0.15	100	NMWQCC	15,000	508,000
Cyclohexane	6.1	13,000	EPA regional SL	79,300,000	496,000,000
Dichlorodifluoromethane	14	390	EPA regional SL	5,460,000	30,900,000
Dichloroethane[1,1-]	0.23	25	NMWQCC	5750	185,000
Dichloroethane[1,2-]	0.048	5	EPA MCL	240	8,120
Dichloroethene[1,1-]	1.1	5	NMWQCC	5500	58,800
Dichloroethene[trans-1,2-]	0.38	100	EPA MCL	38,000	789,000
Dichloropropane[1,2-]	0.12	5	EPA MCL	600	20,300
Dioxane[1,4-]	0.0002	61	EPA regional SL	12.2	413
Ethanol	na ^b	na	na	na	na
Ethylbenzene	0.323	700	EPA MCL	226,100	6,540,000
Ethyltoluene[4-]	na	na	na	na	na
Hexane	74	880	EPA regional SL	65,120,000	344,000,000
Methanol	0.00019	18,000	EPA regional SL	3420	116,000
Methylene Chloride	0.13	5	EPA MCL	650	22,000
Styrene	0.11	100	EPA MCL	11,000	372,000
Tetrachloroethene	0.72	5	EPA MCL	3600	70,500
Tetrahydrofuran	na	na	na	na	na
Toluene	0.272	750	NMWQCC	204,000	6,070,000
Trichloro-1,2,2-trifluoroethane[1,1,2-]	22	59,000	EPA regional SL	1,298,000,000	7,540,000,000
Trichloroethane[1,1,1-]	0.705	60	NMWQCC	42,300	700,000
Trichloroethane[1,1,2-]	0.034	5	EPA MCL	170	5,760
Trichloroethene	0.4	5	EPA MCL	2000	48,100
Trichlorofluoromethane	4	1300	EPA regional SL	5,200,000	37,400,000
Trimethylbenzene[1,2,4-]	0.25	15	EPA regional SL	3750	127,000
Trimethylbenzene[1,3,5-]	0.36	370	EPA regional SL	133,200	3,900,000

Table 4.3-2
Differential Pressure Data at
Sampling Ports Monitored during SVE Operations

Well	Port Depth (ft bgs)	Sampling Interval (ft length along borehole)	Static Pressure (kPa)			
			Baseline 2014	April 15	July 15	November 15
54-01015 ^a	37.6	36–46	-0.106	— ^b	—	—
54-01015 ^a	165.4	182–192	-0.180	—	—	—
54-01015 ^a	308.3	340–352	0.011	—	—	—
54-01015 ^a	333.3	375–385	-0.119	—	—	—
54-01015 ^a	377.7	425–435	-0.126	—	—	—
54-01015 ^a	426.5	480–490	-0.122	—	—	—
54-01015 ^a	462.1	520–530	0.000	—	—	—
54-01016 ^a	30.8	30–40	-0.056	—	—	—
54-01016 ^a	162.2	178–190	0.021	—	—	—
54-01016 ^a	274.7	318–324	0.020	—	—	—
54-01016 ^a	336.3	386–396	0.016	—	—	—
54-01016 ^a	414.3	473–483	0.010	—	—	—
54-01016 ^a	459.5	530–540	0.000	—	—	—
54-01016 ^a	517.6	592–602	0.010	—	—	—
54-02001	20	17.5–22.5	-0.063	-0.314	-0.206	NS-RS ^c
54-02001	40	37.5–42.5	-0.035	-0.545	-0.253	NS-RS
54-02001	60	57.5–62.5	0.000	NS-B ^d	NS-B	NS ^e
54-02001	80	77.5–82.5	-0.113	-0.855	-0.694	NS-RS
54-02001	100	97.5–102.5	-0.038	-0.349	-0.267	NS-RS
54-02001	120	117.5–122.5	-0.167	-0.989	-0.639	NS-RS
54-02001	140	137.5–142.5	-0.380	-1.034	-0.622	NS-RS
54-02001	160	157.5–162.5	0.000	NS-B	NS-B	NS
54-02001	180	177.5–182.5	-0.022	0.317	-0.210	NS-RS
54-02001	200	197.5–202.5	-0.037	NS-B	-0.214	NS
54-02002	20	17.5–22.5	NS-B	NS-B	NS	NS
54-02002	40	37.5–42.5	-0.025	-0.828	0.527	0.565
54-02002	60	57.5–62.5	-0.014	-0.174	0.153	0.187
54-02002	80	77.5–82.5	-0.020	-0.379	NS	NS
54-02002	100	97.5–102.5	NS-B	NS-B	NS	NS
54-02002	120	117.5–122.5	-0.021	-0.746	0.525	0.583
54-02002	140	137.5–142.5	0.000	NS-B	NS-B	NS
54-02002	157/160	154.5–159.5	0.000	NS	0.495	NS
54-02002	180	177.5–182.5	0.100	0.016	0.000	0.00
54-02002	200	197.5–202.5	0.000	-1.092	0.440	0.439
54-02016	18	15.5–20.5	NS-B	NS-B	NS-B	NS

Table 4.3-2 (continued)

Well	Port Depth (ft bgs)	Sampling Interval (ft length along borehole)	Static Pressure (kPa)			
			Annual	April 15	July 15	November 15
54-02016	31	28.5–33.5	0.041	-0.057	-0.061	0.102
54-02016	82	79.5–84.5	NS-B	NS-B	NS-B	NS
54-02020	20	10–30	-0.041	—	—	—
54-02020	40	30–50	-0.068	—	—	—
54-02020	60	50–70	-0.100	—	—	—
54-02020	80	70–90	-0.129	—	—	—
54-02020	95	90–110	-0.146	—	—	—
54-02020	120	110–130	-0.147	—	—	—
54-02020	140	130–150	-0.154	—	—	—
54-02020	160	150–170	-0.157	—	—	—
54-02020	180	170–190	-0.159	—	—	—
54-02020	200	190–210	0.012	—	—	—
54-02021	20	10–30	-0.044	-0.070	-0.098	-0.028
54-02021	40	30–50	-0.053	-0.075	-0.112	NS
54-02021	60	50–70	-0.250	-0.082	-0.306	NS
54-02021	80	70–90	-0.128	-0.075	-0.155	NS
54-02021	100	90–110	-0.216	-0.093	-0.253	NS
54-02021	120	110–130	0.000	-0.056	-0.227	NS
54-02021	140	130–150	-0.239	-0.120	-0.303	-0.616
54-02021	160	150–170	-0.103	-0.079	-0.110	-0.173
54-02021	180	170–190	-0.269	-0.127	-0.282	-0.697
54-02021	198	190–210	-0.271	0.042	-0.173	-1.129
54-02022	20	17.5–22.5	-0.041	NS-B	NS-B	NS
54-02022	40	37.5–42.5	-0.055	-0.177	-0.173	0.025
54-02022	60	57.5–62.5	-0.070	-0.200	-0.192	0.00
54-02022	80	77.5–82.5	-0.101	-0.207	-0.243	-0.023
54-02022	100	97.5–102.5	-0.142	NS-B	NS-B	NS
54-02022	120	117.5–122.5	-0.126	-0.247	-0.259	-0.097
54-02022	140	137.5–142.5	-0.085	-0.239	-0.200	-0.219
54-02022	160	157.5–162.5	-0.041	-0.229	-0.185	-0.289
54-02022	180	177.5–182.5	0.000	-0.212	-0.146	-0.336
54-02022	200	197.5–202.5	0.020	-0.200	-0.127	-0.354
54-02023	20	10–30	0.011	—	—	—
54-02023	40	30–50	0.017	—	—	—
54-02023	60	50–70	0.178	—	—	—
54-02023	80	70–90	0.051	—	—	—
54-02023	100	90–110	0.072	—	—	—

Table 4.3-2 (continued)

Well	Port Depth (ft bgs)	Sampling Interval (ft length along borehole)	Static Pressure (kPa)			
			Annual	April 15	July 15	November 15
54-02023	120	110–130	0.018	—	—	—
54-02023	140	130–149	0.079	—	—	—
54-02023	159	149–169	0.151	—	—	—
54-02023	180	170–190	0.033	—	—	—
54-02023	200	190–210	0.204	—	—	—
54-02024	20	10–30	-0.035	—	—	—
54-02024	40	30–50	-0.034	—	—	—
54-02024	60	50–70	-0.047	—	—	—
54-02024	80	70–90	-0.092	—	—	—
54-02024	100	90–110	-0.132	—	—	—
54-02024	120	110–130	-0.146	—	—	—
54-02024	140	130–150	-0.164	—	—	—
54-02024	160	150–170	-0.182	—	—	—
54-02024	180	170–190	-0.193	—	—	—
54-02024	200	190–210	-0.203	—	—	—
54-02025	20	20	-23.000	—	—	—
54-02025	60	60	0.110	—	—	—
54-02025	100	100	-0.151	—	—	—
54-02025	160	160	-0.174	—	—	—
54-02025	190	190	-0.185	—	—	—
54-02026	20	20	0.000	—	—	—
54-02026	60	60	-0.017	—	—	—
54-02026	100	100	-0.100	—	—	—
54-02026	160	160	-0.217	—	—	—
54-02026	200	200	-0.258	—	—	—
54-02026	215	215	-0.277	—	—	—
54-02027	20	20	0.010	—	—	—
54-02027	60	60	-0.017	—	—	—
54-02027	100	100	-0.112	—	—	—
54-02027	160	160	-0.162	—	—	—
54-02027	200	200	-0.170	—	—	—
54-02027	220	220	-0.173	—	—	—
54-02027	250	250	-0.166	—	—	—
54-02028	20	20	0.000	—	—	—
54-02028	60	60	0.000	—	—	—
54-02028	100	100	0.010	—	—	—
54-02028	160	160	0.068	—	—	—

Table 4.3-2 (continued)

Well	Port Depth (ft bgs)	Sampling Interval (ft length along borehole)	Static Pressure (kPa)			
			Annual	April 15	July 15	November 15
54-02028	200	200	0.086	—	—	—
54-02028	220	220	0.085	—	—	—
54-02028	250	250	0.076	—	—	—
54-02031	20	20	0.000	—	—	—
54-02031	60	60	0.041	—	—	—
54-02031	100	100	0.101	—	—	—
54-02031	160	160	0.106	—	—	—
54-02031	200	200	0.207	—	—	—
54-02031	220	220	0.145	—	—	—
54-02031	260	260	0.235	—	—	—
54-02034	20	20	-0.029	—	—	—
54-02034	60	60	-0.063	—	—	—
54-02034	100	100	-0.041	—	—	—
54-02034	160	160	0.210	—	—	—
54-02034	200	200	0.243	—	—	—
54-02034	220	220	0.247	—	—	—
54-02034	260	260	0.272	—	—	—
54-02034	300	300	0.318	—	—	—
54-02089	13	13	-0.017	-0.049	-0.107	0.106
54-02089	31	31	-0.015	-0.047	-0.107	0.102
54-02089	46	46	-0.024	-0.047	-0.121	0.117
54-02089	86	86	-0.044	-0.192	-0.291	0.314
54-24238	44	43–45	-0.020	-1.728	-0.150	0.017
54-24238	64	63–65	-0.024	-0.258	-0.278	0.293
54-24238	84	83–85	0.011	0.105	0.000	0.324
54-24239	25	24–26	-0.024	0.033	-1.509	0.023
54-24239	50	49–51	-0.029	0.047	0.010	0.146
54-24239	75	74–76	0.064	0.028	-0.029	0.015
54-24239	99.5	98.5–100.5	0.103	-0.233	-0.022	0.095
54-24240	28	27–29	0.000	-0.244	-0.227	-0.208
54-24240	53	52–54	-0.013	-0.897	-0.838	-0.846
54-24240	78	77–79	-0.060	-2.053	-1.983	-1.946
54-24240	103	102–104	-0.116	-1.652	-1.488	-1.405
54-24240	128	127–129	-0.143	-1.187	-0.988	-0.883
54-24240	153	152–154	-0.167	-0.654	-0.435	-0.300
54-24241	73	71–74	-0.127	-0.802	-0.394	NS-RS
54-24241	93	92–94	-0.150	-1.035	-0.565	NS-RS

Table 4.3-2 (continued)

Well	Port Depth (ft bgs)	Sampling Interval (ft length along borehole)	Static Pressure (kPa)			
			Annual	April 15	July 15	November 15
54-24241	113	112–114	-0.180	-1.283	-0.695	NS-RS
54-24241	133	132–134	-0.233	-1.320	-0.659	NS-RS
54-24241	153	152–154	-0.278	-1.409	-0.124	NS-RS
54-24241	173	172–174	-0.282	-1.398	-0.566	NS-RS
54-24241	193	192–194	-0.288	-1.292	-0.585	NS-RS
54-24242	25	24–26	-0.048	—	—	—
54-24242	50	49–51	-0.203	—	—	—
54-24242	75	74–76	-0.112	—	—	—
54-24242	100	99–101	-0.053	—	—	—
54-24242	110.5	109.5–111.5	-0.213	—	—	—
54-24243	25	24–26	0.073	-0.115	-0.129	0.146
54-24243	50	49–51	0.075	-0.145	-0.180	0.139
54-24243	75	74–76	0.109	-0.330	-0.395	0.240
54-24243	100	99–101	0.176	-0.888	-0.961	-0.020
54-24243	125	124–126	0.179	-1.064	-1.253	1.017
54-24399 ^f	561.5–565.5	561.5–565.5	n/a ^g	n/a	n/a	n/a
54-24399 ^f	568–608	568–608	n/a	n/a	n/a	n/a
54-24399 ^f	568–569	568–569	n/a	n/a	n/a	n/a
54-27641	32	29.5–34.5	-0.035	-0.283	-0.300	NS-RS
54-27641	82	79.5–84.5	-0.059	-3.844	-3.919	-3.805
54-27641	115	112.5–117.5	-0.169	-1.169	-1.319	-0.966
54-27641	182	179.5–184.5	-0.178	-0.067	-0.420	-0.053
54-27641	232	229.5–234.5	-0.164	0.053	-0.320	NS-RS
54-27641	271	268.5–273.5	-0.164	0.141	-0.227	-0.257
54-27641	332.5	330–335	-0.175	0.151	-0.195	-0.277
54-27642	30	27.5–32.5	-0.028	-0.094	-0.050	0.066
54-27642	75	71.5–76.5	-0.035	-0.667	-0.264	0.300
54-27642	116	114.5–119.5	0.000	-0.761	-0.480	NS-RS
54-27642	175	172.5–177.5	0.049	-0.985	-0.285	0.191
54-27642	235	232.5–237.5	0.038	-0.793	-0.154	0.701
54-27642	275	272.5–277.5	0.000	-0.722	-0.236	0.485
54-27642	338	335.5–340.5	-0.028	-0.526	-0.088	NS-RS
54-27643	30	27.5–32.5	0.018	—	—	—
54-27643	74	71.5–76.5	0.050	—	—	—
54-27643	117	114.5–119.5	0.129	—	—	—
54-27643	167	164.5–169.5	0.251	—	—	—
54-27643	235	232.5–237.5	0.279	—	—	—

Table 4.3-2 (continued)

Well	Port Depth (ft bgs)	Sampling Interval (ft length along borehole)	Static Pressure (kPa)			
			Annual	April 15	July 15	November 15
54-27643	275	272.5–277.5	0.276	—	—	—
54-27643	354	351.5–356.5	0.133	—	—	—
54-610786 ^h	25	22.5–27.5	0.000	—	—	—
54-610786 ^h	50	47.5–52.5	0.000	—	—	—
54-610786 ^h	75	72.5–77.5	-0.020	—	—	—
54-610786 ^h	100	97.5–102.5	-0.044	—	—	—
54-610786 ^h	118.5	116–121	-0.053	—	—	—

^a Vapor-monitoring borehole angled. Port depth is depth below ground surface. Port-depth interval is length along borehole.

^b — = Not measured as part of quarterly sampling.

^c NS-RS = Not sampled because of radiological concerns.

^d NS-B = Not sampled because port blocked.

^e NS = Not sampled because previous rounds port blocked or partially blocked.

^f Open borehole below 565.5 ft bgs.

^g n/a = Not applicable for packer system.

^h Drilled in December 2009.

Table 5.6-1
Distances from Example Observation Points
to SVE-East and Sudden Drum Failure Location

Well	Distance from SVE-East	Distance from Sudden Release
54-27642	41.9 m (138 ft)	14.2 m (47 ft)
54-24238	29.7 m (98 ft)	7.7 m (25 ft)
54-24241	24.5 m (80 ft)	36.6 m (120 ft)

Appendix A

*Spreadsheet Containing Dwyer Orifice Plate Calculations
(on CD included with this document)*

Appendix B

*Analytical Suites and Results
(on CD included with this document)*

Appendix C

Example Calculations for Effluent Mass Removal

This appendix explains calculations of the total mass of volatile organic compounds (VOCs) being removed in the soil-vapor extraction (SVE) effluent. The numbers presented below are not exact measurements, but they are representative of the data collected during SVE operation at Material Disposal Area L, Technical Area 54, at Los Alamos National Laboratory. The example calculations are a simplified description of several Excel macros that combine both flow and concentration data to create graphs of mass removal versus time.

C-1.0 INITIALIZATION OF THE CALCULATION

For both SVE-East and SVE-West, one data point was added and set 1 min before start time and with flow "0." The concentration at the 1 min before start time is assumed to be equal to the first measured concentration.

C-2.0 GENERATING FLOW RATE VERSUS TIME

Air-flow data, in standard cubic feet per minute (scfm), from both SVE-East and SVE-West are loaded into a spreadsheet. Next, data on flow are numerically integrated over discrete time intervals using the trapezoid method to create volumes associated with each time interval (in m³). Example air-flow data for SVE-West is included in Table C-2.0-1.

Table C-2.0-1
SVE-West Example Air-Flow Data

Time	1/9/2015 12:55	1/9/2015 12:56	1/16/2015 8:58	1/26/2015 9:08	2/25/2015 12:42	2/28/2015 12:42
Flow (scfm)	0	99.9	98.3	101	99.8	99.9

The partial volume pumped for each time interval is calculated using the following formula:

$$\text{Partial volume} = (\text{flow1} + \text{flow2})/2 * \text{time difference} * 0.0283168 \text{ m}^3/\text{ft}^3,$$

where 0.0283168 is a recalculation factor from standard cubic feet to m³.

For the first data point, this leads to the expression,

$$\text{Partial volume} = (0+99.9)/2 * (1/9/2015 12:56:00 \text{ PM} - 1/9/2015 12:55:00 \text{ PM}) * 0.0283168$$

$$\text{Partial volume} = 45.95 \text{ cfm} * 1 \text{ min} = 1.41 \text{ m}^3 \text{ (for time 1/9/2015 12:56:00 PM).}$$

This calculation is repeated for all five pairs of data in Table C-2.0-1 and leads to the values in Table C-2.0-2 (values are rounded to whole numbers).

Table C-2.0-2
SVE-West, Volumes Pumped for Discrete Time Intervals

Time	1/9/2015 12:55	1/9/2015 12:56	1/16/2015 8:58	1/26/2015 9:08	2/25/2015 12:42	2/28/2015 12:42
Flow	0	99.9	98.3	101	99.8	99.9
(Flow1+flow2)/2 (scfm)		50	99	100	100	100
Time difference		1	9842	14,410	43,414	4320
Partial volume (m ³)		1	27,619	40,662	123,426	12,215

Total volume pumped is calculated by adding partial volumes:

- For 1/9/2015 12:56:00 PM: total volume = 1
- For 1/16/2015 8:58:00 AM: total volume = 1 + 27,619 = 27,620
- For 1/26/2015 9:08 AM: total volume = 1 + 27,619 + 40,662 = 27,620 + 40,662 = 68,282 and so on.

The results of the calculated total volume pumped at discrete times is included in Table C-2.0-3.

Table C-2.0-3
SVE-West, Integrated Total Volume Pumped at Discrete Times

Time	1/9/2015 12:55	1/9/2015 12:56	1/16/2015 8:58	1/26/2015 9:08	2/25/2015 12:42	2/28/2015 12:42
Flow	0	99.9	98.3	101	99.8	99.9
(Flow1+flow2)/2 (scfm)		50	99	100	100	100
Time difference		1	9842	14,410	43,414	4320
Partial volume (m ³)		1	27,619	40,662	123,426	12,215
Total volume (m ³)		1	27,620	68,282	191,708	203,923

C-3.0 INTERPOLATING CONCENTRATION VERSUS TIME TO THE FLOW DATA

To obtain total mass on the compound 1,1,1-trichloroethane (1,1,1-TCA) in this example, the concentration data versus time have to be interpolated to the total volume scale because concentration data were not collected at every flow rate measurement. Concentrations at discrete times for SVE-West are included in Table C-3.0-1.

Table C-3.0-1
SVE-West, Effluent Concentration at Discrete Times

Time	1/9/2015 12:55	1/9/2015 14:24	1/16/2015 9:04	1/26/2015 9:19	2/25/2015 12:46
Concentration (µg/m ³)	479,833	479,833	261,727	141,769	87,242.3

The volume pumped at the start, 1 min, is equal to 0. For the next data point (at 1/9/2015 14:24), linear interpolation is used.

To use linear interpolation, two points were selected from Table C-2.0-3, one immediately before and one immediately after the interpolation point. For the interpolated point at 1/9/2015 14:24, these points are 1/9/2015 12:56 and 1/16/2015 8:58. Initially, the equation of the line passing through these points is calculated: $y = ax + b$. At the end of interpolation step, the equation of this line and the time value for interpolated point to find the interpolated total volume are used.

If time is marked as “x” and total volume as “y,” the equations are

$$a = (y_2 - y_1) / (x_2 - x_1),$$

$$b = y_1 - a * x_1,$$

and finally

$$y_c = a * x_c + b.$$

For the example listed above,

$$a = (27620 - 1) / (1/16/2015\ 8:58:00\ AM - 1/9/2015\ 12:56:00\ PM) = 4040.98$$

$$b = 1 - 4040.98 * (1/9/2015\ 12:56:00\ PM) = -169776018.10$$

$$y_c = 4040.98 * (1/9/2015\ 2:24:00\ PM) - 169776018.10 = 248$$

Note: In the explanation above, dates as values of x are used. Within Excel, “date values” are used to remove any problems with incorporating dates into equations. Calculations explained above are repeated for three more points from Table C-3.0-1, and the results are included in Table C-3.0-2.

Table C-3.0-2
SVE-West, Effluent Concentration at Discrete Times

Time	1/9/2015 12:55	1/9/2015 14:24	1/16/2015 9:04	1/26/2015 9:19	2/25/2015 12:46
Concentration (µg/m³)	479,833	479,833	261,727	141,769	87,242.3
Total volume pumped (m³)	0	248	27,637	68,313	191,719

Table C-3.0-3 presents values of the linear coefficients used in the interpolation for each point in Table C-3.0-2.

Table C-3.0-3
SVE-West Flow Volume Integration

Time	1/9/2015 12:55	1/9/2015 12:56	1/16/2015 8:58	1/26/2015 9:08	2/25/2015 12:42	2/28/2015 12:42
Flow (scfm)	0	99.9	98.3	101	99.8	99.9
(Flow1+flow2)/2 (scfm)		50	99	100	100	100
Time difference		1	9842	14,410	43,414	4320
Partial volume (m³)		1	27,619	40,662	123,426	12,215
Total volume (m³)		1	27,620	68,282	191,708	203,923
		a	4040.98354	4063.37821	4093.919934	4071.666667
		b	-169,776,018.10	-1,707,17,050.49	-172,000,730.78	-171,064,746.59

C-4.0 CALCULATION OF MASS REMOVAL SVE-WEST

Data from Table C-3.0-2 may be numerically integrated leading to the total mass of 1,1,1-TCA contained in the effluent stream removed from SVE-West as a function of time mapped to discrete points in time.

Partial mass removed = (concentration1+concentration2)/2*(volume2 – volume1)*1e-9 * 2.20462, where 1e-9 is recalculation factor from µg to kg, and ‘2.20462’ is recalculation factor from kg to lb.

Total mass removed is integrated numerically as the sum of the partial masses.

For time “1/9/2015 2:24:00 PM,” the partial mass removed = (479,833 + 479,833)/2*(248-0)*1e-9*2.20462 = 0.3 lb.

Results of the volume-concentration time alignment and mass removal integration for SVE-West are presented in Table C-4.0-1.

**Table C-4.0-1
SVE-West, Volume-Concentration Integration of 1,1,1-TCA Mass Removal**

Time	1/9/2015 12:55	1/9/2015 14:24	1/16/2015 9:04	1/26/2015 9:19	2/25/2015 12:46
Concentration (µg/m ³)	479,833	479,833	261,727	141,769	87,242.3
Total volume pumped (m ³)	0	248	27,637	68,313	191,719
Partial mass removed (lb)	0	0.3	22.4	18.1	31.2
Total mass removed (lb)	0	0.3	22.7	40.8	72

C-5.0 CALCULATION OF MASS REMOVAL SVE-EAST

The same calculation pattern is used to calculate mass numbers for the SVE-East unit. The results are presented in Tables C-5.0-1 and C-5.0-2.

**Table C-5.0-1
SVE-East Flow Interpolation Coefficients**

Time	1/26/2015 10:20	1/26/2015 10:21	1/27/2015 11:17	2/25/2015 13:18	2/28/2015 13:42
Flow	0	99.5	98.6	98.5	99.1
(Flow1+flow2)/2		50	99	99	99
Time difference		1	1496	41,881	4344
Partial volume (m ³)		1	4196	116,874	12,153
Total volume (m ³)		1	4197	121,071	133,224
		a	4038.930481	4018.494305	4028.618785
		b	-169,757,988.92	-168,899,026.40	-169,324,867.60

Table C-5.0-2
SVE-East Volume-Concentration Integration of 1,1,1-TCA Mass Removal

Time	1/26/2015 10:20	1/26/2015 11:12	1/27/2015 12:27	2/25/2015 13:20
Concentration ($\mu\text{g}/\text{m}^3$)	348,969	348,969	370,780	223,558
Total volume pumped (m^3)	0	144	4392	121,077
Partial mass removed (lb)	0	0.1	3.4	76.4
Total mass removed (lb)	0	0.1	3.5	79.9

C-6.0 CALCULATION OF COMBINED SVE-WEST PLUS SVE-EAST MASS REMOVAL

To calculate the total amount of 1,1,1-TCA removed, SVE-West and SVE-East numbers have to be added. Again, interpolation and data alignment are necessary because there are no total mass removed data at the same times for SVE-West and SVE-East.

The SVE-West unit was always sampled and recorded first, so the dates from the SVE-West unit are used as interpolation dates. For each interpolation date, two time points from SVE-East are used, one immediately before (1/27/2015 12:27) and one immediately after (2/25/2015 13:20). Using the interpolation formulas from section 3.0, the following is derived:

$$a = (79.9 - 3.5) / (2/25/2015\ 13:20 - 1/27/2015\ 12:27) = 2.6311$$

$$b = 3.5 - 2.6311 * (1/27/2015\ 12:27:00\ \text{PM}) = -110587.45$$

Results for interpolation coefficients are listed in Table C-6.0-1.

Table C-6.0-1
Interpolation Coefficients for the Combined Mass Removal

Time	1/26/2015 10:20	1/26/2015 11:12	1/27/2015 12:27	2/25/2015 13:20
Concentration ($\mu\text{g}/\text{m}^3$)	348,969	348,969	370,780	223,558
Total volume pumped (m^3)	0	144	4392	121,077
Partial mass removed (lb)	0	0.1	3.4	76.4
Total mass removed (lb)	0	0.1	3.5	79.9
a		2.769230769	3.231683168	2.631143424
b		-116,391.96	-135,829.05	-110,587.45

When Tables C-4.0-1 and C-6.0-1 are compared, the only date from Table C-4.0-1 when both units, West and East, were operational is 2/25/2015 12:46:00 PM. The amount of 1,1,1-TCA SVE-East removed at 2/25/2015 12:46:00 PM can be calculated using this date and "a" and "b" coefficients from Table C-6.0-1.

$$y_c = a * (2/25/2015\ 12:46:00\ \text{PM}) + b = 2.631143424 * (2/25/2015\ 12:46:00\ \text{PM}) - 110587.45 = 79.8\ \text{lb}$$

By adding SVE-West and SVE-East (East after interpolation), the total amount of the 1,1,1-TCA removed by both units is (72 + 79.8 = 151.8). Table C-6.0-2 presents the combined total mass of 1,1,1-TCA removed by both units.

**Table C-6.0-2
Integration of Combined Mass Removal**

Time	1/9/2015 12:55	1/9/2015 14:24	1/16/2015 9:04	1/26/2015 9:19	2/25/2015 12:46
Concentration ($\mu\text{g}/\text{m}^3$)	479,833	479,833	261,727	141,769	87,242.3
Total volume pumped (m^3)	0	248	27,637	68,313	191,719
Partial mass removed (lb)	0	0.3	22.4	18.1	31.2
Total mass removed West (lb)	0	0.3	22.7	40.8	72
Total mass removed East (lb)*	0	0	0	0	79.8
East + West (lb)	0	0.3	22.7	40.8	151.8

* The first four columns for the East unit list "0" because SVE-East was not operational on 1/9/2015.

The flow data were integrated each time new SUMMA data were obtained. The calculation pattern for concentrations, as described above, is repeated for each detected analyte. (The analyte does not have to be detected in all SUMMA samples; single detection will trigger the calculations described above.) The total "East+West lb" values were added together to obtain total value of VOC removed.

Appendix D

*Video Log of Borehole 54-24399
(on DVD included with this document)*

Appendix E

*Flow Rate Data for SVE-West and SVE-East
(on CD included with this document)*

